



# **RPG-XCH-DP** **X Frequency, Dual Polarized Radiometer** **(6.925 / 10.65 / 18.70 (21.00) / 36.50 GHz h/v)**

**Version 6.8 (18. 2. 2009)**



## **Operating Manual**



**by Th. Rose, H. Czekala**  
**Radiometer Physics GmbH,**  
**[www.radiometer-physics.com](http://www.radiometer-physics.com)**





## Table of Contents

Table of Contents .....	ii
1. Unpacking and Assembly of the Radiometer .....	4
1.1 Radiometer Modules and Positioner .....	4
1.2 Electrical Connections .....	6
1.3 Powering up the Radiometer .....	9
2. Instrument Hardware .....	9
2.1 Operating the Positioner Controller .....	9
2.1.1 BE-01 Controller .....	10
2.1.2 BAD-05 Controller .....	12
2.2 General Radiometer Configuration .....	13
2.3 Receivers .....	14
3. Detailed Description of Receiver Components .....	16
3.1 Antenna Performance .....	16
3.2 Noise Diodes .....	17
3.3 RF-Amplifiers .....	18
3.4 Bandpass Filters .....	18
3.5 Detector, Video Amplifier, ADC .....	18
3.6 Additional Sensors .....	18
3.7 Other Radiometer Details .....	19
3.8 Instrument Specifications .....	19
4. Calibrations .....	21
4.1 Absolute Calibration .....	21
4.1.1 The Internal Dicke Switch Calibration Target .....	21
4.1.2 External Liquid Nitrogen Cooled Calibration Target .....	21
4.1.3 General Remarks on Absolute Calibrations .....	22
4.1.3.1 System Nonlinearity Correction .....	23
4.2 Noise Injection Calibration .....	24
4.3 Sky Tipping (Tip Curve) .....	25
5. Software Description .....	27
5.1 Installation of Host Software .....	27
5.1.1 Hardware Requirements for Host PC .....	27
5.1.2 Directory Tree .....	27
5.2 Getting Started .....	28
5.3 Radiometer Status Information .....	31
5.4 Data Storage Host Configuration .....	32
5.5 Exchanging Data Files .....	34
5.6 Inspecting Absolute Calibration History .....	35
5.7 Inspecting Automatic Calibration Results .....	37
5.8 Absolute Calibration .....	37
5.9 Defining Measurements .....	38
5.9.1 Sky Tipping .....	39
5.9.2 Products + Integration .....	40
5.9.3 Scanning .....	41
5.9.4 Timing + .....	42
5.9.5 MDF + MBF Storage .....	43
5.10 Sending a MBF to the Radiometer .....	44
5.11 Commanding the Radiometer Processes .....	45



5.12 Monitoring Data .....	46
5.13 Concatenate Data Files .....	47
5.14 Cutting Connection .....	47
5.15 Data Display Menus .....	47
5.16 Manual Radiometer Control .....	49
5.16.1 Positioner Control .....	49
5.16.2 Channel Voltages .....	50
5.16.3 Sensor Calibration .....	51
5.16.4 System .....	51
5.17 Transform Data Files to ASCII Format .....	52
6. Instrument Maintenance and Recommendations .....	53
6.1 Cleaning .....	53
6.2 Calibrations .....	54
6.3 Maintenance Schedule .....	54
6.4 Resetting of Radiometer Embedded PC .....	54
6.5 Restarting Host .....	55
6.6 Instrument Viewing Range .....	56
6.7 Upgrading System Software .....	57
7. Theory of Operation (Atmospheric Applications) .....	58
7.1 Introduction .....	58
7.2 Polarisation Signal .....	60
7.3 Model Calculations .....	60
7.4 Proposed Retrieval Method .....	62
7.5 Discussion .....	63
7.6 Conclusions .....	65
7.7 REFERENCES .....	65
8. Soil Moisture Applications .....	66
Appendix A (File Formats) .....	68
A1a: BRT-Files (*.BRT), Brightness Temperature (Single Channels) .....	68
A1b: BRT-Files (*.BRT), Brightness Temperature (Version 2) .....	68
A2: HKD-Files (*.HKD), Housekeeping Data .....	69
A3: LIW-Files (*.LIW), Liquid Water Data .....	69
A4: IWV-Files (*.IWV), Integrated Water Vapour Data .....	70
A5: Structure of Calibration Log-File (CAL.LOG) .....	70
Appendix B (ASCII File Formats) .....	73
Appendix C (Measurement Example) .....	75
C1. Zenith Sky Observations .....	75
C2. Observations Under Low Elevation Angles .....	76



## 1. Unpacking and Assembly of the Radiometer

### 1.1 Radiometer Modules and Positioner

The instrument is delivered in two boxes. Box A contains the elevation / azimuth positioner and the positioner / power / data cables. Unpack this box first. In box B you will find the radiometer modules mounted on a steel frame, the positioner controller, the PC and a LN calibration target, see Fig.1.1:



*Fig.1.1: Content of box B. Radiometer modules are mounted to a steel frame that is also holding the two off axis parabola antennas for the low frequency channels.*

Step 1: Dismount the antenna frame from the main steel frame. The antenna frame is screwed to the main frame by two threaded bolts with black knobs.

Step 2: Dismount the 10.65 GHz and 6.926 GHz receiver modules (see Fig.1.2) from the main frame.

Step 3: Unscrew the main frame from the wooden box's bottom plate (4 screws S1, see Fig.1.3).

Step 4: Lift the main frame together with the 18.7 and 36.5 GHz modules on top of the positioner and screw it tightly on the positioner's mounting plate (use S2 positions, Fig.1.3). Also mount the antenna frame back to the main frame. See Fig.1.4.

Step 5: Mount the 6.925 and 10.65 GHz modules back to the main frame (positions S3, Fig.1.3)

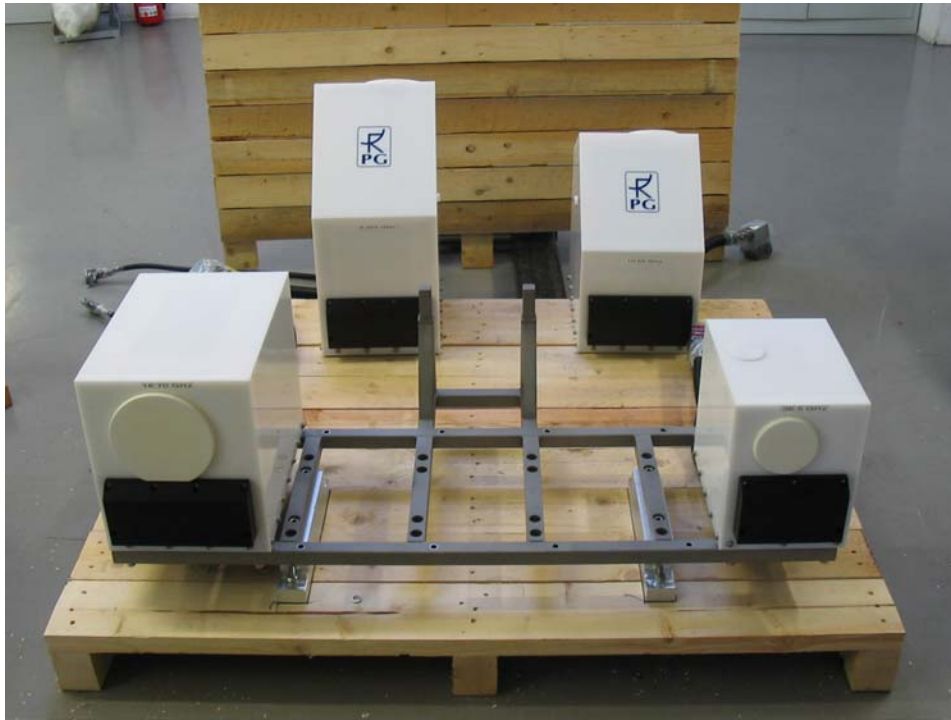


*Fig.1.2: The low frequency modules (6.925 and 10.65 GHz) dismantled from the main frame.*

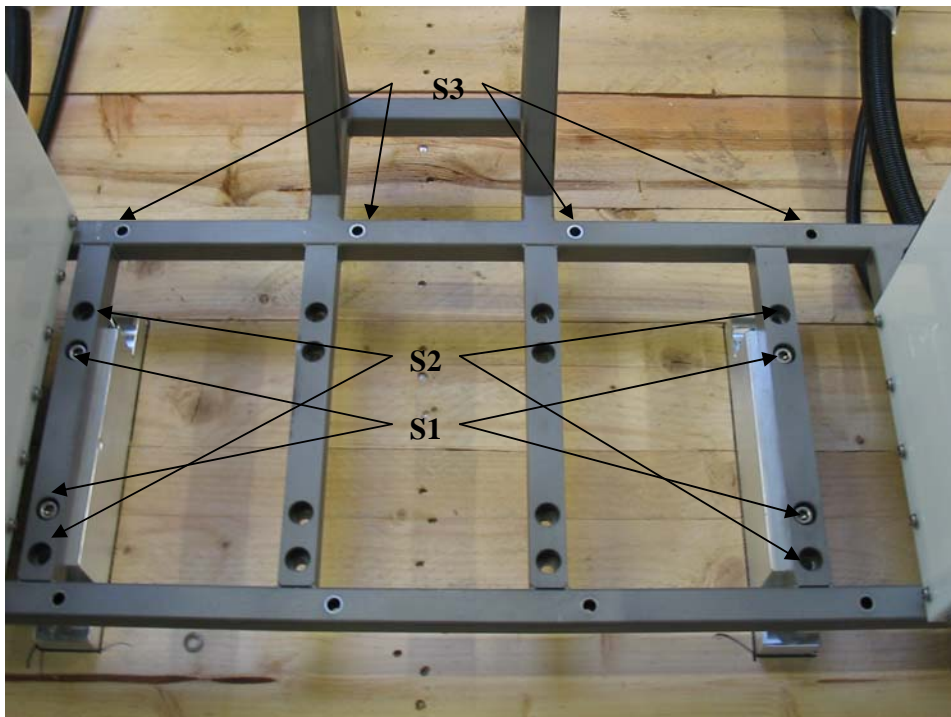


*Fig.1.3: Dismounting the main frame from the box B base plate by unscrewing 4 S1 screws.*



*Fig.1.4: Mounting the main frame on top of the positioner's base plate.*

## **1.2 Electrical Connections**

Fig.1.4 shows the two power supplies PS1 and PS2 located close to the positioner's elevation axis.

Each receiver module has a main power cable (industry standard T12-4 CombiTec connector) and a receiver control cable (15 pin sub-D connector). Plug all sub-D connectors into their associated sockets on PS1 (see Fig.1.5) and screw them tight. They are labelled 1-4. Then plug in the T12-4 connectors (10.65 GHz and 36.5 GHz modules to PS1, 6.925 GHz and 18.7 GHz modules to PS2). The receiver modules are now connected to the data acquisition system.

Furthermore connect the radiometer power connector and the positioner connector to the rear side of the positioner controller box as shown in Fig.1.6. The positioner controller receives its commands from the host PC via an RS-232 cable with 25 pin sub-D connector on the controller side and a 9 pin sub-D connector on the PC side. Use the COM1 interface on the PC for this connection. Then plug in the PC power and monitor power cables into one of the sockets shown in Fig.1.6.

Finally fasten the modul cables with cable ties like shown in Fig.1.7.

Connect the

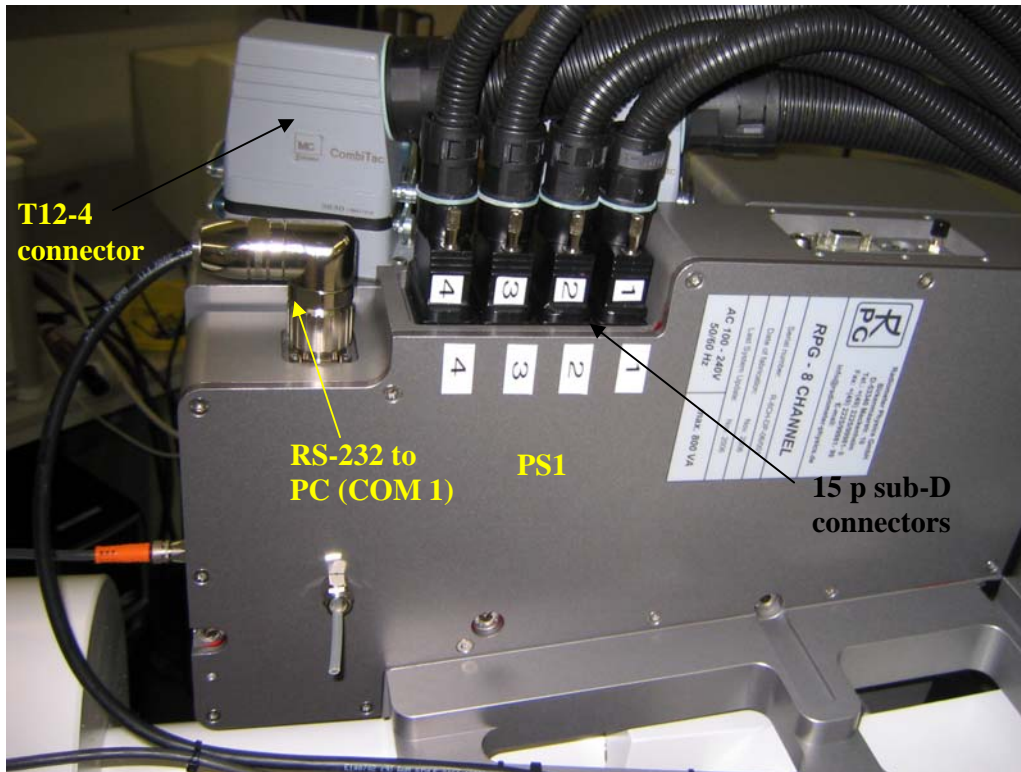


Fig.1.5: Connecting the receiver modules to PS1 / PS2.

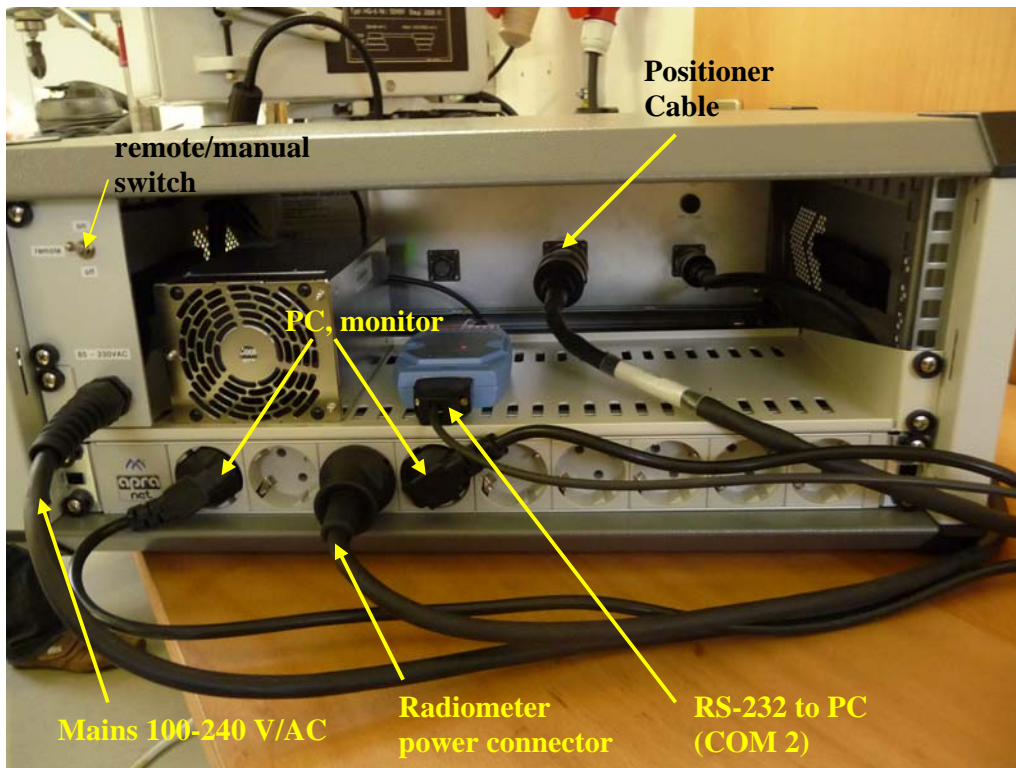


Fig.1.6: Rear panel of positioner controller unit with connections.





*Fig.1.7: Rear side of assembled instrument.*

### 1.3 Powering up the Radiometer

After all mechanical and electrical connections have been established, the radiometer can be turned on (Fig.1.8: Power ON/OFF switch). The embedded PC takes about 60 seconds to boot and start the radiometer software. Also the positioner controller performs a boot-up procedure and automatically enters the remote control mode that is needed to communicate with it via RS-232. Wait at least 30 minutes for warm-up at operating temperatures  $>10^{\circ}\text{C}$  and 45 minutes warm-up time at lower environmental temperatures. The stabilization process can be inspected in the DIAGNOSTICS menu on the host computer.

During warming up the system actively heats the receivers with a total power consumption of 500 Watts. Once the receivers are thermally stabilized, the power consumption drops down to less than 300 Watts.



*Fig.1.8: Front side of power and positioner controller.*

## 2. Instrument Hardware

### 2.1 Operating the Positioner Controller

The instrument positioner controller is by default set to automatically switch to REMOTE mode when the unit is powered on. In this mode the controller communicates with the external PC via RS-232 interface. In general this mode should not be changed. Otherwise the PC software might lose the ability to access the positioner status (elevation and azimuth position) and to initiate movements. When the PC software is active and has connected to the



radiometer, the REMOTE mode is essential for a smooth radiometer operation. **If the controller is accidentally in LOCAL mode while the PC software is active, the software might crash or stop execution until the controller is reset to REMOTE operation.**

However, it is sometimes useful to manually move the positioner without the control of the operating software. E.g. during the instrument setup process and horizontal alignment a manual controller operation is mandatory. The following description of the controller functions is limited to those commands that are needed for this system setup and does not include information about how to change the controller driver parameters or other critical parameters that affect the smooth operation of the device. For further details please refer to the controller operating manual delivered with the radiometer package.

There are two different controller models, the BE-01 and the BAD-05.

### 2.1.1 BE-01 Controller

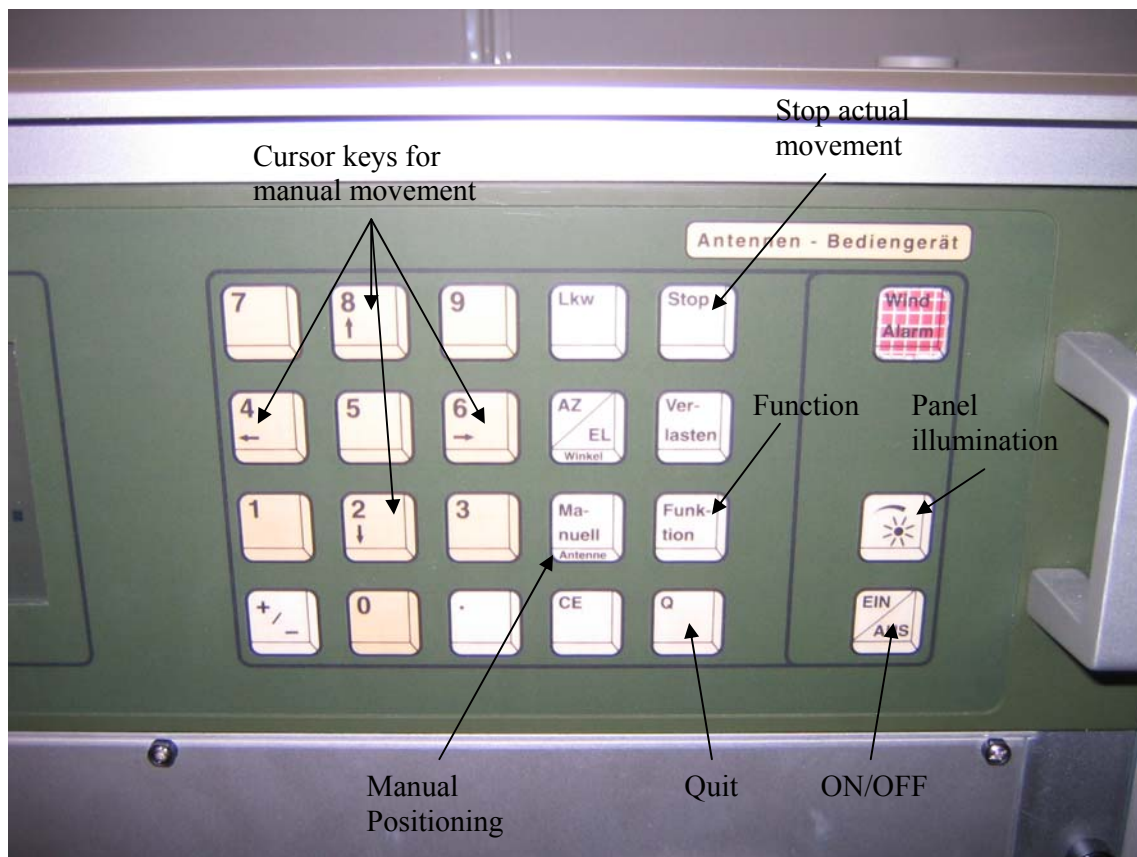


*Fig. 2.1: Positioner controller operating panel (controller model BE-01).*

#### **Panel Keys:**

**AZ/EL:** The positioner model AR/AE 1040 is a two axis positioning device with simultaneous axis control. The delivered controller unit can also handle other positioner models with only a single axis or two distinct positioners. In LOCAL mode the **AZ/EL**-key allows to enter elevation and azimuth coordinates for manual movement control. First the antenna no. is entered (always **1**). Then one enters the new azimuth target position. If the azimuth position shall be unchanged quit the entry with **Q** and continue with the elevation



angle. Press the **Q**-key to leave this menu. The positioner will then move to the defined coordinates.

**EIN/AUS**: ON/OFF-key. The controller is programmed to turn on automatically when power is applied to the unit. If the user wants to turn the controller off without turning off the radiometer and PC (by switching the main switch shown in Fig.1.8) he can press this key. When power is applied to the controller or the **EIN/AUS**-key is pressed to turn the controller on, the device is running through a setup sequence for detecting the connected positioner model and to load the driver parameters. After this initialization procedure the controller automatically enters REMOTE mode.

**Funktion:**

NEVER change the settings accessible with the **Function**-key followed by the **1**-key, **2**-key or **3**-key. These settings are critical for the positioner operation and have been factory pre-defined. Changing these parameters might lead to strange positioner behaviour or damage the positioner!

Pressing the **Function**-key followed by the **4**-key one enters the AZ/EL step width menu. This step width is used during manual movements with the cursor keys. First of all the azimuth step width has to be entered with the numerical keys which is quitted with the **Q**-key. Then the elevation step width is entered and quitted in the same way.

Pressing the **Function**-key followed by the **7**-key the user may switch between English and German for the LCD display language.

Pressing the **Function**-key followed by the **8**-key toggles between LOCAL and REMOTE mode for the power on default.

Pressing the **Function**-key followed by the **9**-key toggles the controller between REMOTE and LOCAL mode. The default is REMOTE mode when the unit is powered on. In this mode all keys except for the Function-key, the STOP-key and the **EIN/AUS**-key are disabled.

**Panel illumination**: see Fig.2.1. The user might change the panel illumination with this key. After pressing the key one of the 0 / 1 / 2 / 3 / 4 keys should be pressed to set the panel illumination to one of the four different illumination levels. Level 4 ist the brightest illumination level. Both, the LCD display and the keys are illuminated so that the controller can be operated at dark places. After switching on the controller the default level is 2. One can turn off the illumination by entering level 0.

**Manuell**: Manual movement key. When the controller is in LOCAL mode the operator can press the **Manuell**-key to move the positioner axis with the cursor keys. First the antenna number (always 1) has to be entered and then the positioner will move as long as one of the cursor keys is pressed. The vertical arrow keys control the elevation axis and the horizontal arrow keys the azimuth axis. One can leave the menu by pressing **Q**.

**Stop**: The positioner movement can be stopped at any time by pressing the **Stop**-key. This works in both, LOCAL and REMOTE mode.

**Offset Adjustment**

When the radiometer is set up for the first time its horizontal adjustment has to be performed in order to remove a possible elevation offset angle. The radiometer is automatically calibrating itself by the sky tipping method (on regular intervals) which relies on the correct horizontal adjustment of the elevation axis. The following procedure is used for the adjustment:



Step 1: Move the positioner to the desired reference position which is intended to be azimuth  $0.0^\circ$  and elevation  $0.0^\circ$ . For the elevation axis the operator should use a leveler to adjust the radiometer table to be horizontally aligned.

Step 2: Turn off the controller with the **EIN/AUS**-key.

Step 3: Press and hold the **Function**-key and turn on the controller (**EIN/AUS**-key).

Step 4: Release the **Function**-key.

Step 5: Press the **1**-key, **2**-key and **3**-key in this order.

The new reference positions are then stored into an EEPROM inside the controller unit. From now on all positioning angles are displayed relative to the new references.

### 2.1.2 BAD-05 Controller

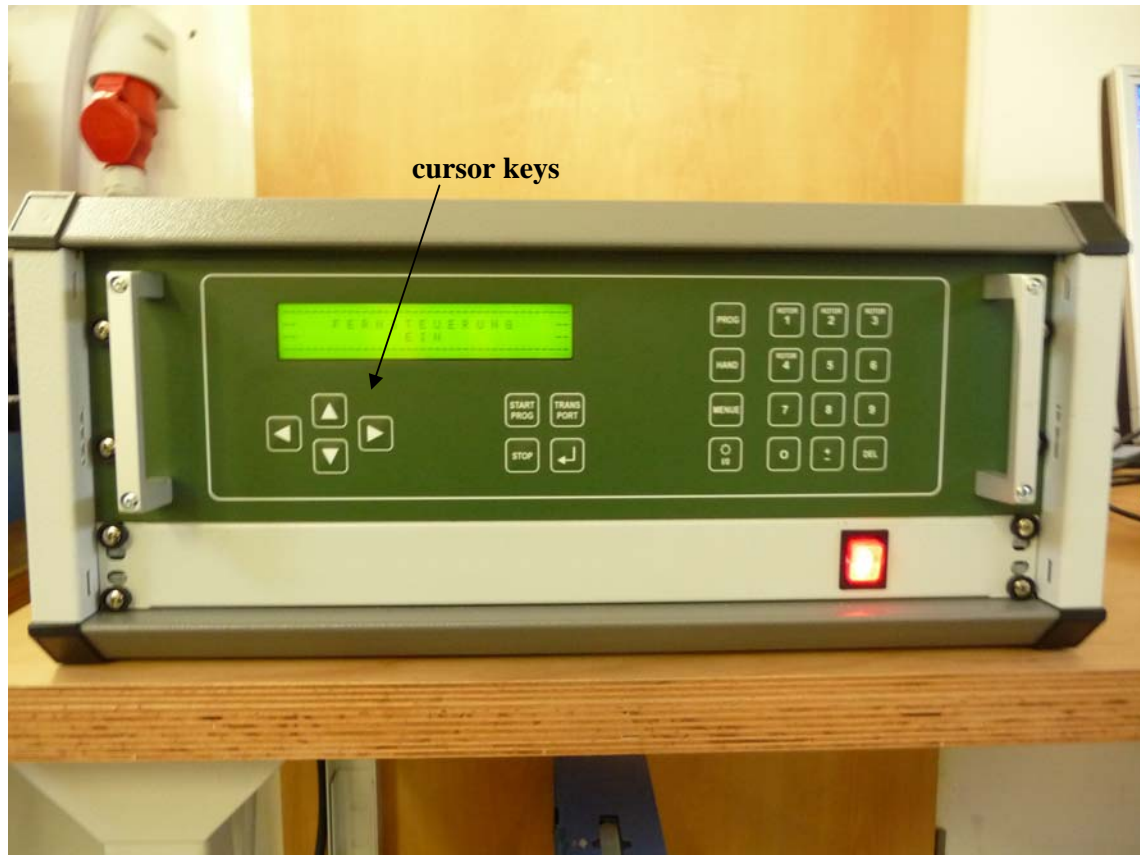


*Fig.2.1.2: Controller model BAD-05*

The BAD-05 has a Remote/Manual switch on its rear panel (see Fig.1.6). To switch to manual mode, set this switch to 'Manual' and turn off/on the controller's power (main switch). Then the controller will automatically enter the manual control mode. In this mode the user can move the positioner manually via the cursor keys. To get back to the 'Remote' mode, switch back the switch on the rear panel to 'Remote' position and turn off/on the controller power. It will then return to remote mode and can be accessed by the PC.

#### **Limiting Switches**

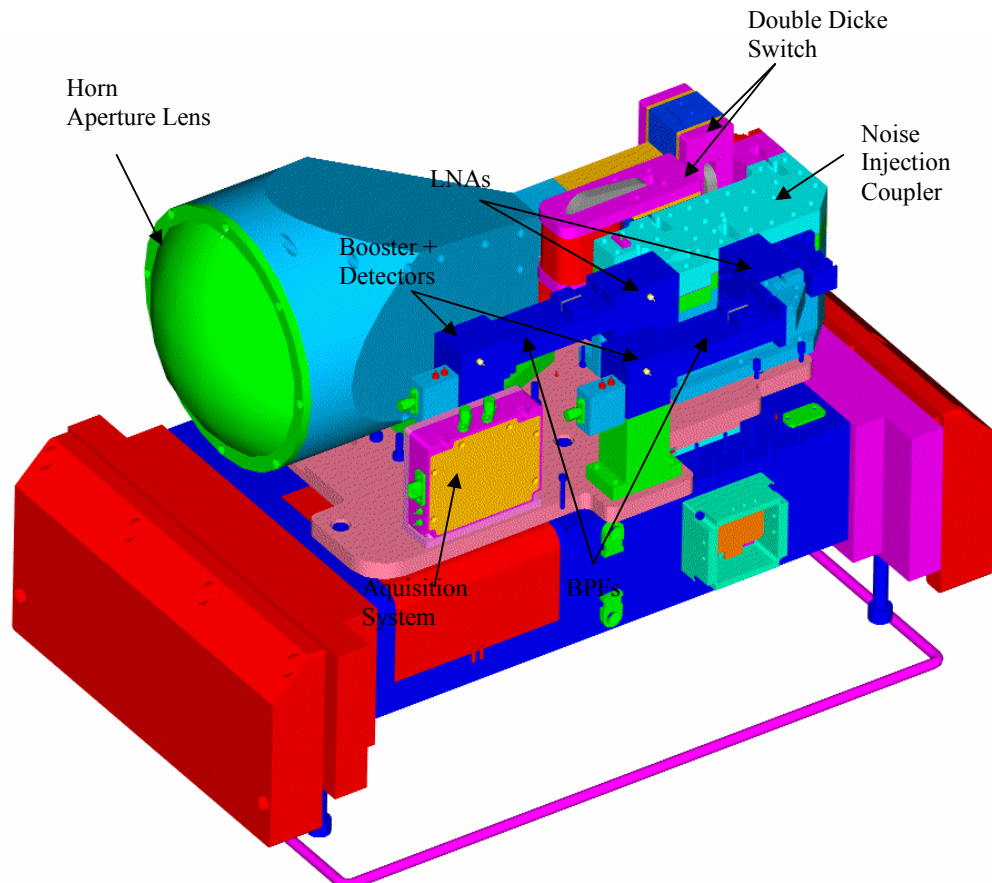
The positioner is equipped with hardware limiting switches on both axis. When it reaches one of these switches the movement is stopped and cannot be continued in the same direction. The

elevation axis limiting switches are close beyond the maximum angles of  $\pm 90^\circ$ . The radiometer hardware mounted on the positioner platform cannot be damaged accidentally due to the limiting switch protection.

## 2.2 General Radiometer Configuration

Fig.2.2 shows a schematic drawing of one of the internal receivers, illustrated as an example for the 18.7 GHz radiometer. The following functional blocks can be identified:

- Receiver optics comprising corrugated feed horn with aperture lens (encapsulated in thermal insulation)
- OMT (Ortho Mode Transducer) for splitting the signal into vertical and horizontal polarization channels.
- Calibration system comprising a double Dicke switch (system noise temperature calibration) and noise injection section (gain calibration).
- Signal processing components like isolators, LNAs, BPFs (band pass filters) and detectors.
- The instrument electronics sections
- Data acquisition system



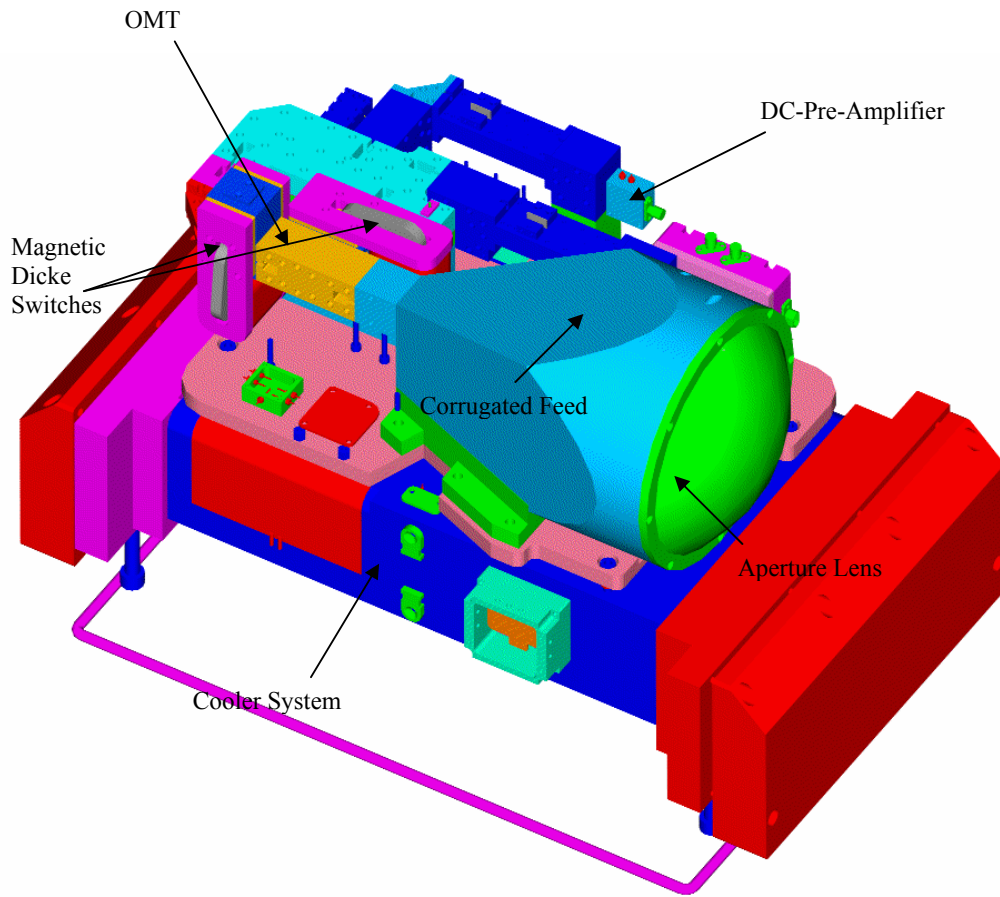


**Fig. 2.2: Radiometer configuration (18.70 GHz radiometer).**

The optical section is optimized for a beam of approximately  $5.0^\circ$  HPBW for all channels. At 6.925 GHz and 10.65 GHz the beam is formed by a combination of corrugated feed horn and off-axis parabola antenna while at 18.7 and 36.5 GHz a corrugated feed with aperture lens is sufficient to achieve the desired beam width. The corrugated feed horn offers a low cross polarization level and a rotationally symmetric beam pattern.

The receivers are integrated together with their feeds and lenses and are thermally insulated to achieve a high thermal stability.

## 2.3 Receivers

The RPG-XCH-DP (X stands for 4,6 or 8) receiver concept is motivated by the following design goals:

- The design of the receiver section focuses on maximum thermal and electrical stability, a compact layout with a minimum of connectors and thermally drifting components, an integrated RF design, low power consumption and weight.
- The receivers comprise a reliable calibration system with precision secondary standards and Dicke switches. The accuracy of calibration target temperature sensors and the minimization of thermal gradients are critical items to achieve an absolute brightness temperature accuracy of 1K.

- A high temporal resolution in the order of seconds is achieved. The minimum integration time for each channel is 1 second.

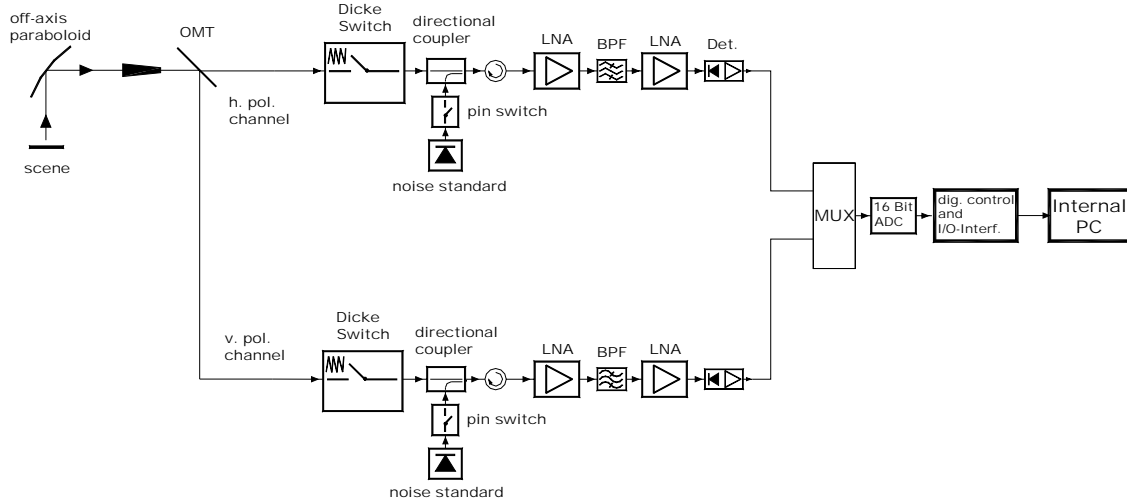


**Fig.2.3: RPG-XCH-DP schematic receiver layout. All radiometers are direct detection systems without the need for local oscillators and mixers.**

Fig.2.3 shows a schematic of the receiver system. At the receiver inputs a Dicke Switch periodically switches the receiver inputs to an internal black body with well know brightness temperature. It is used to continuously determine the system noise temperature of the radiometers. The Dicke Switch is followed by a directional coupler which allows for the injection of a precision noise signal generated by an on/off switching calibrated noise source. This noise signal is used to determine system nonlinearities (four point method, described in section ‘Calibration’) and system gain drifts during measurements.

A 40 dB low noise amplifier (LNA) boosts the input signal before it is filtered and again boosted by another 20 dB amplifier. The waveguide bandpass filters’ (BPF) bandwidths and centre frequencies are listed in table 2.1. In the host software, the different receiver modules are numbered 1-4:

$f_c$ [GHz]	<b>6.925</b>	<b>10.65</b>	<b>18.70</b>	<b>36.50</b>
Receiver #	1	2	3	4
$b$ [MHz]	400	400	400	400

**Table 2.1: RPG-XCH-DP channel centre frequencies and corresponding bandwidths.**

Each channel has its own detector diode. This allows for a parallel detection and integration of all channels. The detector outputs are amplified by an ultra low drift operational amplifier chain and multiplexed to a 16 bit AD converter for each of the four frequency modules.

The receivers are based on the direct detection technique without using mixers and local oscillators for signal down conversion. Instead the input signal is directly amplified, filtered and detected. The advantages over a heterodyne system are the following:





- No mixers and local oscillators required (cost reduction)
- Local oscillator drifts in amplitude and frequency avoided (stability improvement)
- Mixer sideband filtering not required (cost reduction)
- Reduced sensitivity to interfering external signals (mobile phones etc.) due to avoidance of frequency down conversion

A high integration level is achieved due to the use of state of the art low noise amplifier MMICs, which offer superior sensitivity performance compared to mixers.

The total power consumption of each receiver package is < 4 Watts. This includes biasing of RF- and DC- amplifiers, noise diodes, Dicke switch drives, ADCs and digital control circuits. The low consumption simplifies the thermal receiver stabilization with an accuracy of < 0.05 K over the whole operating temperature range (-30°C to +40°C).

### 3. Detailed Description of Receiver Components

#### 3.1 Antenna Performance

To meet the optical requirements of minimum reflection losses and compactness a corrugated feed horn is an optimal choice. It offers a wide bandwidth, low cross polarization level and a rotationally symmetric beam. Corrugated feed horns can be designed for a great variety of beam parameters. The horn should be as small as possible to reduce weight and costs.

In order to generate a beam with the desired divergence (6.0° HPBW) a focussing element is needed at 6.925 GHz and 10.65 GHz. An off axis parabola antenna has negligible losses.

The side-lobe levels produced by the feed horn/parabola system is below -30 dBc so that brightness temperature errors can be kept < 0.2 K in the case that the side-lobe crosses the sun.

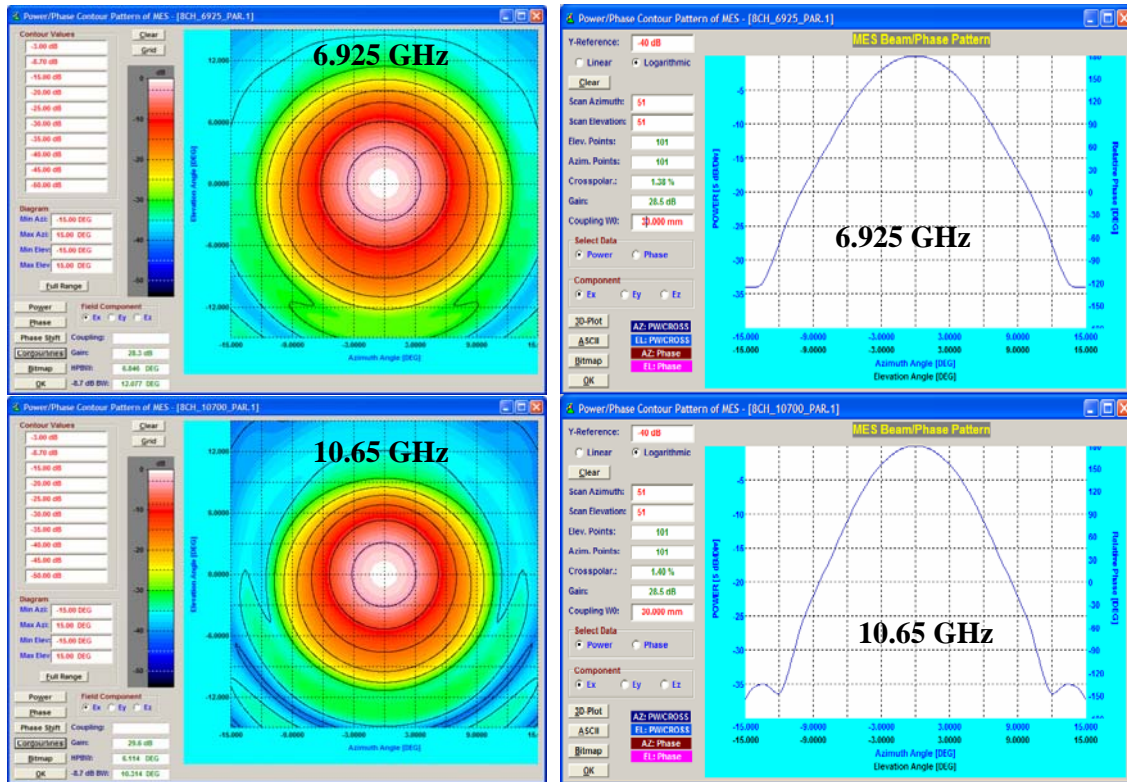
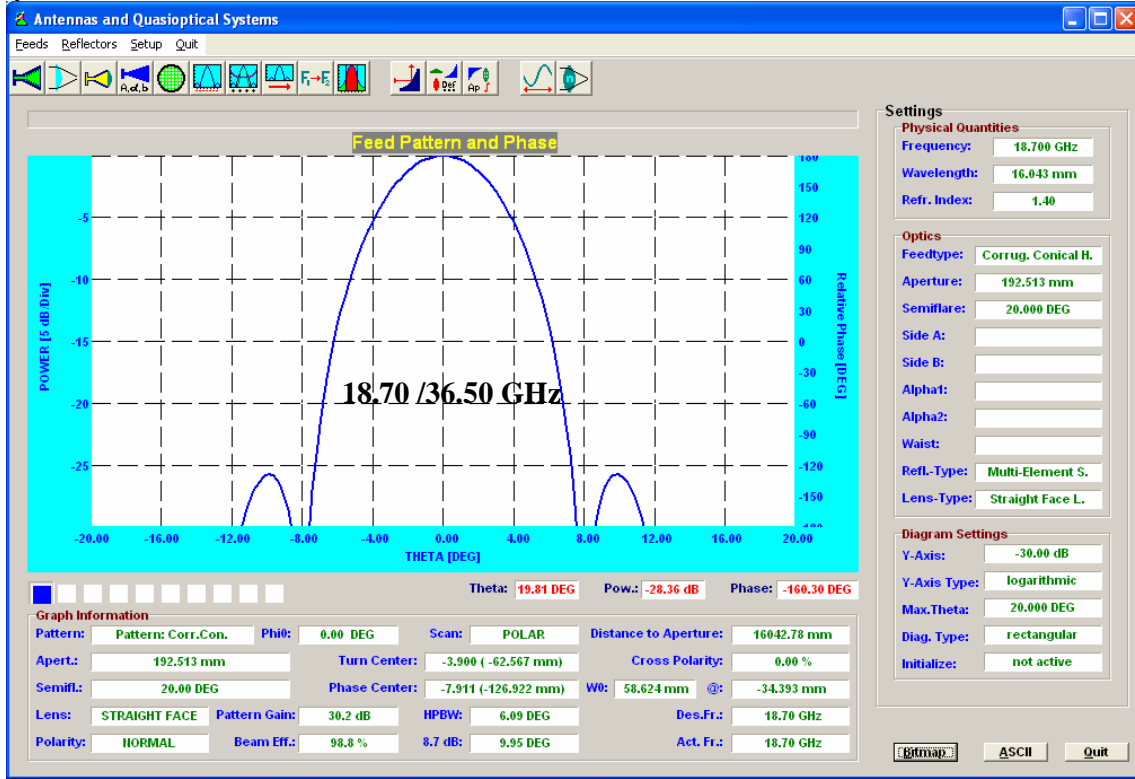


Fig.3.1: Left: 2d amplitude distributions of the parabola/corrugated feed @ 6.925 and 10.65 GHz and H-and E-plane cuts on the right. H/E plane cuts of the corrugated feed/lens system @ 18.70 and 36.5 GHz.



Frequency [GHz]	6.925	10.65	18.70	36.50
sidelobe level [dBc]	<-30	<-35	<-40	<-40
directivity [dB]	28.3	29.6	30.2	30.2
HPBW [°]	6.85	6.11	6.09	6.09
Aperture Diameter [mm]	450	330	192.0	86.0

Table 3.1: Optical antenna performance of corrugated feed / off-axis parabola systems.

### 3.2 Noise Diodes

The noise diode is one of the most critical receiver components because the system's brightness temperature critically depends on the calibration reliability. For this reason a careful circuit design and component selection is essential. The noise diode meets MIL-STD202, is hermetically sealed and has been burned in for 170 hours in order to achieve a precisely constant symmetrical white Gaussian noise level. The waveguide circuit layout including a -25 dB directional coupler guarantees the required mechanical stability needed to operate the calibration standard for several month without recalibration. The thermally stabilized diode is biased by a self adjusting current source. The directional coupler offers an isolation of >30 dB to the input signal path so that the noise injection does not significantly affect the antenna temperature. The equivalent noise temperature injected by the noise diode is in the range 150K-300K at the isolator input.



### 3.3 RF-Amplifiers

The advances in MMIC technology during recent years have led to low noise amplifiers up to 220 GHz. A key feature of this technology is the possibility of integrating the receiver into a compact planar structure without the need for bulky waveguide designs. In the frequency range between 7 and 40 GHz noise figures of 3.5 dB and bandwidth of 20 GHz are available. Each amplifier comprises a thermal compensation circuit to reduce gain drifts. The amplifier inputs are equipped with isolators to ensure a proper matching between successive stages. Assuming a 3.5 dB noise figure for the first amplifier and additional 1.0 dB for losses in the feed horn, isolator and directional coupler results in a system noise temperature of 450 K. With a scene temperature of 300 K the overall RMS noise, assuming a 400 MHz bandwidth and 1 second integration time) is 0.2 K in Dicke switch operation mode.

### 3.4 Bandpass Filters

The receiver channel bandwidths are determined by waveguide bandpass filters. The 3 pole Chebychev-type filters with 0.2 dB bandpass ripple and 1.0 dB typical transmission loss have a cutoff slope of 20 dB/200 MHz. The high Q design (2.0% rel. bandwidth) is realized by waveguide cavity resonators.

### 3.5 Detector, Video Amplifier, ADC

The zero bias highly doped GaAs Schottky detector diodes can handle frequencies up to 170 GHz with a virtually flat detection sensitivity from 7 GHz to 40 GHz. In addition, the detector diode offers superior thermal stability when compared to silicon zero bias Schottky diodes.

The rectified DC-signal enters an ultra stable OP-Amp circuit with internal analogue integrator. The utilized OP-Amps offer a thermal drift stability of 0.03  $\mu\text{V}/^\circ\text{C}$  which is roughly equivalent to a brightness temperature drift of 10 mK/ $^\circ\text{C}$  assuming a broadband detector with a sensitivity of 1 mV/ $\mu\text{W}$ . The long term stability is 0.2  $\mu\text{V}/\text{month}$ .

The 16 bit AD-converter is part of the video amplifier's circuit board to avoid noise from connecting cable pickup. It is optimized for low power dissipation (10 mW) and the high resolution makes a variable offset- and gain-control of the video amplifier superfluous.

The detector, video amplifier and ADC are integrated within a single hermetically shielded unit which is part of the receiver block (thermally stabilized to  $<0.03\text{K}$ ).

### 3.6 Additional Sensors

Apart from the microwave receivers the RPG-XCH-DP radiometers are equipped with the following additional sensors:

**Environmental Temperature Sensor:** Accuracy:  $\pm 0.5^\circ\text{C}$ , used to estimate  $T_{\text{mr}}$  (mean atmospheric temperature) needed for sky tipping calibration procedure.

**Barometric Pressure Sensor:** Accuracy:  $\pm 1$  mbar, used to estimate  $T_{\text{mr}}$  (mean atmospheric temperature) needed for sky tipping calibration procedure and for the determination of liquid nitrogen boiling temperature (absolute calibration).

All meteorological sensors are calibrated without the need for further recalibration.



### 3.7 Other Radiometer Details

In order to fulfil the requirement of low maintenance regarding absolute calibrations, the instrument is equipped with a two-stage thermal control system for all receivers with an accuracy of  $\pm 0.05$  K over the full operating temperature range. Due to this extraordinary high stability the receivers can run freely without any calibration (not even the automatic gain calibration) for 20 minutes while maintaining an absolute brightness temperature accuracy of  $\pm 0.5$  K. Each receiver is equipped with a precision noise standard (long term stability) at its signal input which replaces the external cold target in the internal absolute calibration procedure.

The system performs many automatic tasks like data interfacing with the external host, data acquisition of all housekeeping channels and detector signals, controlling of azimuth/elevation positioner, backup storage of measurement data, automatic and absolute calibration procedures etc. These tasks are handled by a build in embedded PC with 1.0 Gbyte flash memory for data storage. This PC is designed for operating temperatures from  $-30^{\circ}\text{C}$  to  $60^{\circ}\text{C}$  and is therefore ideal for remote application. The software running on this PC can easily be updated by a password protected file transfer procedure between host and embedded PC.

The host computer software operates under Windows NT4.0, Windows 2000 and Windows XP. A complete host software description is given in chapter 5.

### 3.8 Instrument Specifications

Parameter	Specification
System noise temperatures	<900 K typical for all receiver (including calibration frontend)
Radiometric resolution	0.2 RMS @ 1.0 sec integration time
Channel bandwidth	400 MHz
Absolute system stability	1.0 K
Radiometric range	0-350 K
Absolute calibration	with internal Dicke switch & external cold load, automatic sky tipping
Internal calibration	gain: with internal Dicke Switch + noise standard automatic abs. cal.: sky tipping calibration
Receiver and antenna thermal stabilization	Accuracy <0.05 K
Gain nonlinearity error correction	Automatic, four point method
Brightness calculation	based on exact Planck radiation law
Integration time	$\geq 1$ second for each channel
Data interface	RS-232, 115 kBaud
Data rate	9.5 kByte/sec., RS-232
Instrument control	Industrial PC, Pentium based
Housekeeping	all system parameters, history documentation
Optical resolution	HPBW: $6.1^{\circ}$
Sidelobe level	<-30dBc
Pointing speed	elevation: $3^{\circ}/\text{sec}$ , azimuth: $5^{\circ}/\text{sec}$
Operating temperature range	$-30^{\circ}\text{C}$ to $+45^{\circ}\text{C}$



*RPG-XCH-DP / 2-4 Frequency Dual Polarized Radiometers*

---

Power consumption	<350 Watts average, 500 Watts peak
Input voltage	100-230 V AC, 50 to 60 Hz
Weight	105 kg for receiver modules, 300 kg for positioner

## **4. Calibrations**

Calibration errors are the major source of inaccuracies in radiometric measurements. The standard calibration procedure is to terminate the radiometer inputs with two absolute calibration targets which are assumed to be ideal targets, meaning their radiometric temperatures are equal to their physical temperature. This assumption is valid with reasonable accuracy as long as proper absorber materials are chosen for the frequency bands in use and barometric pressure corrections are applied to liquid coolants in the determination of their boiling temperature.

### **4.1 Absolute Calibration**

A calibration target is considered to be an absolute standard when it is not calibrated by another standard. The RPG-XCH-DP is shipped with two calibration targets of this category.

#### **4.1.1 The Internal Dicke Switch Calibration Target**

The Dicke switch target (see Fig.2.2 and Fig.2.3) is one of the instrument's key components. The switch magnetically terminates the receiver inputs with an absorber target of well known physical temperature (ON position). This absorber serves as a termination of the same brightness temperature and is thus equivalent to a quasi-optical target (of the same temperature) when positioned in front of the receiver. The Dicke switch is located behind the feed horn and cannot calibrate changes in the feed horn BT. It is therefore essential to thermally stabilize the feed horn and lens of each receiver to keep this contribution constant. The switches are operated once per second and are used to adjust drifts in the system noise temperature. Of course it is important to measure the Dicke switch physical temperature as accurate as possible.

The main advantage of using a Dicke switch instead of a quasi-optical target for absolute calibration is that this calibration can be performed frequently (every second!) while the radiometers are pointing to the scene. The switches work in combination with the built-in noise injection system which is used to calibrate gain drifts. In contrast to the Dicke switches (these are absolute standards), noise diodes are secondary standards that have to be calibrated by a hot/cold calibration with liquid nitrogen or by a tip curve calibration on the clear sky.

#### **4.1.2 External Liquid Nitrogen Cooled Calibration Target**

Another absolute calibration standard is the liquid nitrogen cooled target (see Fig.4.1). This target is only used during absolute calibrations. The positioner's elevation axis is tilted down to  $-90^\circ$  and the target is located underneath the receiver antenna of the module which is actually calibrated. The calibration is repeated for each modul. This standard - together with the internal Dicke switch target - is used for the absolute calibration procedure. The cooled load is stored within a 40 mm thick polystyrene container. 25 litres of liquid nitrogen is needed for one filling.

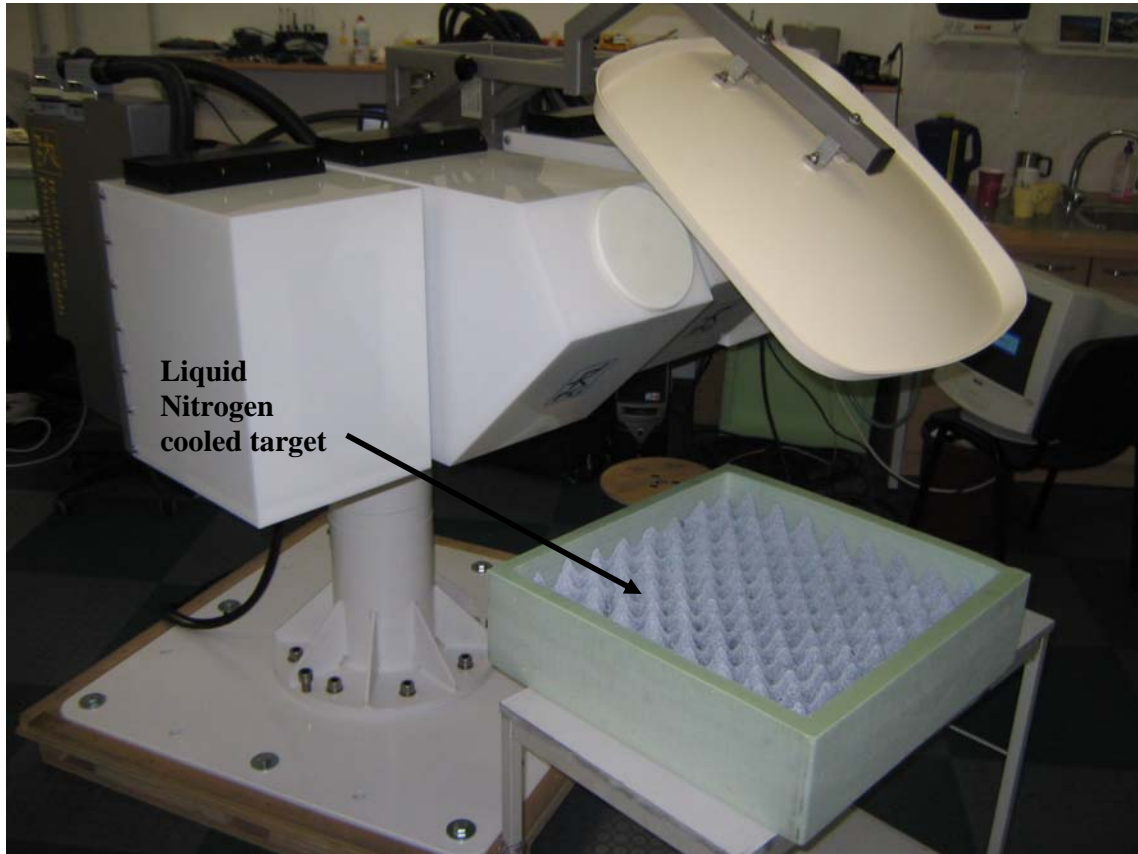


*Fig.4.1: External cold load attached to the radiometer box.*

The boiling temperature of the liquid nitrogen and thus the physical temperature of the cold load depends on the barometric pressure  $p$ . The radiometer's pressure sensor is read during absolute calibration to determine the corrected boiling temperature according to the equation:

$$T_c = T_0 - 0.00825 \cdot (1013.25 - p)$$

$T_0 = 77.25$  K is the boiling temperature at 1013.25 hPa.

The calibration error due to microwave reflections at the LN/air interface is automatically corrected by the calibration software (embedded PC). It is recommended to wrap a plastic foil around the load + radiometer (wind protection) during absolute calibration to avoid the formation of condensed water above the liquid surface (caused by wind etc.).

#### **4.1.3 General Remarks on Absolute Calibrations**

After the system has been turned on, at least 30 minutes are required for warming up and stabilization of all receiver components. To ensure accurate measurements, an absolute calibration should be performed only after completed warm-up.

The liquid nitrogen calibration was performed once at RPG to calibrate the noise standards. Usually it is not required to repeat this calibration when the radiometer regularly performs sky tipping calibrations. Sky tipping is the most accurate calibration method.

### 4.1.3.1 System Nonlinearity Correction

A common simplification in the design of calibration systems for total power receivers is the assumption of a linear radiometer response. In this case a simple two point calibration (hot/cold) is sufficient to determine the system noise equivalent temperature ( $T_{sys}$ , offset noise) and system gain ( $G$ , slope of the linear response). Accurate noise injection measurements [2], [3] have shown that the assumption of linear system response is not valid in general. Calibration errors of 1-2 K have been observed at brightness temperatures in between the two calibration target temperatures. This system nonlinear behaviour is mainly caused by detector diodes [1] needed for total power detection. Even in the well defined square law operating regime (input power  $< -30$  dBm) the detector diode is not an ideal element with perfect linearity. The noise injection calibration algorithm implemented in all RPG radiometers corrects for these nonlinearity effects.

The system nonlinearity is modelled by the following formula:

$$U = GP^\alpha, \quad 0.9 \leq \alpha < 1 \quad (1)$$

where  $U$  is the detector voltage,  $G$  is the receiver gain coefficient,  $\alpha$  is a nonlinearity factor and  $P$  is the total noise power that is related to the radiometric brightness temperature  $T_R$  through the Planck radiation law:

$$P(T_R) \cong \frac{1}{e^{\frac{h\nu}{k_B T_R}} - 1}$$

(the proportionality factor is incorporated in  $G$ ).  $T_R$  is the sum of the system noise temperature  $T_{sys}$  and the scene temperature  $T_{sc}$ .

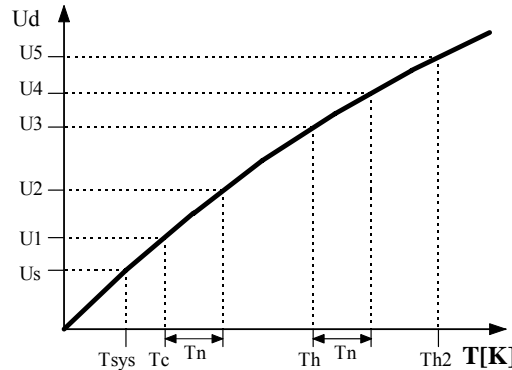


**Fig.4.7: Detector response as a function of total noise temperature.  $T_{sys}$  is the system noise temperature,  $T_n$  the additionally injected noise,  $T_c$  the total noise when the radiometer is terminated with a cold load (e.g. liquid nitrogen cooled absorber) and  $T_h$  the corresponding noise temperatures for the ambient temperature load.**

The problem is how to determine  $G$ ,  $\alpha$  and  $T_{sys}$  experimentally (three unknowns cannot be calculated from a measurement on two standards). A solution is to generate four temperature points by additional noise injection of temperature  $T_n$  which leads to four independent equations with four unknowns ( $G$ ,  $\alpha$ ,  $T_{sys}$  and  $T_n$ ) The procedure is illustrated in Fig.4.7:

During the calibration cycle the elevation mirror automatically scans the two absolute targets.



The initial calibration is performed with absolute standards and leads to the voltages  $U1$  and  $U3$ . By injection of additional noise  $U2$  and  $U4$  are measured. For example  $U2$  is given by

$$U_2 = G(P(T_{sys}) + P(T_{cold}) + P(T_n))^\alpha \quad (2)$$

where  $T_{cold}$  is the radiometric temperature of the cold target. The evaluation of the corresponding equations for  $U1$ ,  $U3$  and  $U4$  results in the determination of  $T_{sys}$ ,  $G$ ,  $\alpha$  and  $T_n$ . It is important to notice that the knowledge of the equivalent noise injection temperature  $T_n$  is not needed for the calibration algorithm. It is only assumed that  $T_n$  is constant during the measurement of  $U1$  to  $U4$ .

After finishing the procedure the radiometer is calibrated. With the four point calibration method also the noise diode equivalent temperature  $T_n$  is determined. Assuming a high radiometric stability of the noise injection temperature, following calibrations can use this secondary standard (together with the built-in ambient temperature target) to recalibrate  $T_{sys}$  and  $G$  (considering  $\alpha$  to be constant) without the need for liquid nitrogen.

## **References**

- [1] Cletus A. Hoer, Keith C. Roe, C. McKay Allred, 'Measuring and Minimizing Diode Detector Nonlinearity', IEEE Trans. on Instrumentation and Measurement, Vol. IM-25, No.4, Dec. 1976, page 324 pp.
- [2] Sandy Weinreb, 'Square Law Detector Tests', Electronics Division Internal Report No. 214, National Radio Astronomy Observatory, Charlottesville, Virginia, May 1981
- [3] Hvatum Hein, 'Detector Law' Electronics Division Internal Report No.6, National Radio Astronomy Observatory, Green Bank, West Virginia, Dec. 1962

## **4.2 Noise Injection Calibration**

It is not convenient to use a liquid nitrogen cooled load for each calibration. For this reason the radiometer has four built-in noise sources (one for each receiver) that can be switched to the receiver inputs. The equivalent noise temperature  $T_n$  of the noise diode is determined by the radiometer after a calibration with two absolute standards (hot/cold or sky tipping) and is in the range 250 K to 1000 K. The noise diode is also used to correct for detector diode nonlinearity errors. The accuracy of a calibration carried out with this secondary standard and the Dicke Switches is comparable to the results obtained with a liquid nitrogen cooled load. The advantage of the secondary standard is obvious: A calibration can be automatically done at any time. All system parameters are recalibrated including system noise temperatures.

The noise diode is optimized for precision built-in test equipment (BITE) applications and meets MIL-STD202 standard with 170 hours burn-in. This process guarantees highest reliability and performance repeatability. The repeatability error is expected to be  $<0.1$  K / month.

Due to the fact that only two calibration points are generated with this calibration type ( $T_a$ = Dicke Switch temperature,  $T_{a+n}$  = Dicke Switch temperature + noise standard), it has to be assumed that the non-linearity factor  $\alpha$  does not change with time. This is a reasonable assumption because  $\alpha$  is basically an intrinsic detector diode parameter.

### 4.3 Sky Tipping (Tip Curve)

Sky tipping (often referred to as tip curve calibration) is a calibration procedure suitable for those frequencies where the earth’s atmosphere opacity is low (i.e. high transparency) which means that the observed sky brightness temperature is influenced by the cosmic background radiation temperature of 2.7 K. All RPG-8CH-DP channels are candidates for this calibration mode.

Sky tipping assumes a homogeneous, stratified atmosphere without clouds or variations in the water vapour distribution. If these requirements are fulfilled the following method is applicable:

The radiometer scans the atmosphere from zenith to around 20° in elevation and records the corresponding detector readings for each frequency. The path length for a given elevation angle  $\alpha$  is  $1/\sin(\alpha)$  times the zenith path length (often referred to as “air mass”), thus the corresponding optical thickness should also be multiplied by this factor (if the atmosphere is stratified!).

The optical thickness is related to the brightness temperature by the equation:

$$\tau(\infty) = -\ln\left(\frac{T_{mr} - T_i}{T_{mr} - T_{B0}}\right) \sec(\theta)$$

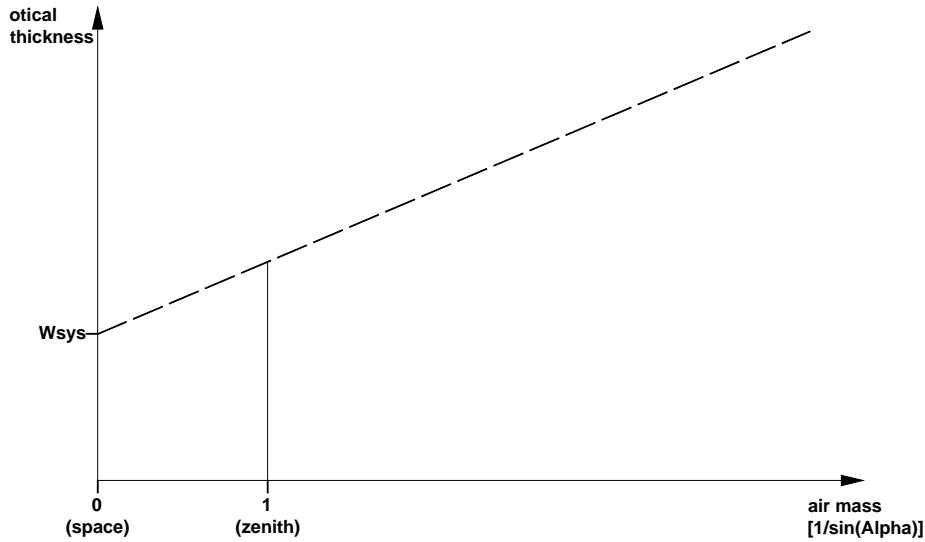


**Fig.4.9: Extrapolation of tipping response to 2.7 K free space temperature.**

$T_{mr}$  is a mean atmospheric temperature in the direction  $\theta$ ,  $T_{B0}$  is the 2.7 K background radiation temperature and  $T_i$  is the brightness temperature of frequency channel  $i$ .  $T_{mr}$  is defined as:

$$T_{mr} = \frac{\int_0^{\infty} T(z) e^{-\tau(z)} \sigma_a dz}{1 - e^{-\tau(\infty)}}$$



$T_{mr}$  is a function of frequency and is usually derived from radiosonde data. A sufficiently accurate method is to relate  $T_{mr}$  with a quadratic equation of the surface temperature measured directly by the radiometer.

The optical thickness as a function of air mass is a straight line (see Fig.4.9) which can be extrapolated to zero air mass. The detector reading  $U_{sys}$  at this point corresponds to a radiometric temperature which equals to the system noise temperature plus 2.7 K:  $U_{sys} = G*(T_{sys} + 2.7 \text{ K})$ . The proportionality factor (gain factor)  $G$  can be calculated when a second detector voltage is measured with the radiometer pointing to the ambient target with known radiometric temperature  $T_a$ . The sky tipping calibrates the system noise temperature and the gain factor for each frequency without using a liquid nitrogen cooled target.

The disadvantage of this method is that the assumption of a stratified atmosphere is often questionable even under clear sky conditions due to invisible inhomogeneous water vapour distributions (e.g. often observed close to coast lines). The built-in sky tipping algorithm investigates certain user selectable quality criteria to detect those atmospheric conditions that do not fulfil the calibration requirements. The most important criteria are:


- Linear correlation factor. This measures the correlation of the optical thickness samples (as a function of air mass) with a straight line. Typical linear correlation factor thresholds are  $>0.9995$ . The linear correlation factor is not sensitive for the noise of the optical thickness samples caused by clouds etc.
- $\chi^2$ -test. This measures the variance of the optical thickness samples relative to the straight line in Fig.4.9. Typical threshold values are  $<0.8$  for a good quality calibration.

The tip curve calibration is considered to be the most accurate absolute calibration method. The brightness temperatures acquired in the elevation scan are close to the scene temperatures measured during zenith observations.



## 5. Software Description

The following conventions are used in this software description:

- Messages generated by the program that have to be acknowledged are printed in red. Example: *The specified port in 'R2CH.CFG' has no data cable connected to it!*
- Button labels are printed in green: *Cancel*
- Messages that have to be answered by *Yes* or *No* are printed in light blue: *Overwrite the existing file?*
- Labels produced by the software are printed in grey: *UTC*
- Names of group boxes are printed in blue. Example: *Radiometer Status* on the main screen.
- Names of tabs are printed in violet: *Sky Tipping*
- Names of menus are printed in black: *File Transfer*
- When a speed button shall be pressed this is indicated by its symbol: 
- Hints to speed buttons are printed in brown: *Define Serial Interface*
- Selections from list boxes are printed in magenta: *Celsius*
- Selections from radio buttons are printed in dark green: *COM1*
- File names are printed in orange: *MyFileName*
- Directory names are printed in dark blue: *C:\Programs\RPG-HATPRO\*

### 5.1 Installation of Host Software


#### 5.1.1 Hardware Requirements for Host PC

The hardware requirements for running the host software are:

- Pentium based PC, 500 MHz clock rate minimum
- 200 MB free RAM for software execution
- Serial interface (RS-232), 9 pin Sub-D connector

An industrial PC is included in the standard delivery package and pre-installed software comes with it. However the host software R2CH.EXE can be installed and run on any other computer that fulfils the hardware requirements listed above.

#### 5.1.2 Directory Tree

By clicking on the desktop icon  the executable host program *R2CH.EXE* is invoked (runs on Windows NT4.0, Windows 2000, Windows XP). On pre-installed PCs this file is located in *C:\RPG-8CH-DP\*. This directory path can be changed to any other path (in the following referred to as *MY\_DIRECTORY\RPG-8CH-DP\*). Of course the corresponding desktop link has to be modified accordingly.

In the case that the user wants (or has) to install the software himself the following steps should be performed:

- Start your Windows operating system
- Start the Windows Explorer
- Insert the Radiometer CD-ROM
- In Windows Explorer click on the CD-ROM drive icon



- Click on the **RPG-XCH-DP**-folder and drag the whole folder to **MY\_DIRECTORY** (user selectable). X stands for 4,6 or 8, depending on the number of installed receiver modules.

Example: If '**MY\_DIRECTORY**' is the directory **D:\Programs** the complete tree should look like this:

```
D:
|---Programs
|   |---RPG-4CH-DP
|   |   |---DATA
|   |   |---MBFs
|   |   |---MDFs
```

The **RPG-4CH-DP** -directory contains the following files:

- **VCL50.BPL** : System library extension file
- **VCLX50.BPL** : System library extension file
- **BORLNDMM.DLL** : Dynamic link library, Memory Management functions
- **CC3250MT.DLL** : Dynamic link library, Core functions
- **INPOUT32.DLL** : Dynamic link library needed for serial communication
- **R2CH.EXE** : Radiometer software
- **R8CH.CFG** : Radiometer software configuration file
- **BAD05.POS** : Positioner controller model file
- **BAUDRATE.POS** : Positioner controller baudrate file
- **RAD.ID** : Radiometer Identification file

The **MBFs** and **MDFs** directories are empty after installation and are intended for the Measurement Batch Files and Measurement Definition Files needed to initiate a measurement. **DATA** is reserved for measurement data files including user defined sub-directories. Of course the user can create any other directory for his data file storage.

Click into **MY\_DIRECTORY\RPG-4CH-DP** and locate **R2CH.EXE**. When clicking on this file with the right mouse button a list of actions is displayed. Select the 'Desktop (Create Shortcut)' option to generate an icon on the desktop.

## 5.2 Getting Started



When clicking on the desktop icon **RPG** to start the host software (**R2CH.EXE**) the program first tries to locate a data cable connected to any of the RS-232 host serial interfaces. If it does not find a data cable the message **The specified port in 'R8CH.CFG' has no data cable connected to it!** is generated. This message is referring to the file **R8CH.CFG** (located in **MY\_DIRECTORY\RPG-4CH-DP**) which is a configuration file that is loaded by **R2CH.EXE** at program start. This file contains information (among other data) about the standard serial interface port used for the communication link to the radiometer.

For certain reasons it is desirable to operate the software even without a data link to the radiometer. For instance, the user may wish to inspect recorded data files, calibration history or prepare **MDFs** (Measurement Definition Files) for the next measurements etc. These tasks do not require a radiometer communication link. In this case the message **The specified port**



in 'R8CH.CFG' has no data cable connected to it! can be ignored. All commands requiring a radiometer connection are then disabled.

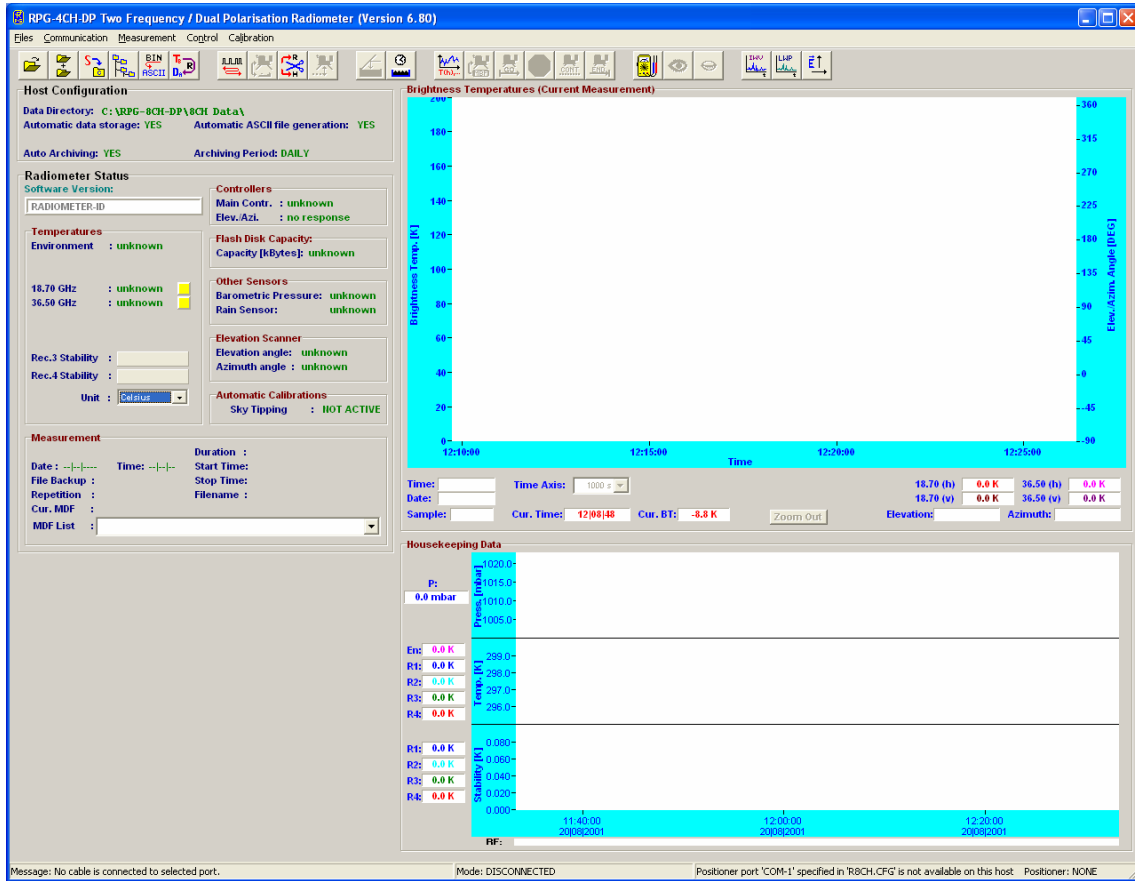



Fig.5.1: Starting host software with a data cable connected to one of the RS-232 interfaces.

If a data cable is installed between the host and the radiometer (see section 1.2), the user can define the serial interface parameters for the communication (only required the first time when the host PC is installed). This is done by clicking  (*Define Serial Communication Ports*). The command opens the menu in Fig.5.2.

The selectable COM-ports are enabled in the upper short cut button list. The user can select only one of the possible ports for interconnection with the radiometer and another one for the communication with the positioner controller.

The baud rate parameter defines the communication speed. For cable lengths up to 40 m the highest baud rate should be used (*115200*). This is particularly important when files that have been backed up on the radiometer Flash Memory need to be transferred to the host. Some of these data files might be several MBytes in size so that an optimally fast transfer rate is desirable. At *115200* baud the transfer speed is about 9 kByte/sec.

The positioner controller is only operated with 9600 Baud. We recommend to use COM1 for the connection to this controller and COM3 or COM4 for the connection to the radiometer.

If *Auto Connect* is checked, the host software automatically tries to connect to the radiometer (if a data cable is detected) when it is started. This feature enables an auto-start up function after a power failure of the host PC. The radiometer embedded PC will automatically continue a measurement when the power returns after a power failure. To start the host software automatically after reboot of the operating system, the *R2CH.EXE* should be copied into the



Auto Start directory of the operating system or an appropriate task should be defined in the operating system scheduler.

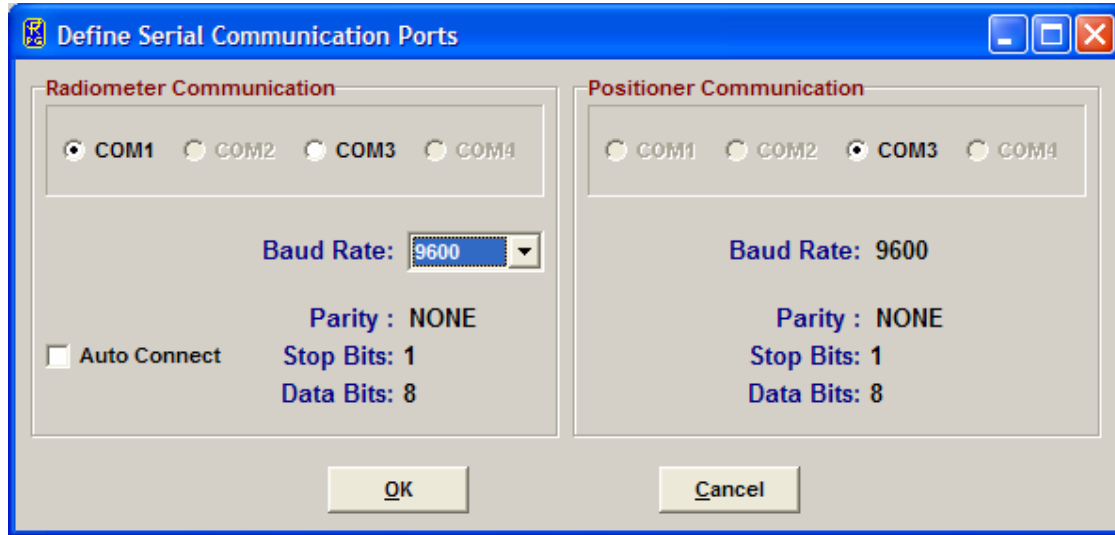




Fig.5.2: Definition of radiometer and positioner controller interface parameters.

The interface parameters are stored in the configuration file (*R2CH.CFG*) that is loaded each time *R2CH.EXE* is started. This file is backed up on exiting *R2CH.EXE*. A definition of the serial interface parameters is only necessary at the first start of *R2CH.EXE* or when the transfer speed must be reduced due to longer cable length.

The sequence for setting up a communication link to the radiometer is the following:

- Install the interface cable between host and radiometer as described in section 1.2 (the radiometer power has to be turned off).
- Turn on the system power, see section 1.3.
- Wait for 2 minutes until the radiometer PC has booted up.
- Start the host software (if not already done) and define the serial interface parameters as described above (if necessary).
- The next step is to initiate the communication between the host and radiometer PC by pressing  (*Connect to Radiometer*). *R2CH.EXE* then establishes the same baud rate on the radiometer embedded PC as was selected in *Define Serial Communication Port*. This operation takes a couple of seconds. If successful, the message *Connection to radiometer successfully established. Baud Rate adjusted.* is displayed. Otherwise the message *Radiometer does not respond! Connection could not be established...* appears. In this case try the following to handle the problem:
  - Repeat the  command.
  - If not successful, check the data cable (is it properly connected to host and radiometer?).
  - Check that the radiometer power is turned on.
  - Repeat the turn on procedure.
  - If not successful, contact RPG.

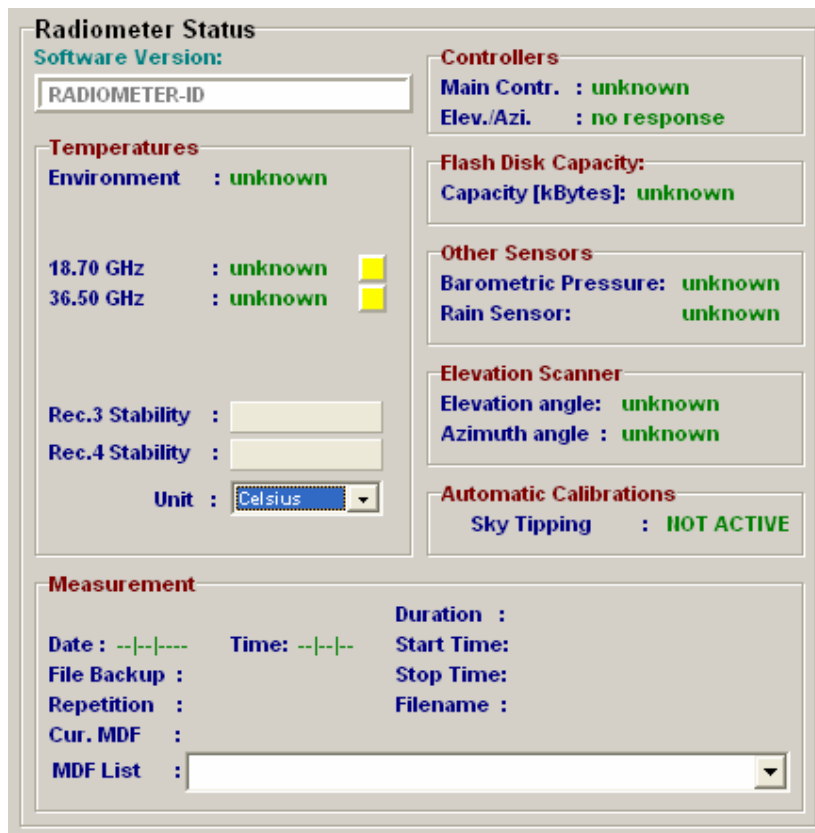
The connection status is displayed in the status bar (bottom line of the main screen) and includes the COM port number and baud rate. The radiometer responds to the host by sending



the status report (listed in **Radiometer Status** on the host main screen) comprising its ID, the status of the various controllers, the system’s housekeeping data (temperatures, surface sensor readings, inclination in elevation axis and azimuth position) and Flash Memory capacity (disk on module, the embedded PC’s hard disk. When a measurement is started, additional information is displayed here like the calibration status, reference time and date, the duration of the actual measurement, its start and end time, the measurement filename, whether file backup is enabled on the embedded PC or not and the repetition number of the running batch (explained later). The radiometer status display can be disabled (🚫) or enabled (👁️) at any time. In general the display should be enabled because certain automatic tasks (like logging of all calibration activities) are only performed when the status display is enabled.

### 5.3 Radiometer Status Information


The various status displays in the **Radiometer Status** group box are:



- Software Version: Indicates the version number of the radiometer PC software **8CH.EXE** for reference (the host software version is printed in the main window caption).
- Instrument ID: The radiometer identifies itself by sending the instrument ID to the host when a connection is established (e.g. **RPG-8CH-DP**, **RPG-6CH-DP**, **RPG-4CH-DP**).
- **Controllers**: Lists the status of the two instrument controllers:
  - The main controller handles all communication activities between the radiometer PC and the radiometer hardware.





- The elevation / azimuth controller generates the driving signals for the positioner.
- **Flash Memory Capacity:** The radiometer PC is equipped with a flash memory hard disk (no movable parts) called DOM. Its capacity – when empty - is 1.0 Gbytes. The status indicates, how much memory (measured in kBytes) is left for the backup of measurement files. If the remaining free memory is less than 20 Mbytes the backup files should be flushed (see section 5.4). When 10 Mbytes are reached no further file backup is performed.
- **Temperatures:** Five temperature sensors are implemented:
  - The environmental temperature sensor is located outside of the radiometer box below the positioner mounting plate. The sensor data is an important parameter for the absolute calibration hot target temperature measurement and is also used to derive  $T_{mr}$  (needed for tip curve calibrations, see section 4.4).
  - Receiver1 / Receiver 2 / Receiver 3 / Receiver 4: These temperature sensors reflect the physical temperatures of the receiver modules which are stabilized to an accuracy of  $< 0.05$  K. Typical sensor readings are around  $40^{\circ}\text{C}$ . The thermal receiver stabilisation is continuously monitored. If the receiver temperature is kept constant to within  $\pm 0.03$  K the status indicator on the right of the temperature display is green. If it turns to red the stability is worse than this threshold. In addition the actual stabilisation values are listed. The colour of the stability status indicator turns to yellow if not enough temperature samples have been acquired to determine the stability.
- **Other Sensors:**
  - Barometric Pressure: The pressure sensor measures the barometric pressure in mbar (accuracy  $\pm 1.0$  mbar). The data is used in the determination of the precise boiling temperature of the liquid nitrogen coolant used in the external calibration target during absolute calibration.
- **Automatic Calibrations:** Here the status of automatic calibrations (sky tipping, see section 4) is monitored during measurements. All calibration data is automatically logged in the **CALLOG** file located in `MY_DIRECTORY\RPG-4CH-DP\`. The contents of that file can be inspected with the  command (described later).
- **Elevation Scanner:** The data displayed here is the current position of the elevation and azimuth scanner.
- **Measurement:** During measurements this group box displays details like the file name of the current measurement, when the measurement was started and when it will end, if file backup is enabled on the radiometer PC and the batch repetition factor.

## 5.4 Data Storage Host Configuration

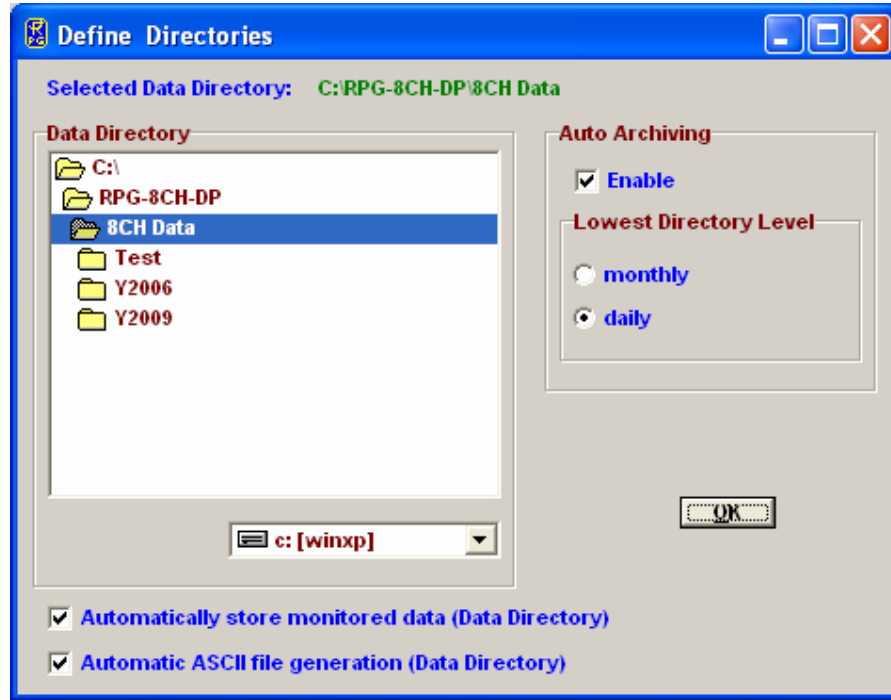
There are two different ways of data storage during measurements:

- Data files are stored on the radiometer PC by enabling the file backup option in the measurement definition file (MDF, explained later). The data transferred to the host for online display are not stored by the host PC. If the data files need to be inspected or further processed then they have to be transferred from the radiometer to the host PC. This procedure can be quite time consuming due to the relatively low transfer speed via the RS-232 connection (9 kBytes / sec. max.). The only advantage of this storage mode is that once the measurement has started, the host can be disconnected from the radiometer (it is then replaced by a Host Replacer Termination) while the




radiometer continues its operation. No positioner activity is possible while the host PC software is out of use because the positioner is controlled directly by the host PC.

- File backup on the radiometer PC is enabled or disabled and the data transferred to the host PC is stored by the host in a predefined data directory. This is the most common operation mode for long term measurements because data files are transferred online from the radiometer to the host. Of course the host computer has to be permanently connected to the radiometer PC. When the host is connected to a network it can regularly send the data files to an FTP server located far away from the measurement site. The file backup on the radiometer is only used as a safety option in the case that the host PC has a power failure or hard disk problem.



*Define Directories Menu including data file directory and quicklook file directory selection.*

The *Host Configuration* group box on the main screen displays the data storage details. It is possible to change the settings by clicking  (*Define Directories*). The automatic host data storage during measurements can be enabled or disabled and the data storage directory is selected from the directory tree shown in *Data Directory*. In the same menu one can specify if an ASCII version of the data files (which are in binary format by default) shall be generated. ASCII files will then (if this option is selected) be stored to the same data directory as the binary files.

Data archiving is a useful feature to prevent the data directory to be filled with ten thousands of files which may overload the operating system. MS operating systems cannot handle many (in the order of ten thousands) files in a single directory. If *Enable* is checked, the software automatically creates sub-directories in the data directory and stores the data files according to the year, month and day they are generated. E.g. a file *08111623.LIW* would be stored in a directory *...\RPG-4CH-DP\Data\Y2008\M11\D16\* if *daily* is checked or in *...\RPG-4CH-DP\Data\Y2008\M11\* if *monthly* is checked.

## 5.5 Exchanging Data Files

The radiometer PC's hard disk has two directories which are accessible from the host computer:

- Data Files Directory
- System Files Directory

The data files directory is used to store all backup measurement files with unlimited access for READ and WRITE. The system files directory contains files that are essential for the radiometer operation. That is why the access for this directory is READ ONLY. Its files should not be manipulated or deleted by the user. If one tries to write to this directory the host prompts for a password to be entered. Only the radiometer administrator should know this password for software updating (overwriting **8CH.EXE**). **Overwriting 8CH.EXE with a non-operating software or deleting this executable file will disable all radiometer functions and requires a system re-initialisation by RPG!**

To get access to the radiometer directories click (Exchange Data and System Files with the Radiometer). The menu in Fig.5.2 will be displayed.

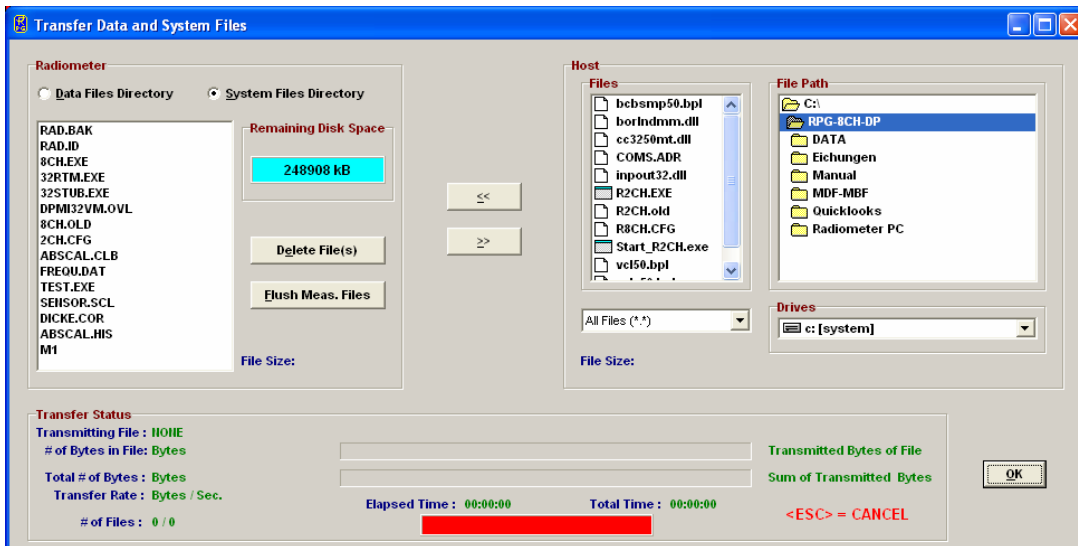


Fig.5.2: File transfer menu.

File transfer is necessary when backup data files need to be copied from the radiometer hard disk to the host computer. If file backup is enabled for a measurement, the instrument stores all data files in its **Data Files Directory**.

The **System Files Directory** contains the following files:

- **32RTM.EXE** runtime library
- **32STUB.EXE** stub file loaded by **8CH.EXE** to enter protected mode
- **DPMI32VM.OVL** overlay file for DOS protected mode interface
- **8CH.EXE** radiometer software
- **FREQU.DAT** contains frequency list of radiometer
- **RAD.ID** contains radiometer ID (RPG-8CH-DP, etc.)
- **SENSOR.SCL** sensor calibration file



- **ABSCAL.CLB** absolute calibration parameters
- **ABSCAL.HIS** absolute calibration history file

**8CH.EXE** is the executable that boots up when the radiometer is turned on. The program handles all automatic tasks like detector readout, calibrations, scanning, file storage etc. The only reason for writing to the system file directory is the installation of a **8CH.EXE** software update. Write operations to the system files directory are password protected and are reserved for authorized personnel only (contact RPG for password information).

Reading from the system files directory is required when the absolute calibration history file shall be inspected. The file **ABSCAL.HIS** stores all absolute calibrations (including successful tip curve calibrations). Once copied to any directory on the host hard disk its

contents can be browsed by the  command (see section 5.6).

Toggling between data files directory and system files directory display is achieved by pressing the **Data Files Directory** or **System Files Directory** radio buttons in the **Radiometer** group box.

By double clicking on one of the files in the list, the file size in bytes is displayed. In order to delete the backup files from the data files directory press **Flush Meas. Files**. This will delete all backup files from the radiometer. It is not possible to delete single backup files because they are packed together in bigger files to reduce the total number of files on the flash drive. DOMs have problems in handling large numbers of files. During a 18 month continuous operation up to 20.000 data files are generated by the RPG-8CH-DP radiometer which would overload the DOM file system capabilities if they were stored as single files. Packing these files is the only way to handle the problem. Before flushing the backup files they should all be copied to the host first (if the data was not monitored on the host PC with automatic data storage). By pressing **Delete Files** only single files are removed from the system files directory (password entry required).


When a file needs to be copied from the host to the radiometer, first browse through the host directory tree and mark the file in the file list. Then select **Data Files Directory** or **System Files Directory** and press <<. The copy progress is displayed in the **Transfer Status** group box. Copying in the other direction (from radiometer to host) is done with the >> command.

Multiple files may be selected for deleting and file transfer in both directions. If a file transfer in progress is aborted, the user may terminate the operation by pressing <ESC>.

## 5.6 Inspecting Absolute Calibration History

As mentioned in section 5.4 the **ABSCAL.HIS** file, located in the system file directory on the radiometer PC, stores all absolute calibration results. This also includes the successful tip curve calibration of the K-band channels. In order to inspect this calibration history, first copy

**ABSCAL.HIS** from the radiometer to the host. Then press  (**Open Data Files**) and select

 to invoke the **Absolute Calibration History** menu. Load the previously copied **ABSCAL.HIS** file with **Load History File** and the list of calibrations is displayed (see Fig.5.3).

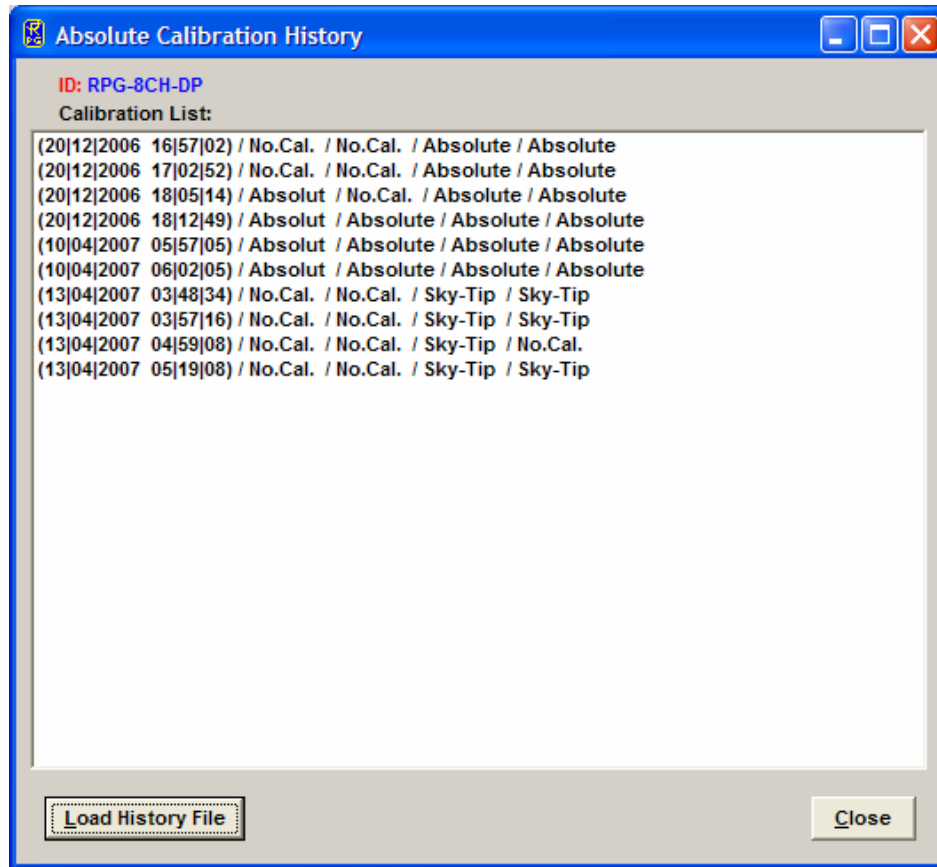


Fig.5.3: Loading the calibration log file *ABSCAL.HIS* into the calibration history list.

The list entries show the date and time of the calibration and the type of calibration for each receiver module in the sequence 6.925 GHz / 10.75 GHz / 18.70 (21.0) GHz / 36.50 GHz. Double clicking on one of the entries opens the *Calibration Results* menu in Fig.5.4. For each receiver channel the three parameters  $G$ ,  $T_{\text{sys}}$  and  $T_n$  (see section 4.1.3) are listed. In addition the calibration type, calibration time and physical temperature of calibration targets are stated.

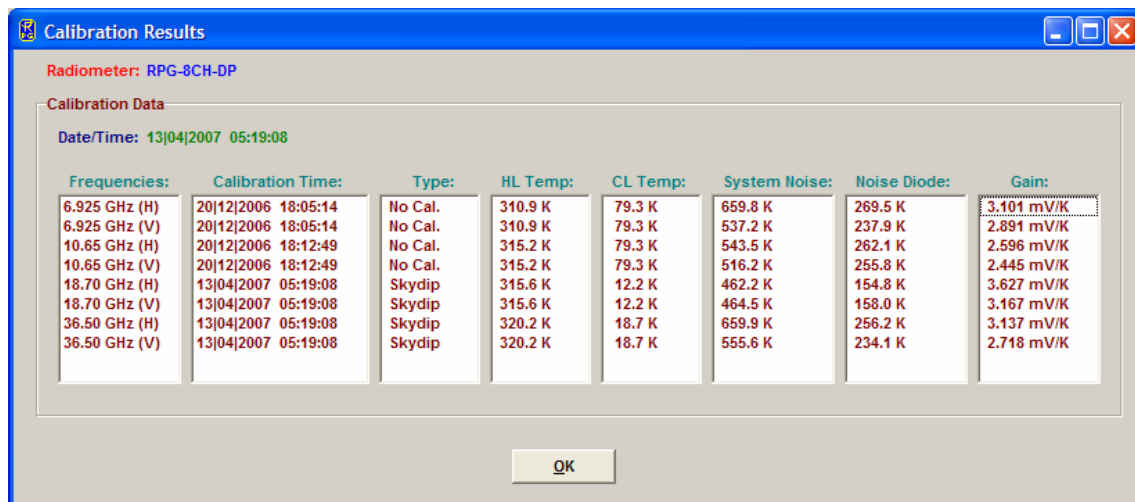


Fig.5.4: Display of absolute calibration parameters.

## 5.7 Inspecting Automatic Calibration Results

Automatic calibrations are those described in section 4.3 (Tip Curve). These calibrations are performed automatically by the radiometer following the calibration settings in the measurement definition file (see section 5.9.1). Monitoring of automatic calibrations is carried out by the (enabled) *Radiometer Status* window on the main screen. The corresponding log file is *CAL.LOG* located in *MY\_DIRECTORY\RPG-8CH-DP\*.

For inspecting this log file press (*Display Automatic Calibration History*). The menu in Fig.5.5 appears. In the *Sky Tipping Calibrations* gain parameters,  $T_{sys}$  (*Tsys*) and  $T_n$  (*Tnoise*) are selectable. The user may zoom into the data by clicking on the graphics display (holding the left mouse button pressed) and dragging the mouse cursor to a second position. When the mouse button is released the new data window appears. *Zoom Out* reverts to the previous zoom. The precise moment of each calibration is indicated by a dot (• and toggle this feature).

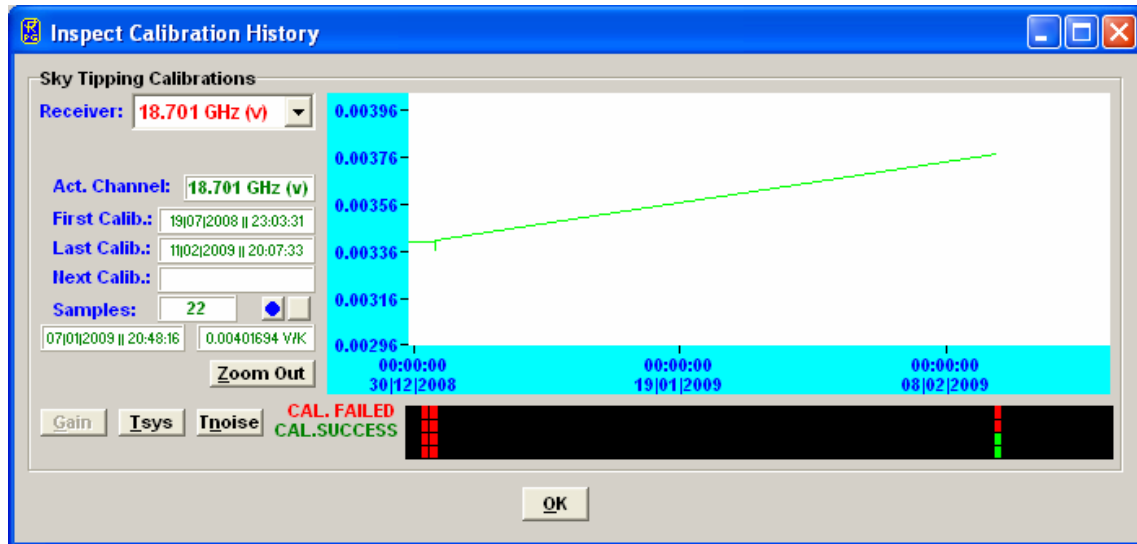


Fig.5.5: Display of automatic calibration parameters.

Below the *Sky Tipping Calibrations* data display the successful calibrations are marked by a green bar while failed calibrations are marked in red. By clicking on one of these bars the tip curve calibration details are listed and a graphical display of the sky dip is shown.

## 5.8 Absolute Calibration

After setting up the external cold target as described in chapter 4.1.2, an absolute calibration is initiated by pressing (*Perform Absolute Calibration*). The menu in Fig.5.6 is shown.

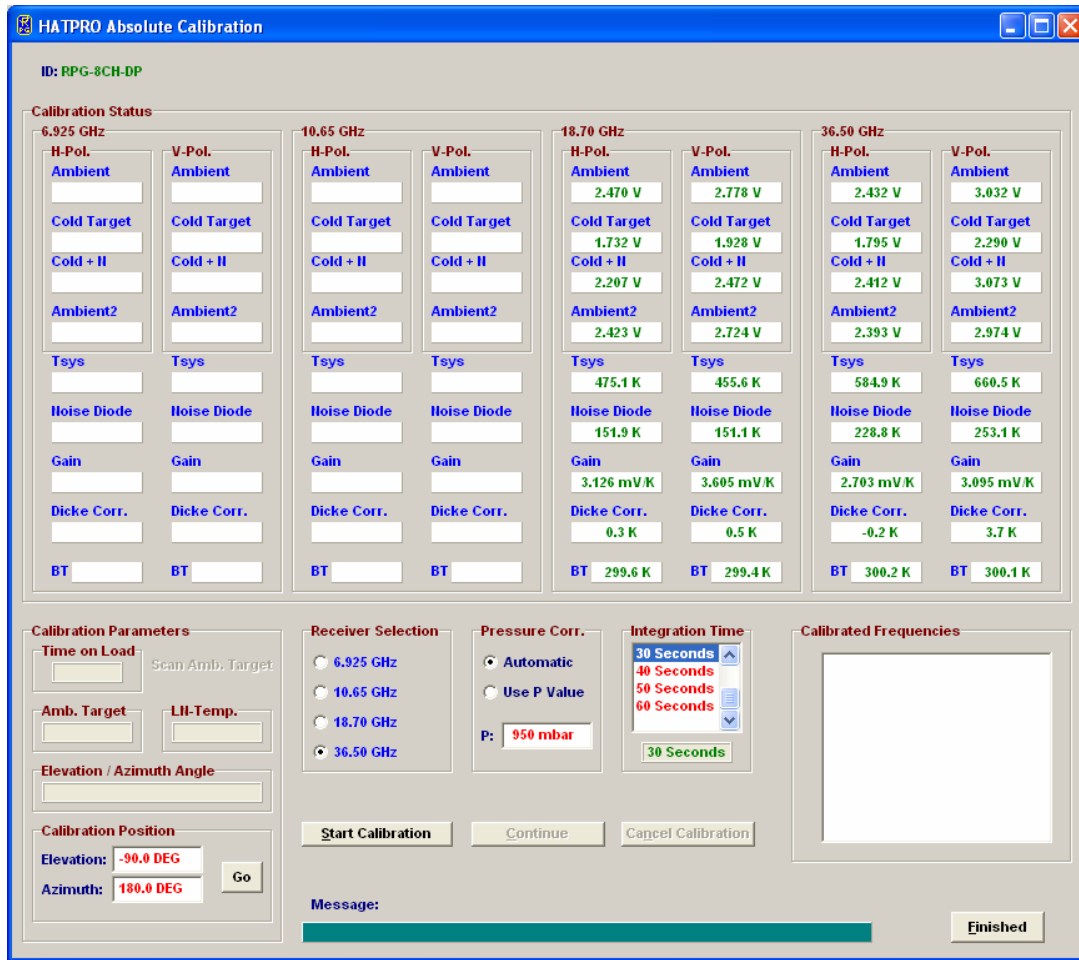


Fig.5.6: Absolute calibration menu.

The integration time  $T_i$  is selectable between **5 Seconds** and **60 Seconds** (*Integration Time* group box) and defines the integration time period for each calibrated channel.

The four receivers are calibrated independently because the cold target has to be pushed underneath the antenna of each receiver package. The receiver to be calibrated is specified in the *Receiver Selection* group box.

**Start Calibration** starts the absolute calibration procedure. During calibration the current activity is displayed in the message line. When the integration cycles have completed, the message **Calibration successful! Save?** is displayed and the user has to confirm to save the calibration with **Continue**. The absolute calibration parameters are then stored on the radiometer PC. Leave the calibration menu by clicking **Finished**.

If the error message **No response to cold load. Calibration terminated!** appears, the cold target was probably not filled with liquid nitrogen or was not installed at all.

**No noise diode response. Calibration terminated!** indicates a malfunction of one of the noise sources. Contact RPG for help in this case.

## 5.9 Defining Measurements

Before a measurement can be started, it has to be defined. The various measurement parameters are then stored in a MDF (Measurement Definition File, extension **.MDF**). The radiometer is capable of processing multiple MDFs automatically which are combined in a



MBF (Measurement Batch File, extension **.MBF**). The MBF is a batch file similar to DOS batch files but only intended to group MDFs. Only MBFs can be sent to the radiometer, not MDFs, even if just a single MDF shall be sent. It has to be encapsulated in a MBF file first!

To enter the **Definition of Measurement and Calibration Parameters** menu press  (Define Measurement Parameter Files (MDF and MBF)).

The measurement definition menu has several tab sheets (*Sky Tipping*, *Standard Calibrations*, *Products + Integration*, *Elevation Scanning*, *Timing + ...*, *MDF + MBF Storage*) which should be processed from left to right (see Fig.5.7).

### 5.9.1 Sky Tipping

The sky tipping (or tip curve) calibration is described in detail in section 4.4. Fig.5.7 shows the corresponding definition tab sheet.

The scanning angles listed in the *Elev. Scan Angles [DEG]* group box are predefined to give equidistant air mass samples in the sky tipping scan (the air mass is proportional to  $1 / \sin(\alpha)$ , see section 4.4). They can be modified by *Add* and *Delete* but it is recommended to only define angles  $>20^\circ$ . If the radiometer's horizontal view is blocked by obstacles the lowest elevation angle should be adjusted appropriately but should not be  $>30^\circ$  to maintain the calibration accuracy.

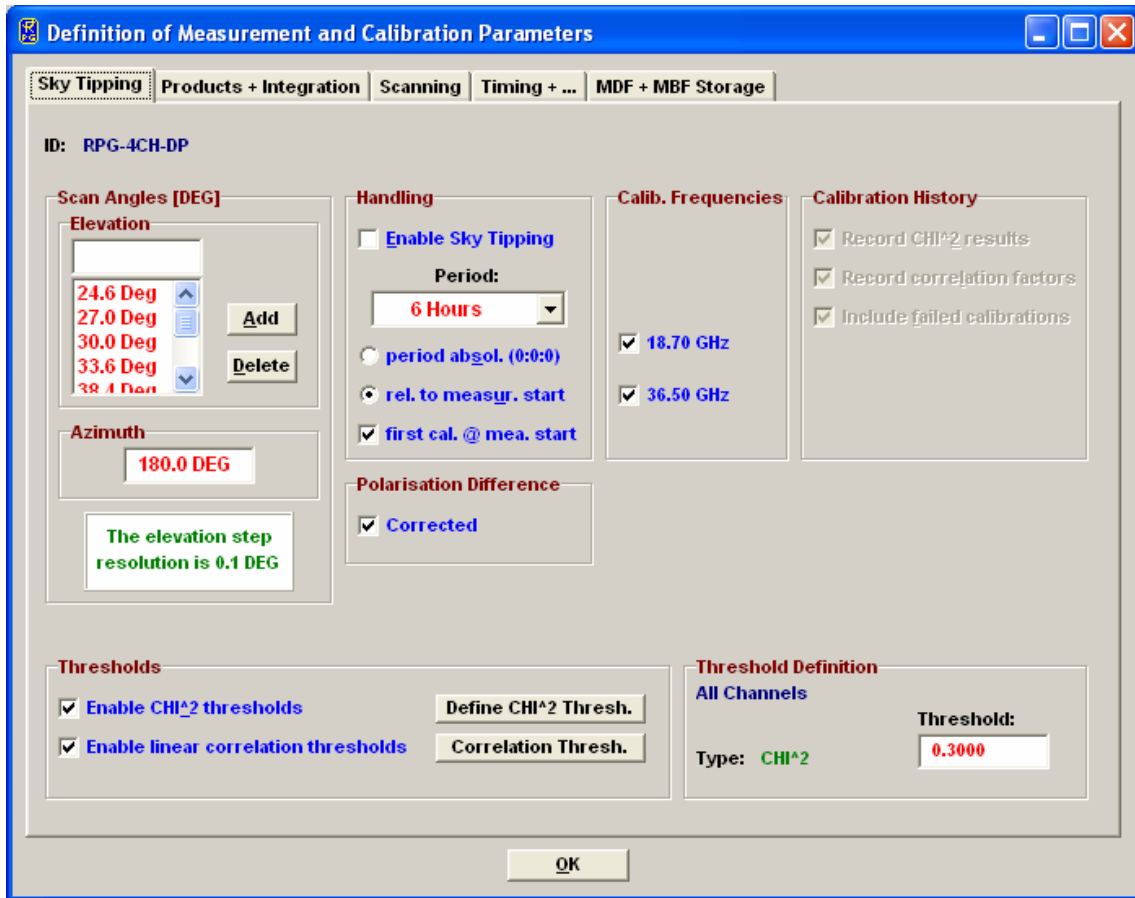


Fig.5.7: Measurement definition file menu, sky tipping tab sheet.

Sky Tipping is enabled by checking *Enable Sky Tipping*. The user can specify how often a calibration shall be performed by selecting a period between *10 Minutes* and *24 Hours*. Practical periods are 2 to 24 hours because the radiometer gain is continuously calibrated by





the noise standards and a noise diode recalibration is not required so frequently. In addition a tip curve interrupts the measurement for more than three minutes which should be kept to a minimum.

Furthermore it is possible to define the time of the first tip curve calibration in the measurement. By checking *period absol. (0:0:0)* the calibration will start relative to midnight time, e.g. with a period of 6 hours and a measurement start at 3:00 pm the first calibration will take place at 18:00 assuming that *first cal. @ mea. start* is not checked. If *rel. to measure. start* is checked the calibration timing is relative to measurement start time.

So far two quality checks (thresholds) are implemented which can be individually enabled or disabled:

- Linear correlation factor. This measures the correlation of the optical thickness samples (as a function of air mass) with a straight line. Typical linear correlation factor thresholds are  $>0.9995$ . The linear correlation factor is not very sensitive to the noise of the optical thickness samples caused by clouds etc.
- $\chi^2$ -test. This measures the variance of the optical thickness samples relative to the straight line. Typical threshold values are  $\leq 0.3$  for a good quality calibration.

With *Define CHI<sup>2</sup> Thresh.* and *Correlation Thresh.* the corresponding thresholds can be entered in the *Threshold Definition* group box.

## 5.9.2 Products + Integration

On the *Products + Integration* sheet the user selects the products he wants to be acquired and calculated by the system.

For each enabled product a separate integration time is selectable.

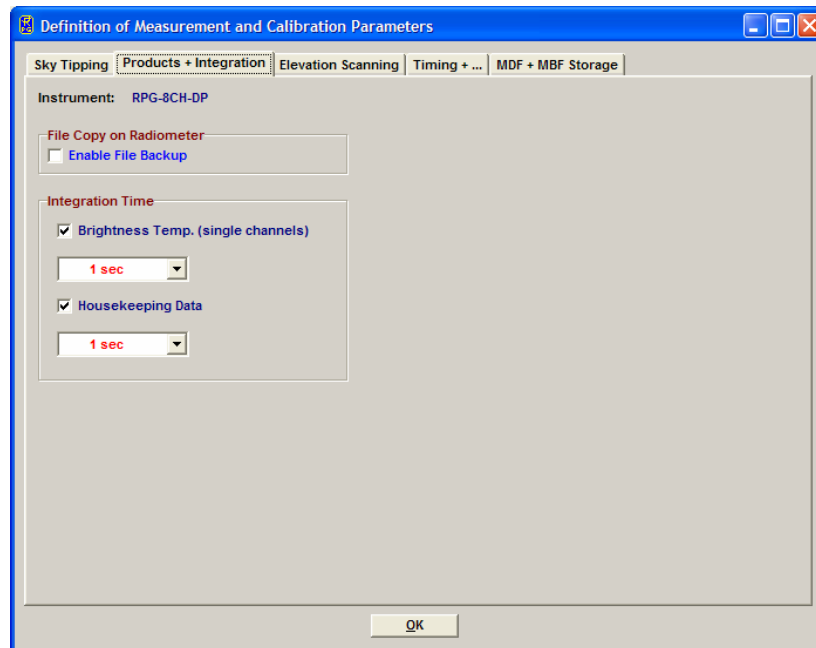
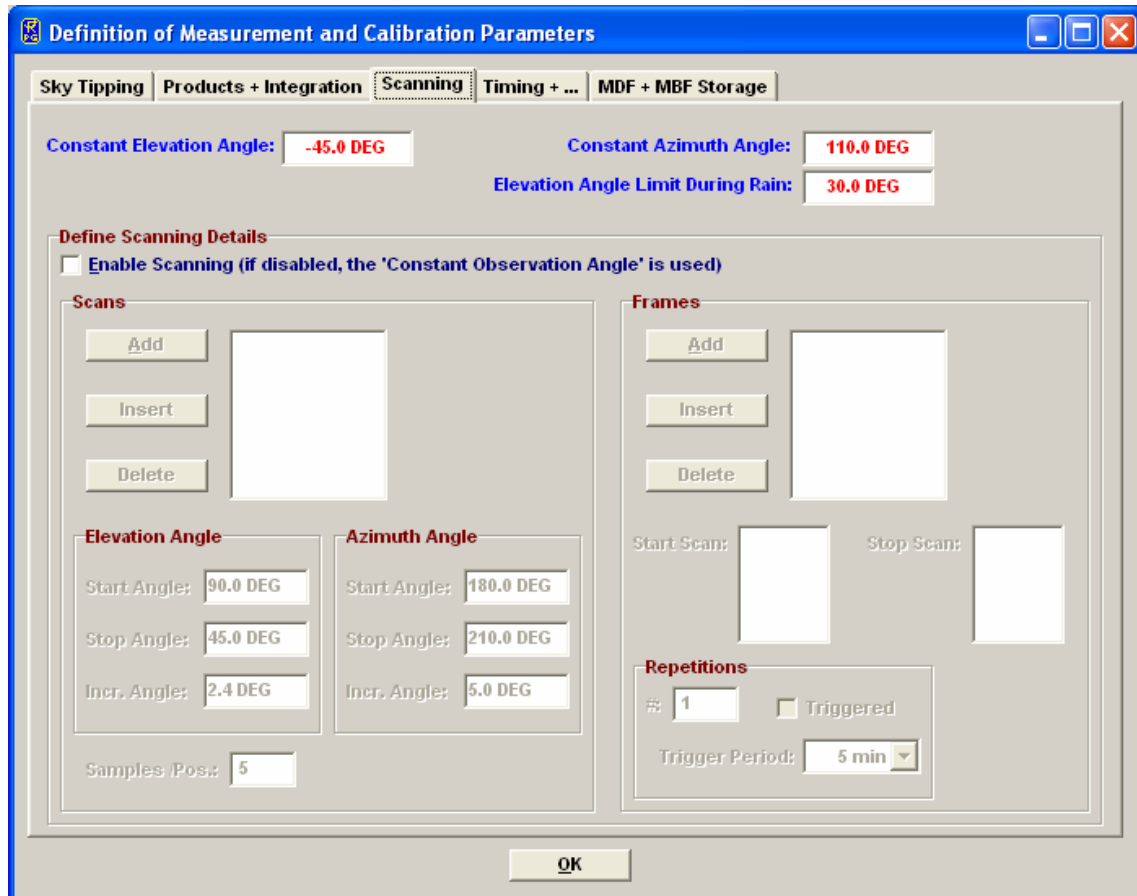


Fig.5.8: Specifying the products available for the radiometer configuration.



Another feature of the **Products + Integration** tab sheet is the ability to enable a file backup on the radiometer PC. When backup is enabled, the checked products will be automatically stored in the radiometer's data directory. This is usually done for safety reasons because the standard mode of measurements is to enable automatic data storage on the host (online monitored data). With this method the data transfer virtually does not require any time. Without monitoring the data on the host and only storing it on the radiometer as backup the user will sooner or later have to transfer the data from the embedded PC to the host with the **Transfer Data and System Files** menu.

### 5.9.3 Scanning



Sometimes it is desirable to scan the elevation / azimuth angle while taking measurement samples. The details for this scanning are defined in the **Scanning** tab sheet. When scanning is disabled a constant elevation / azimuth angle is used for observations.

The radiometer is equipped with a rain sensor. If the sensor detects rain, the elevation positioner automatically limits the maximum elevation angle to the value entered in the 'Elevation Angle Limit During Rain' entry box. This way a wetting of the receiver module microwave windows can be avoided.

The positioner moves are subdivided into elementary scans from a start angle to a stop angle with a certain incremental angle and a given number of samples measured at each position. These scans are numbered as Scan#1, Scan#2.

The radiometer does not execute single scans but only frames of scans. Each frame has a start scan and a stop scan (can be identical) which form a 'loop' of scans that can be repeated



arbitrarily. The concept of having two levels of movement definitions allows for designing complex scan procedures. The positioner speed is always constant. A frame is simply defined by clicking on one of the scans in the start scan list and then clicking on one in the stop scan list. After entering the repetition number the frame is added (or inserted) to the frame list (*Add* or *Insert*). Three examples illustrate how a frame is executed:

- 1) Start: Scan#4, stop: Scan#6, repetitions: 3 ⇒  
Scan#4,Scan#5,Scan#6,Scan#4,Scan#5,Scan#6,Scan#4,Scan#5,Scan#6
- 2) Start: Scan#4, stop: Scan#2, repetitions: 2 ⇒  
Scan#4,Scan#3,Scan#2,Scan#4,Scan#3,Scan#2
- 3) Start: Scan#2, stop: Scan#2, repetitions: 1 ⇒  
Scan#2

### 5.9.4 Timing +...

Start time and end time are important parameters for a measurement setup. There are two ways of triggering a measurement: Immediately after launching the measurement batch or at a certain time and date. Using a start time before the current time is equivalent to an immediate start.

Two options are available for measurement termination. In LIMITED mode the user can set a duration or termination time. If the stop time is before the start time the measurement duration is adjusted to 100 seconds.

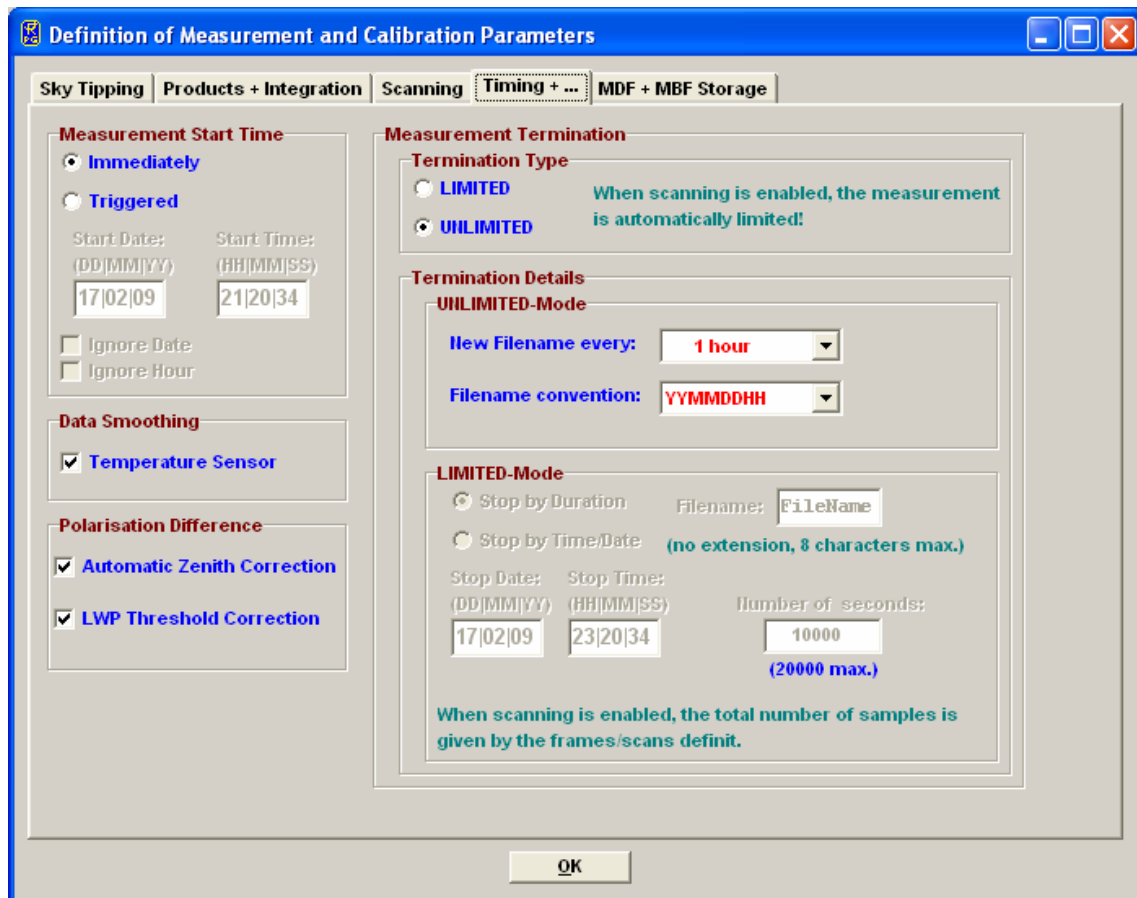


Fig.5.9: Timing definition menu.



In the case that the measurement has a well-defined end time (automatic measurement termination, LIMITED mode) the radiometer needs a filename for storing backups. The user may enter any filename not longer than 8 characters. The host also uses this filename when it is operated in automatic storage mode. If measurement timing is set to UNLIMITED mode the radiometer automatically generates filenames deduced from the actual time and date and ignores the measurement filename entry.

In UNLIMITED mode the user must terminate the measurement manually. A new filename is generated every X hours where X is selected from the ‘New Filename every’ list box. The file format is one of 14 possible versions given in the ‘Filename convention’ list box. In the format string HH=hours, DD=days, MM=month and YY=year of the actual time and date. During measurement this filename is also transmitted to the host, which uses it for file storage of monitored data (assuming that the host is operated in “Automatic Storage” mode).

Since the temperature environmental sensor responds quickly to changes of the corresponding parameter (caused by turbulence in the vicinity of the radiometer) it is sometimes desirable to smooth the data samples of temperature. The detailed surface turbulence at the radiometer location are not of interest. In *Data Smoothing* one can activate a 10 minutes LIFO filter to smooth the environmental temperature readings.

It is useful to activate the *Polarisation Difference* corrections in order to maintain zero polarisation difference under conditions when no polarisation difference can occur.

### 5.9.5 MDF + MBF Storage

It is **not** possible to send a MDF directly to the radiometer. MDFs are gathered into a MBF (measurement batch file). The concept is similar to the Scan/Frame relationship for scanning. The MDFs in a batch file are executed sequentially in the order they are listed in the MDF list (see Fig.5.10). The batch repetition number has the same meaning as the frame repetition factor for scanning: The MDF list forms a loop, which is repeated an arbitrary number of times. This offers the user a flexibility of combining different measurement tasks, which would otherwise not be compatible in a single MDF, e.g. if one wants to do a scanning measurement (not possible with retrieved products) followed by a temperature profiling measurement (a retrieved product) and repeat this 100 times the solution is to define two different MDFs, one for scanning and one for temperature profiling and combine them in a batch file with a repetition factor of 100. The only restriction for MDFs in multi-MDF batches is that the UNLIMITED mode should be avoided.

It is a good practice to store all MDFs in one directory (e.g. ...*RPG-8CH-DP\MDF\_MBF*). All MDFs in the selected directory are listed in the box in the lower right corner. From this list the user may select each MDF he wants to add or insert to the MDF batch list (with *<==Add* and *<==Insert*). MDFs may also be deleted from the MDF batch list. Store your measurement batch files (MBFs) in a single directory (like “...*RPG-8CH-DP\MDF-MBF*”). If file backup is enabled in the MDFs and the batch repetition factor is >1 there is only one filename for each MDF available. The data of successive executions of a certain MDF in the batch loop is stored to a single file. Each time the MDF is repeated in the loop, its measurement data is appended to the file.

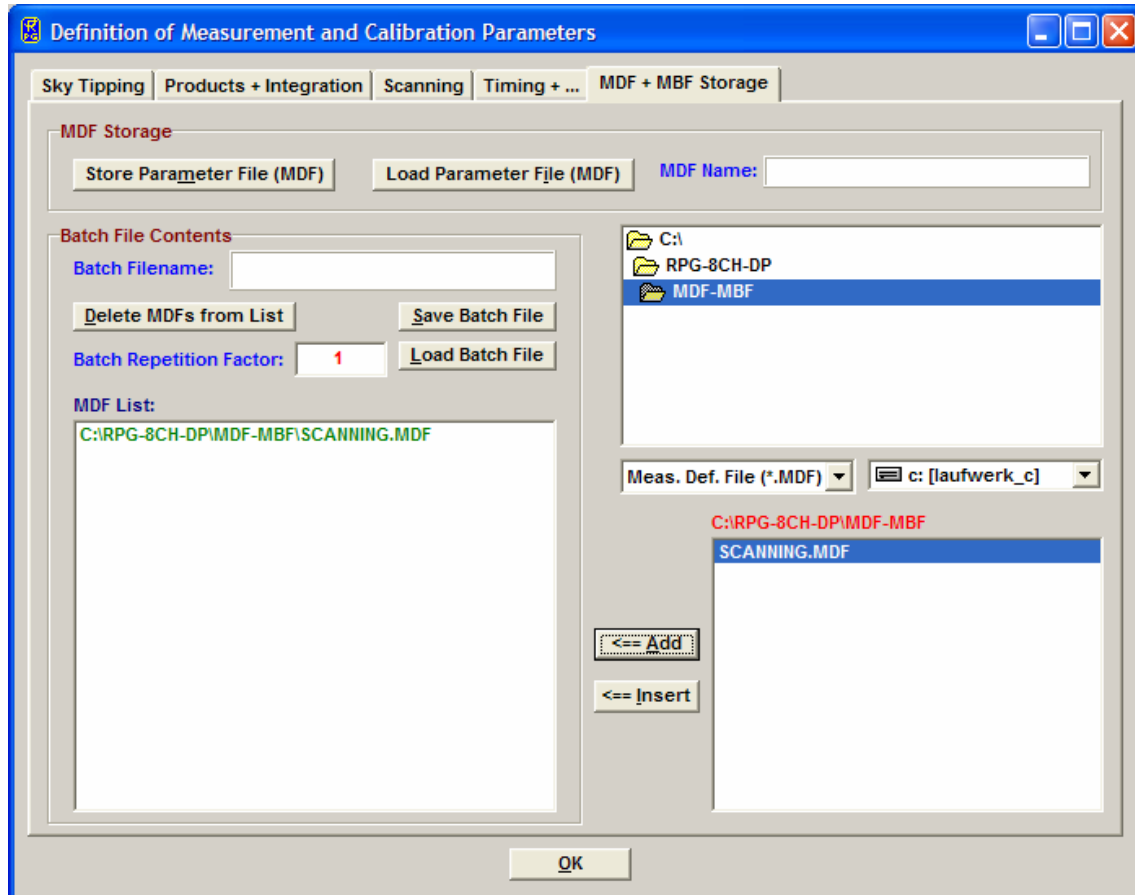


Fig.5.10: Batch file configuration menu.

## 5.10 Sending a MBF to the Radiometer

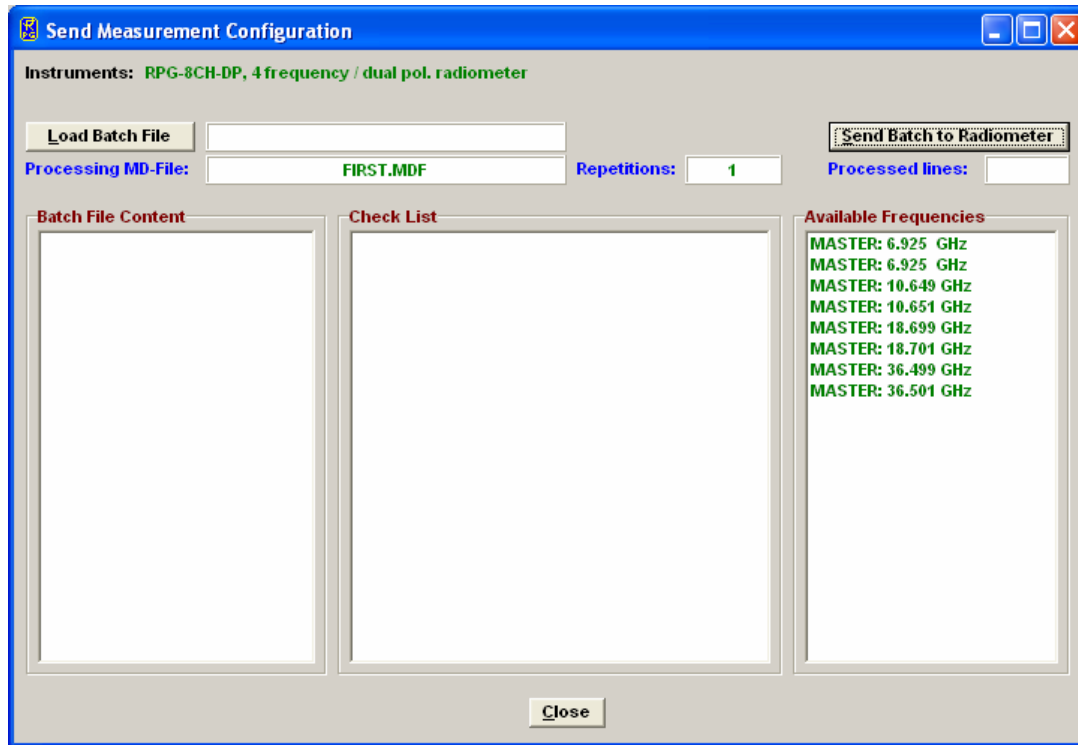
After a batch is created it can be sent to the radiometer (assuming the host is connected to it).

This is done with  (*Send Measurement Batch File to Radiometer*).

By entering this menu the host determines the current radiometer configuration (RPG-8CH-DP in the example to the left).

When an MBF is loaded (*Load Batch File*) its contents and repetition factor are displayed. In addition some pre-checks are performed, e.g. correct radiometer configuration, frequency list consistency, etc. A variety of other checks ensure that no erroneous command data is sent.

When the consistency check of a MDF is finished, the test result is displayed in the *Check List*. The batch can only be sent to the radiometer if all consistency checks have finished with the status OK. Then the MBF is transmitted with *Send Batch to Radiometer*.




## 5.11 Commanding the Radiometer Processes

When a valid non-empty batch has been transmitted to the instrument the following functions are enabled:




### *(Start Processing Batch)*

Although the batch is now stored on the radiometer's embedded PC, **8CH.EXE** remains in STANDBY mode, displayed in the status line on the bottom of the screen. By pressing  the batch process is initiated. The status line entry changes to "MEASUREMENT RUNNING...".



### *(Halt Running Batch)*

A running measurement can be halted any time. This might be useful when the user wants to change the elevation angle manually. The status bar display changes to "MEASUREMENT HALTED" and the manual control button (, discussed later) is enabled which offers manual control over elevation stepper and other radiometer features.



### *(Continue Interrupted Batch)*

Used to continue a halted measurement. The status bar display changes back to "MEASUREMENT RUNNING" and the manual control button is disabled.



(Terminate Running Batch)

This command terminates the execution of the currently running batch. The radiometer switches to STANDBY mode and is ready to receive the next MBF.

### 5.12 Monitoring Data

The best way to perform measurements is:

- Define a MDF with “File Backup” enabled and include it in a batch file (Tch).)
- Check *Automatically store monitored data* in the *Define Data Directory*.
- Send the batch file to the radiometer (MBF).
- Start the batch file on the radiometer (GO).

The monitoring windows of the products that were selected in the MDF are automatically opened and the measured data is displayed (see Fig.5.11). Since the data is transmitted online from the radiometer to the host no additional file transfer is required afterwards. The file backup on the radiometer is activated for safety reasons to prevent data loss in the case of a host PC malfunction (e.g. hard disk crash, etc.).

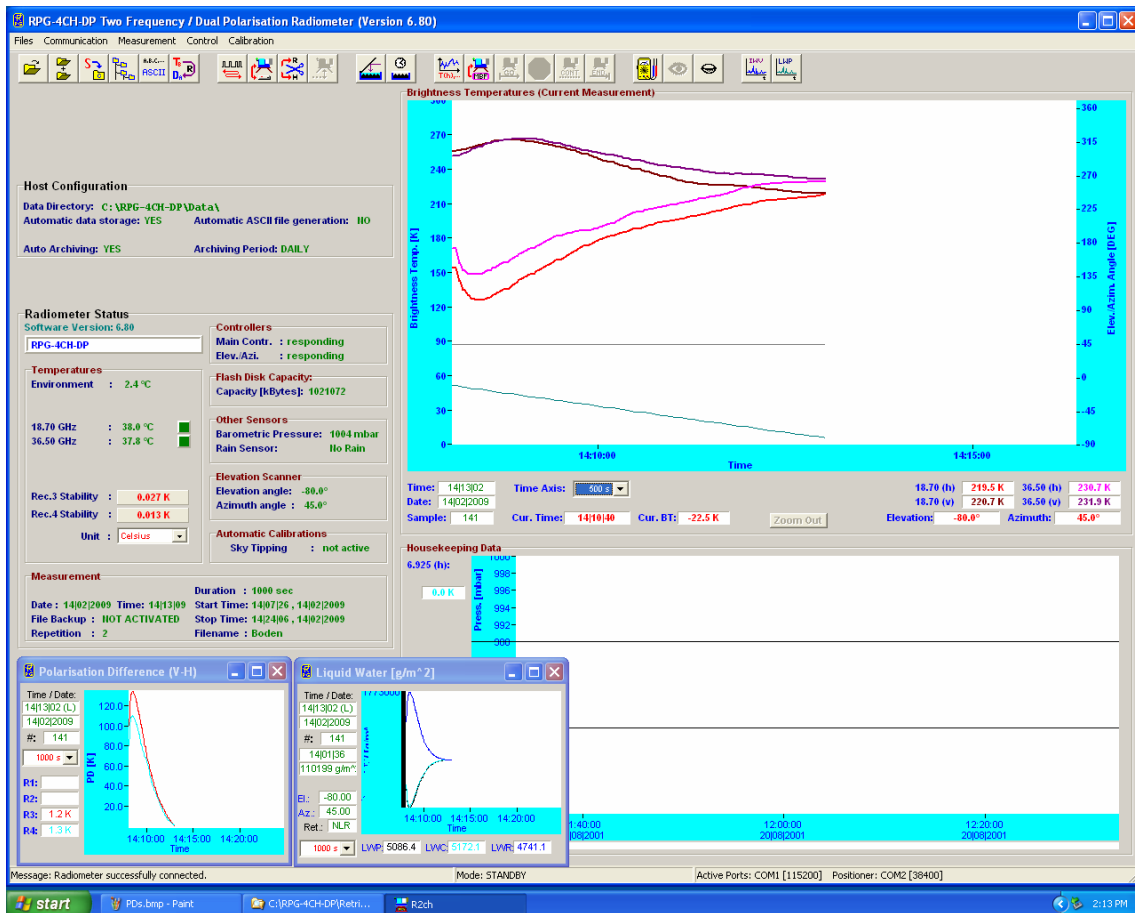



Fig.5.11: Active monitoring window.



The time axis scale is modified by selecting the time axis width in the drop-down list of the window. The monitor window displays the current time, date, sample number, sample value and cursor position (if the mouse cursor is moved into the display area).

### 5.13 Concatenate Data Files

In UNLIMITED termination mode the radiometer periodically generates new data filenames (e.g. every hour). It is often desirable to concatenate data files of the same type (\*.BRT, \*.HKD etc.) to form bigger files (e.g. 24 hour files). This is possible by clicking  (**Concatenate Data Files**) which opens the menu in Fig.5.12. A set of filenames is selected from the list and then concatenated to a single file with **Generate Concatenated File**.

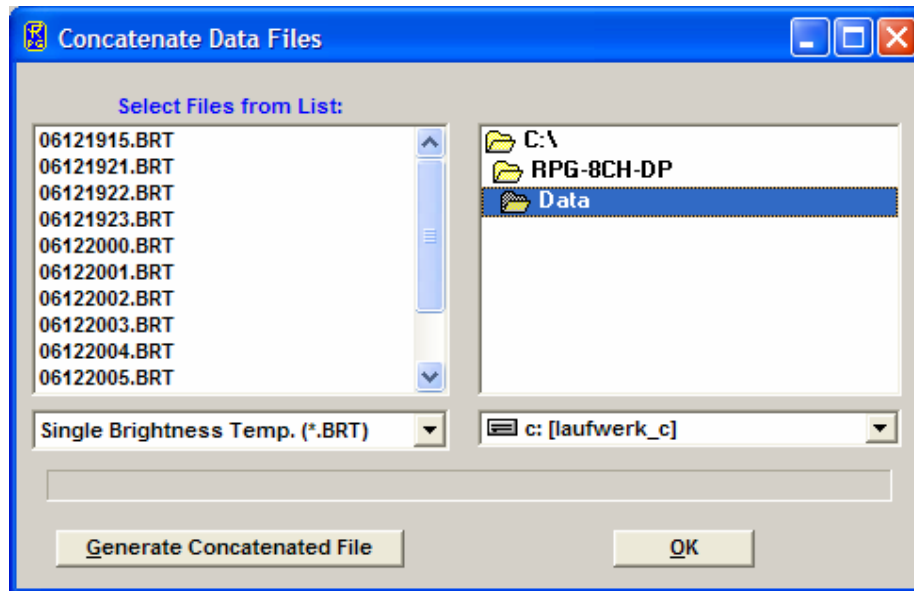


Fig.5.12: Concatenating data files.


### 5.14 Cutting Connection



(**Cut Connection to Radiometer**)

If the user wants to disconnect the host from the interface cable or turn off the radiometer after having been connected this command should be used first. It ensures that all communication activities between host and radiometer are disabled so that the host will not crash after disconnection.

### 5.15 Data Display Menus

For each measurement data product a display window is available. Click on the open button  and select a product from the pull down list. Then load a product data file. Fig.5.14a is an example of a BT chart.





All data display menus indicate start time, end time, time reference, duration, and number of samples.

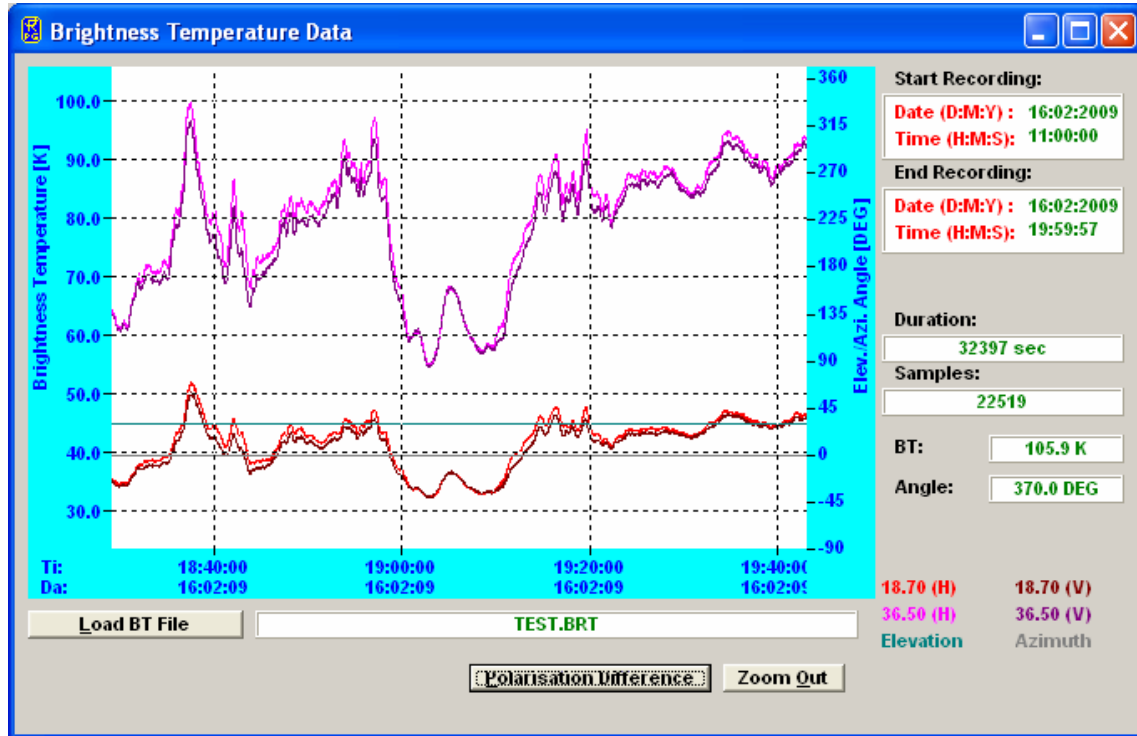
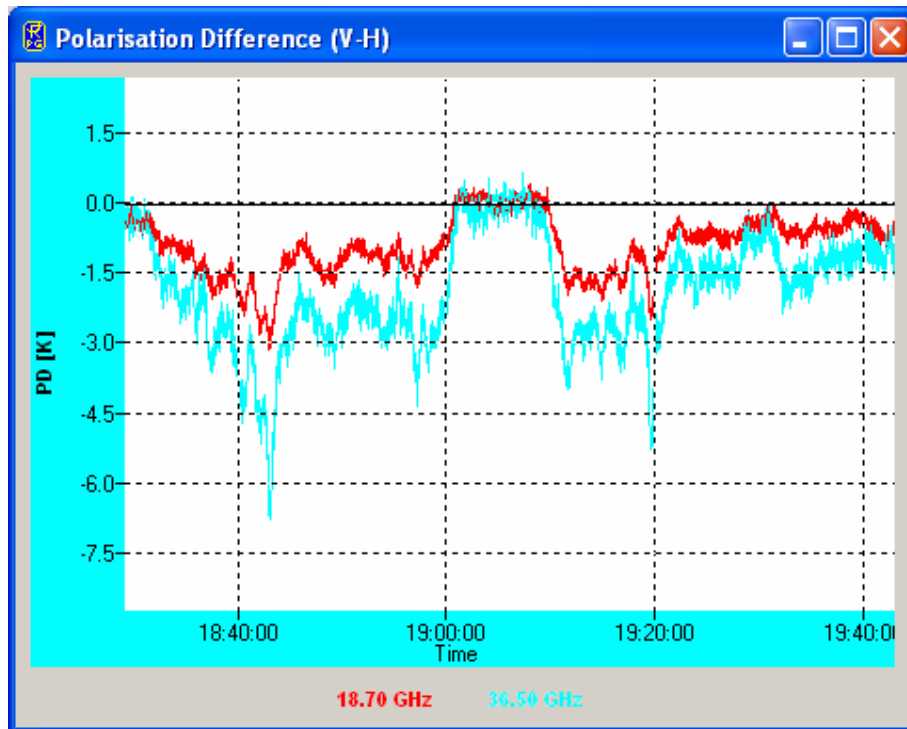


Fig.5.14: BRT chart window.




One may zoom into the data by pressing the left mouse button in the display area and drag the mouse to a different position (mouse button still pressed) to define a rectangle (indicated by a black frame). For zooming back click *Zoom Out*.



Brightness temperature data files contain the elevation / azimuth angle information for each sample. The elevation / azimuth angles are also displayed.

Most display menus can be stretched in size (resized) by positioning the mouse on the menu window edge and drag it to the desired size. The display is then adjusted in size. The Brightness Temperature Data Display menu offers an additional display feature *Polarisation Difference* which opens another window showing the difference in the TBs (V-H polarisation).

### 5.16 Manual Radiometer Control

When the host is connected to the instrument and the radiometer is in STANDBY- or HALTED-mode, the manual control functions are enabled. Click  (*Manual Radiometer Control*) to enter the *Diagnostics and manual control* menu in Fig.5.16.

The reason of implementing these functions is mainly for diagnostic purposes. When a radiometer is assembled every single electronic component must be tested. The receivers' long term stability is checked for several weeks by monitoring the detector voltages. However, some of the diagnostic functions are also useful for other tasks.

#### 5.16.1 Positioner Control

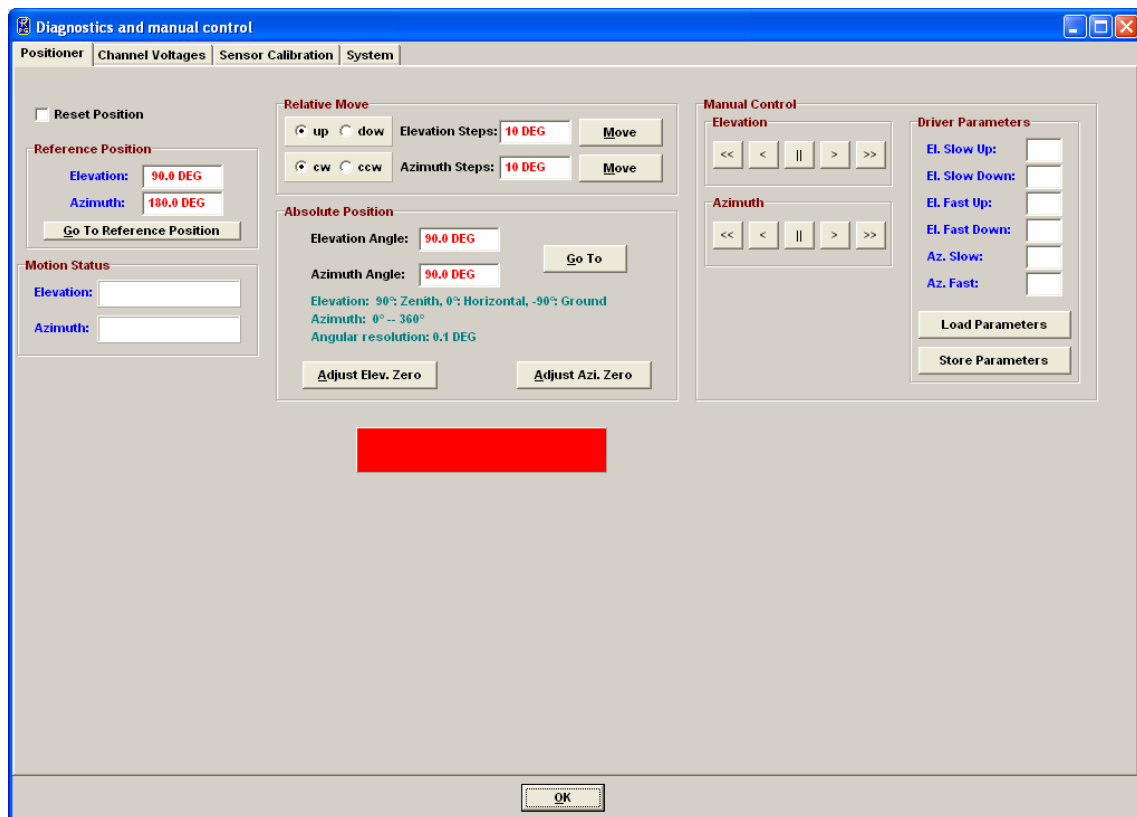


Fig.5.16: The positioner control tab sheet.

The *Positioner* tab sheet is used (for instance) to change the observation angle during a measurement in HALTED mode. If *Reset Position* is checked the stepper is reset to its



original position after leaving the diagnostics menu. If the user wishes to keep the new position he must uncheck **Reset Position**.

Stepping positions can be set relative or absolute in DEG. The absolute elevation stepper positions in elevation are as follows:

- Zenith: +90°
- Horizontal: 0°
- To ground: -90°

The angular stepper resolution is 0.1°. The azimuth value range is set to 0° to 360°  
With the '<<', '<', '||', '>' and '>>' keys the positioner can be moved like with the cursor keys on the controller's front panel. Slow and fast motions can be selected and stopped by pressing the '||' key.

The user should not manipulate the driver parameters in order to maintain a smooth positioner motion.

### 5.16.2 Channel Voltages

The **Channel Voltages** tab sheet is the main diagnostics tool (Fig.5.17).

The following data is displayed:

- Receiver 1-4 detector voltages (1:1)
- Receiver 1-4 board temperatures (T=voltage\*100 [K])
- Environmental temperature (T=voltage\*100 [K])
- Barometric pressure (P=voltage\*1000 [mbar])

The sample rate and maximum number of samples are set in **General Parameters**.

While sampling detector voltages, one can manually turn the noise diodes on and off to check for a correct operation (**Noise Diode**). The channel readings are displayed graphically and also in the **Receivers** frame. Data zooming is possible. After stopping the sampling one can use a ruler to measure the precise voltage at a certain time (↕).

**Reset** clears the acquisition display and sets the Y-axis to +5 V (maximum).

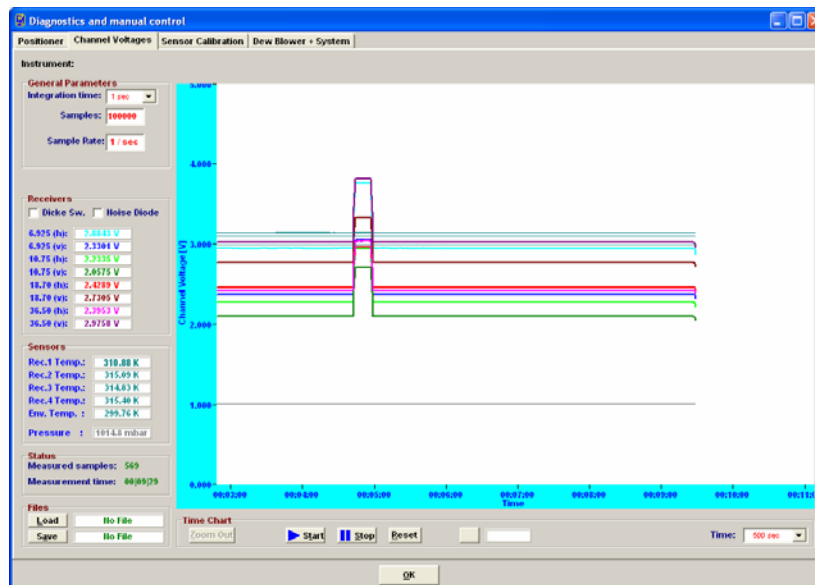


Fig.5.17: Channel voltages tab sheet.



### 5.16.3 Sensor Calibration

This tab sheet is needed to calibrate the thermal sensors and pressure sensor. It is not intended for user purposes. The sensor calibration must be performed by qualified personal only and is done before the radiometer delivery.

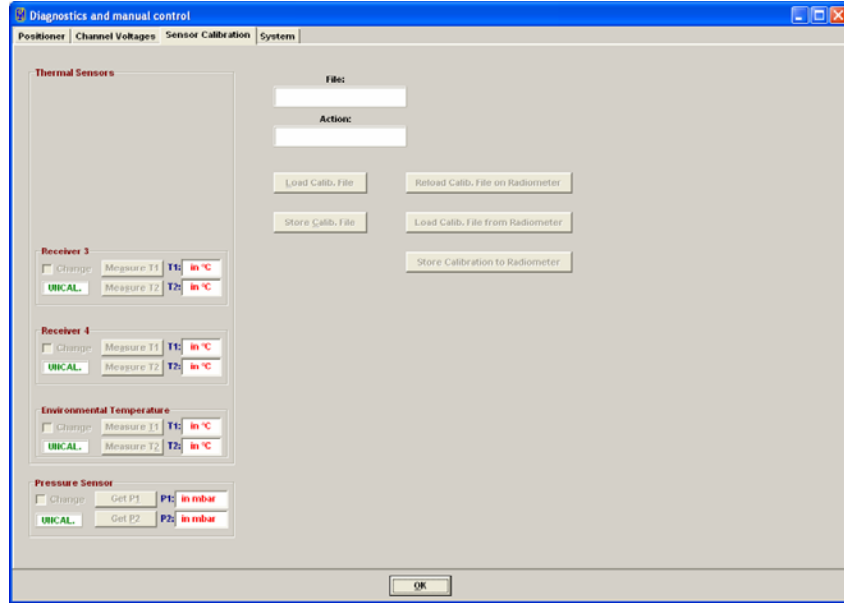


Fig.5.18: Sensor calibration tab sheet.

### 5.16.4 System

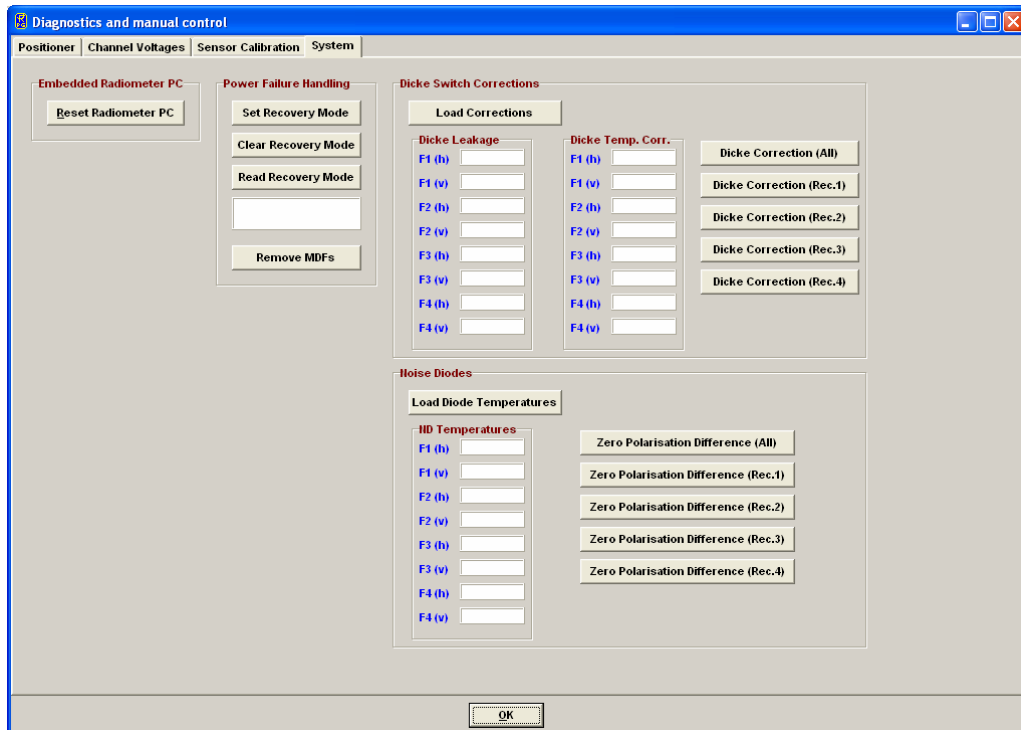


Fig.5.19: How to reset the radiometer software.




The tab sheet in Fig.5.18 is related to system issues.

A very useful feature is the **Reset Radiometer PC** function. When an update of the radiometer software has been performed by transferring a new **8CH.EXE** file to the radiometer's system file directory, a radiometer reset is required to run the new software version. When clicking on the **Reset Radiometer PC** button a warning message is displayed to inform the user that if he confirms to continue this command this will result in a radiometer reset and requires a re-connection to the radiometer afterwards.

The radiometer is capable of an automatic recovery from power failures. When a MDF is sent to the radiometer, the measurement parameters are stored on the radiometer's internal flash disk. This information is deleted when a measurement is terminated. In the case of a power failure, the parameter file(s) are not deleted and after power return the software checks for undeleted parameter files. If recovery mode is activated, the radiometer PC automatically restores the measurement that had been interrupted by the power failure. The commands **Set Recovery Mode**, **Clear Recovery Mode** and **Read Recovery Mode** allow the user to activate / deactivate this mode.

The other features of the 'System' tag are reserved for system engineers and should not be touched by operators.

### 5.17 Transform Data Files to ASCII Format

The standard data file format is binary (file structures listed in Appendix A) because it is more compact than other formats. In the case that a readable format is required the binary files can be transformed to ASCII. By using the  command (**Transform Data Files to ASCII Format**) a binary data file is converted to an ASCII file. The file name of the new file is the binary file name with appended '.ASC', e.g. the BT binary format file **MyFileName.BRT** is converted to **MyFileName.BRT.ASC**.

Beside this manual ASCII file generation it is possible to automatically store data in ASCII format during the monitoring process (active measurement). See section 5.4 for details.

Examples of ASCII files are described in Appendix B.

## 6. Instrument Maintenance and Recommendations

This chapter summarizes recommended maintenance activities to ensure a reliable radiometer.

### 6.1 Cleaning

Due to environmental conditions the radiometer can be covered with dust, spider webs, etc. The following should be considered:

- Cleaning the microwave windows: Clean the microwave windows once per month with pure water or soap and a soft cloth. Never use any aggressive chemicals like acetone, alcohol, benzene or others. These substances might damage the window coating.
- It is recommended to cover the radiometer with a tarpaulin when not in use. This is in particular advisable if the instrument is exposed to a lot of dust, humidity and rain.
- Cleaning of radiometer housing: Clean the housing of the radiometer every few month. Use a soft cloth and soap and water.



*Fig.6.1: Location of the microwave windows for cleaning.*

## 6.2 Calibrations

Except for the automatic calibrations performed by the instrument a manual calibration is required when the system is transported or turned off for a longer period (> several days) and no sky tipping is possible due to cloudy atmosphere. This calibration is called an absolute calibration. To perform this calibration follow the procedure in section 4.1. The calibration is

started by pressing  (**Perform Absolute Calibration**). The menu in Fig.5.6 is shown.

**Start Calibration** starts the absolute calibration procedure. During calibration the current activity is displayed in the message line. When the integration cycles have completed, the message **Calibration successful! Save?** is displayed and the user has to confirm to save the calibration with **Continue**. The absolute calibration parameters are then stored on the radiometer PC. Leave the calibration menu by pressing **Finished**.

If the error message **No response to cold load. Calibration terminated!** appears, the cold target was probably not filled with liquid nitrogen or was not installed at all.

**No noise diode response. Calibration terminated!** indicates a malfunction of one of the noise sources. Contact RPG for help in this case.

The absolute calibration or at least the sky tipping should be repeated every 6 month to maintain measurement accuracy of the built-in noise standards.

## 6.3 Maintenance Schedule

In the table below the given maintenance intervals are average periods. Depending on the deployment site these intervals should be optimized. For instance required cleaning intervals strongly depend on climate zones (arctic, sub-tropic, etc.), the vicinity to polluted areas (cities, sand deserts, airports etc.) or the abundance of insects or other animals (e.g. spider webs).

Activity	Recommended Service Interval
Cleaning of radiometer housing	3 month
Cleaning of microwave window	2 month
Cleaning of cooler slits	12 month
Absolute calibration with liquid nitrogen or sky tipping	6 month
Inspection of cables	12 month

## 6.4 Resetting of Radiometer Embedded PC

Sometimes it is necessary to reset the internal embedded PC. This may be the case after disconnecting the radiometer from the host computer during a measurement or after transfer of a new software version. Fig.6.2 shows the location of the embedded PC interface which is protected from humidity and dust by a black plastic cover. When this cover is removed the PC's interface connectors (monitor socket, keyboard connector, disk drive connector socket and reset button) become visible. By pressing the reset button the embedded PC is rebooted. After 1 minute this initialization is finished and the user can connect the host to the

radiometer PC by clicking on  (**Connect to Radiometer**). **Do not forget to re-install the black plastic protection cover.**



The radiometer can also be reset by turning off the power and turn it on again. This will require a re-balancing of the thermal stabilisation system which requires about 5 minutes. It is therefore recommended to reset the PC by using the reset button.

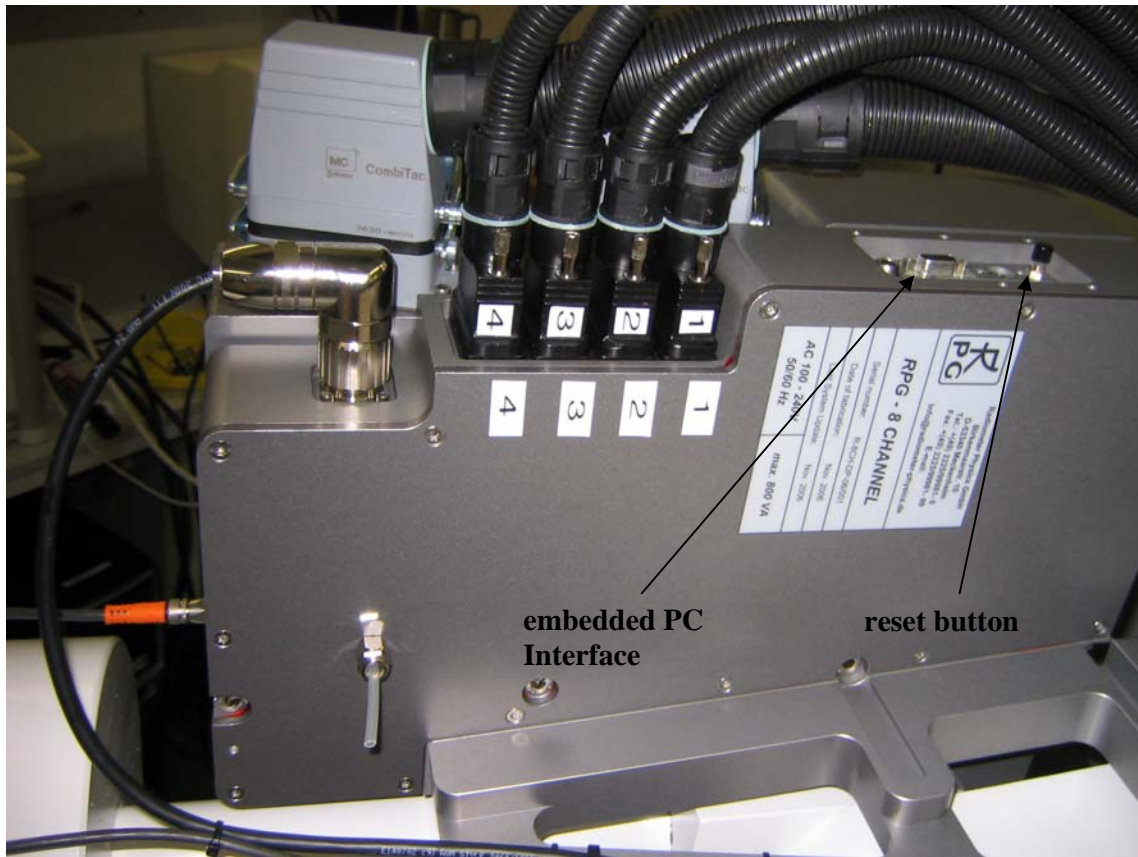





Fig.6.2: Position of radiometer PC interface and reset button.


### 6.5 Restarting Host

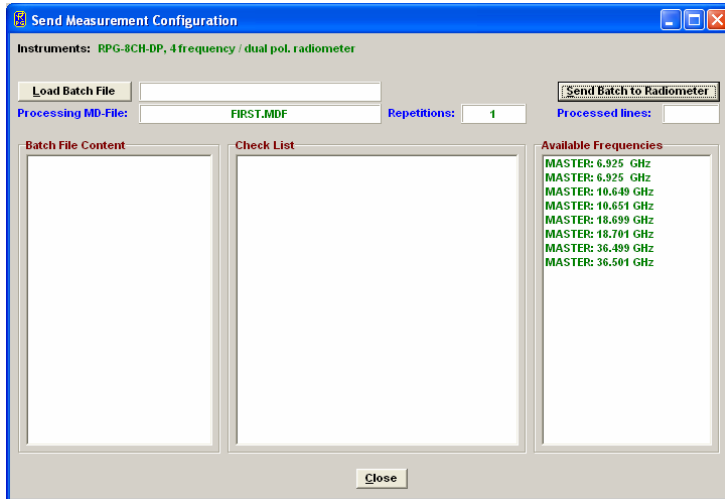
After a power failure of the host computer (with a laptop computer this occurs after about 3 hours of power failure) the host PC has to be restarted. The following steps will restart the host:

- Click  on the desktop after the host has rebooted to start the host software.
- The next step is to initiate the communication between the host and radiometer PC by pressing  (*Connect to Radiometer*). This operation takes a couple of seconds. If successful, the message *Connection to radiometer successfully established. Baud Rate adjusted.* is displayed. Otherwise the message *Radiometer does not respond! Connection could not be established...* appears. In this case try the following to handle the problem:
  - Repeat the  command.






- If not successful, check the data cable (is it properly connected to host and radiometer?).
  - Check that the radiometer power is turned on.
  - Repeat the turn on procedure.
  - If not successful, contact RPG.
- Send the measurement batch to the radiometer with  (*Send Measurement Batch File to Radiometer*).



By entering this menu the host determines the current radiometer configuration (RPG-HATPRO in the example to the left).

When an MBF is loaded (*Load Batch File*) its contents and repetition factor are displayed. In addition some pre-checks are performed, e.g. correct radiometer configuration, frequency list consistency, etc. A variety of other checks ensure that no erroneous command data is sent.

When the consistency check of a MDF is finished, the test result is displayed in the *Check List*. The batch can only be sent to the radiometer if all consistency checks have finished with the status OK. Then the MBF is transmitted with *Send Batch to Radiometer*.

Although the batch is now stored on the radiometer’s embedded PC, *8CH.EXE* remains in STANDBY mode, displayed in the status line on the bottom of the screen. By pressing  the batch process is initiated. The status line entry changes to “MEASUREMENT RUNNING...”.

### 6.6 Instrument Viewing Range

Fig.6.3 shows the requirement for the free viewing range when sky-dip (tip curve) calibration is enabled. The radiometer performs an elevation scan from zenith to close to 20° elevation. No obstacles should be in that viewing range to ensure a good calibration.

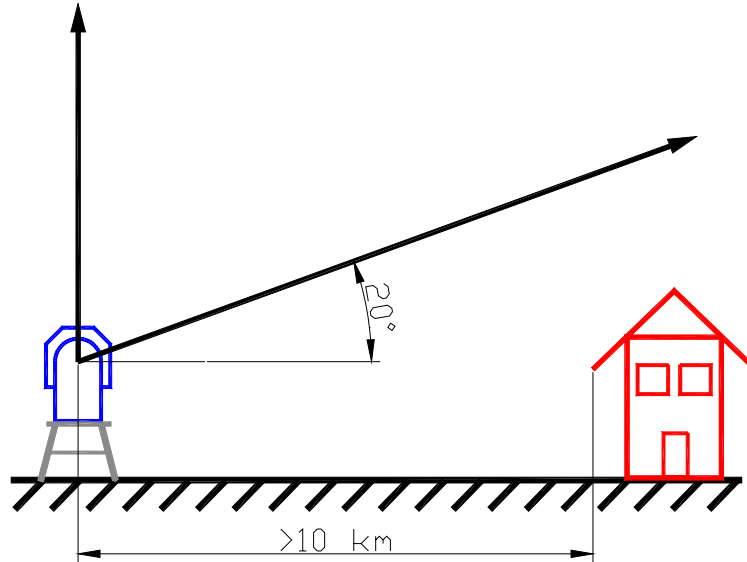


Fig.6.3: Tip curve calibration viewing range.

## 6.7 Upgrading System Software

**Assumption:** You want to install a new radiometer software version (8CH.EXE) on the embedded radiometer PC and a new version of R2CH.EXE on the host PC.

### 1. Step: Save the old software versions

- a) Create a directory to save the old software versions (e.g. C:\MyPath\RPG-8CH-DP\SAVE).
- b) Connect the host to the radiometer and enter the File Transfer Menu (Fig.6.4). On the right side (Host) browse to the directory for saving the files (e.g. C:\MyPath\RPG-8CH-DP\SAVE) and on the left side (Radiometer) in the System Files Directory mark the 8CH.EXE file. Then press the '>>' button to initiate the copy process.

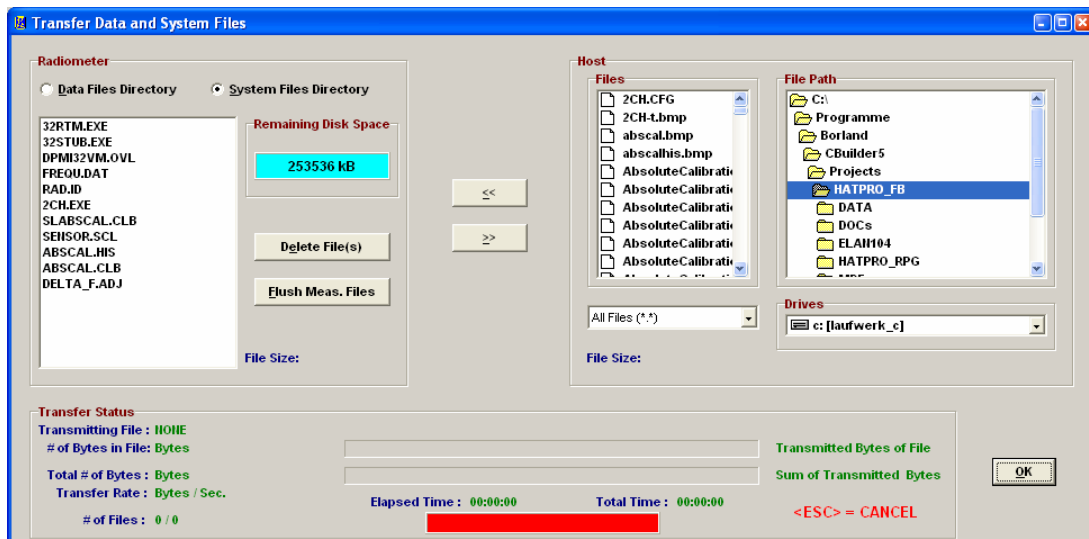


Fig.6.4: File Transfer Menu






c) locate the R2CH.EXE file in the MyPath\ RPG-8CH-DP directory and copy this file to the C:\MyPath\ RPG-8CH-DP\SAVE directory (by using the Operating System Explorer).

**2. Step:** Overwrite the old versions by the new ones

- a) Copy the new version of 8CH.EXE (the radiometer PC software) on an arbitrary directory on your hard disk (e.g. MyPath\ RPG-8CH-DP\Radiometer PC). Then enter the file transfer menu in Fig.6.4 and browse to that directory. Mark the 8CH.EXE file in the Files-list and press the “<<” button. Because you are now going to overwrite a file in the System Files Directory (which is password protected for write access) a password entry window pops up. Please enter the following password in exactly the way as it is printed here:

theringsofsaturn

Press OK and the 8CH.EXE on the radiometer PC will be overwritten by the new 8CH.EXE version. Exit the File Transfer Menu after that.

- b) Boot the radiometer PC to make the new 8CH.EXE the running version. You can do this by entering the Manual Control Menu () and selecting the “System” tag. Press the “Reset Radiometer PC” button and confirm the command with YES. Wait for about 2 minutes to give the boot process time enough to finish. Then reconnect to the radiometer (). The Radiometer Status box now indicates the new radiometer software version.
- c) Terminate R2CH.EXE and overwrite the old R2CH.EXE in MyPath\ RPG-8CH-DP with the new version.
- d) Execute R2CH.EXE to start the new host version and reconnect to the radiometer with .

The software upgrade is finished. You can confirm the successful upgrade by reading the software version numbers of both, the embedded radiometer PC (see main window radiometer status display) and the host PC (see main window caption).

## 7. Theory of Operation (Atmospheric Applications)

### 7.1 Introduction

We present a new approach for ground based remote sensing of liquid water path (LWP) in the presence of precipitating clouds. Dual polarized ground based microwave radiometers are capable of detecting the unique scattering signature of non-spherical precipitation sized particles. This polarization signal is only produced by the precipitation particles for which the brightness temperature emission has a different sensitivity to LWP than the smaller cloud drops. By using the information that is contained in the polarization difference of the down-

welling brightness temperature, the cloud and rain liquid water fractions can be estimated independently.

Future retrieval algorithms based on our proposed approach will enable the detection of small precipitation fractions in thick clouds and also allow for estimates of cloud and rain LWP in raining conditions.

The path-integrated liquid water content (liquid water path, LWP) is of considerable interest to the meteorological community for a number of applications, ranging from climate research to radio telecommunications. Measurements of LWP can be provided by different methods, such as satellite imagery, cloud radar, and ground based passive microwave radiometry.

The latter is the most precise method for LWP estimation over land surfaces. Thus, ground based microwave radiometers are used operationally for the remote sensing of integrated water vapour and LWP, offering the capability of performing measurements in nearly all types of weather conditions (Gueldner and Spaenkuch, 1999). The main limit on their capabilities is the occurrence of rain, which reduces the precision of LWP retrievals by current microwave methods. The retrieval techniques for LWP from brightness temperatures (TB) at microwave frequencies used so far are limited to cloud LWP (called LWC) in the absence of rain LWP (called LWR). The reason for this limitation is the varying sensitivity of emitted TB with drop size. Above a certain radius  $r$  the dependence of TB on radius slightly exceeds being proportional to  $r^3$ . The LWP (proportional to the third moment of the drop size distribution) is no longer unambiguously coupled to the TB signal if such large drops are mixed with smaller cloud droplets.

As a consequence, a LWP retrieval in raining clouds is highly ambiguous with current methods. This fact not only reduces the operational utility if raining conditions are masked out, but also adds a possible error source to LWP retrievals in many clouds.

Radar measurements do not offer an advantage when cloud and rain particles simultaneously occur because the sensitivity of the radar signal to drop size is even worse: The radar reflectivity factor is proportional to the sixth moment of drop radius. Thus the signal will always be dominated by the largest drops in the sampled volume (Fox and Illingworth, 1997}. While a change of the drop size distribution (DSD) from a cloud drop spectra to a convective rain drop size distribution will increase the TB signal of a microwave radiometer by a factor of 2 to 3, the reflectivity factor will change by several orders of magnitude. Thus LWP values derived from the radar reflectivity factor depend more critically on the assumption of the true drop size distribution than those derived from microwave radiometry.

Up to now passive ground based microwave measurements only used the brightness temperature information, which alone cannot deal with the ambiguity introduced by large raindrops within the cloud. New findings from radiative transfer models (Czekala and Simmer, 1998} suggest a possibility to resolve this size dependent ambiguity by measuring a second signal that is also related to raindrop size: The polarization difference (PD), which is defined as the amount of linear polarization  $PD = TB_V - TB_H$ . This scattering induced signal depends on drop deformation, and hence on drop size. The modeling of somewhat realistically shaped non-spherical rain drops has recently become possible due to advances in single scattering methodology and computer efficiency.

The aim of this chapter is to propose a new approach for LWP retrieval in the presence of raining clouds by adding polarization information to the current un-polarized measurement systems and retrieval methods. We will illustrate the physical processes which relate the TB and PD signal to the varying partitioning of total LWP between cloud and rain. We will show how the information content due to the unique scattering signature of non-spherical rain drops can be used to improve the accuracy of widely used LWP retrieval techniques.

However, we do not propose a complete retrieval algorithm for a specific instrument that properly incorporates all the uncertainties that may arise from imperfect instruments, uncertain temperature and humidity profiles, and uncertain cloud microphysics. At this stage

we focus on explaining the general method and its possible advantage for obtaining a LWP retrieval without restriction to non-raining clouds.

Such improvements are expected to have significant impact on future operational services as well as cloud process studies which may be based on the new retrieval approach. Such studies offer the opportunity to gain knowledge about internal structures and cloud microphysical properties. The onset of precipitation, specifically the transition from small particle dominated cloud DSD to precipitation sized DSD (which is very important in cloud parameterizations in numerical weather prediction models), should be detectible. A systematic bias in LWP retrieval is expected if rain drops are not considered.

## **7.2 Polarisation Signal**

The shape of raindrops is known to be non-spherical (Pruppacher and Pitter, 1971) due to wind stress, surface tension and internal hydrostatic pressure. Chuang and Beard (1990) describe the shape of raindrops falling at terminal velocity by a series of Chebyshev polynomials. The radiative transfer results of Czekala and Simmer (1998) revealed remarkable differences between the effects of (commonly assumed) spherical and oblate spheroid shapes on polarized microwave brightness temperatures. The latter shape is used as a close approximation to the Chebyshev shape. While the brightness temperature (TB, defined as the average brightness temperature calculated from the vertically and horizontally polarized brightness temperatures according to  $(TB_V + TB_H)/2$ ) showed only a weak dependence on the hydrometeor shape, the polarization difference for down-welling radiation (as seen by a ground based sensor) was altered from small positive values (always well below 2 K) in the case of spherical raindrops to large negative values (down to -15 K) in the case of oblate spheroids. The polarization in both cases is only produced by drops that are large enough (compared to wavelength) to cause a significant amount of scattering. The precise amount of negative PD varied with the optical thickness within the observed volume. Specifically, the amount of precipitation, the chosen frequency, and the elevation angle of the hypothetical ground based observation, and the cloud top and cloud base height controlled the amount of PD predicted by the radiative transfer model. The theoretically predicted signal of negative PD arising from precipitation sized water drops has recently been validated with ground based measurements (Czekala et al, 2000).

## **7.3 Model Calculations**

The above mentioned studies (Czekala and Simmer, 1998) imply that polarization measurements might be exploited to learn more about the amount of precipitation sized particles within clouds. In order to illustrate the radiometric sensitivities to the partitioning of water between cloud and rain in a clear and simple way, we carried out a sensitivity study. Within an atmospheric column with a fixed vertical profile of temperature and humidity we positioned a cloud between 1 and 2 km height with a specified fraction of cloud water and rain water. For reasons of simplicity we assume a constant vertical profile of cloud and rain water within the cloud. This model is meant to simulate situations like a viewing of an isolated rain event from outside the rain cell or a cloud with no observed surface rain rate. Precipitating clouds with no surface rain rate frequently occur when precipitation starts to evolve within the cloud, but evaporates below the cloud base before reaching the surface.

Cloud and rain fractions were varied independently so that the resulting LWC ranges from 0.0 kg/m<sup>2</sup> to 2.5 kg/m<sup>2</sup> and the LWR from 0.0 kg/m<sup>2</sup> to 2.5 kg/m<sup>2</sup>. The total LWP simply is the sum  $LWP = LWC + LWR$ . All possible combinations of both kinds of LWP were calculated,

resulting in total LWP ranging from 0.0 to 5.0 kg/m<sup>2</sup>. Although the pure rain cases without any LWC make sense for observations where the rain shaft of isolated showers is observed against a clear sky background, some of the LWC/LWR combinations (especially those with large LWC) are certainly unrealistic for the given vertical cloud extension. Nevertheless, the complete coverage of all possible combinations is well suited for explaining the nature of the signal expected from raining clouds, even in the presence of severe rain events.

The cloud LWP was modeled with a DSD given by a modified gamma distribution with a modal radius of 5.5 micron and an integration interval from 0.1 to 100 μm. The rain LWP was produced by a Marshall-Palmer distribution and an integration interval from 100 μm to 5 mm. Oblate spheroids with a fixed orientation and a size dependent aspect ratio were used for rain, spheres for cloud particles. The T-Matrix code from Mishchenko (Mishchenko, 2000) was used to calculate the amplitude scattering function for these particles. The surface emission, which has hardly any effect on the down-welling radiation, was set to 0.9, a reasonable value for land surfaces.

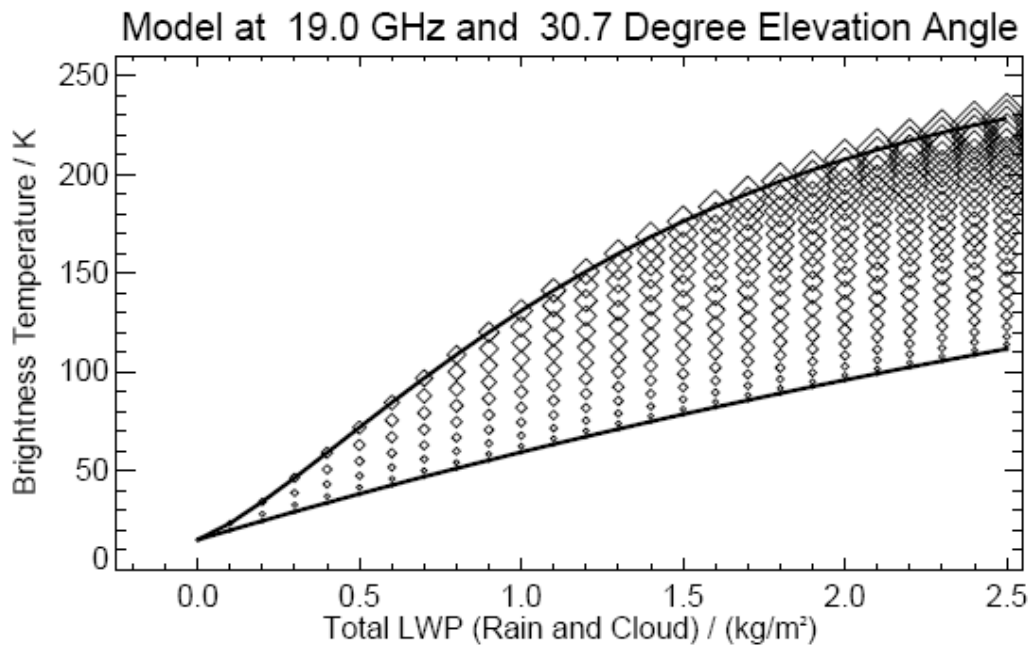
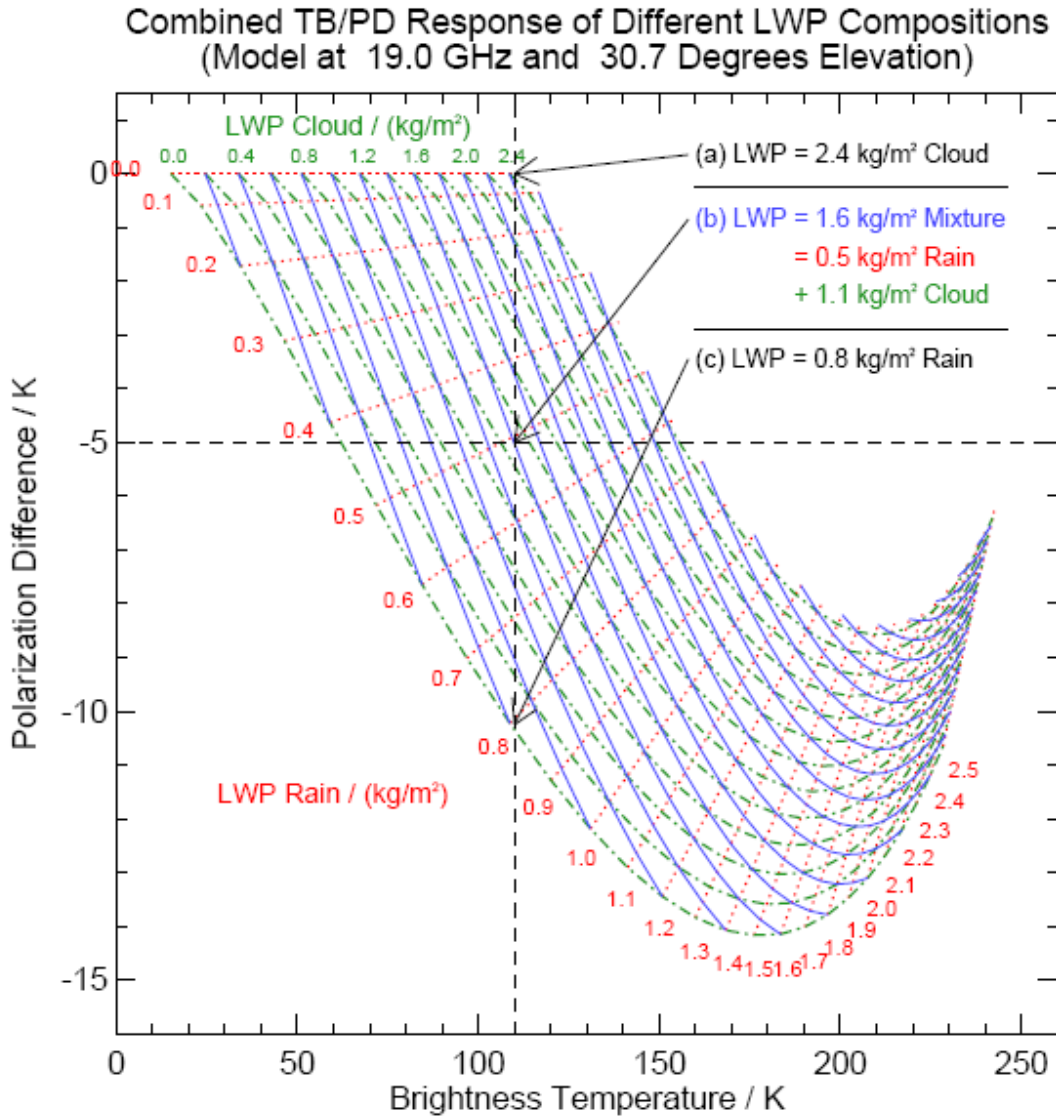


**Fig.7.1**

Fig.7.1 shows the brightness temperature obtained at 19 GHz with an elevation angle of 30.7 degrees for a hypothetical ground based observation. The amount of LWP due to rain is indicated by the size of the symbols. Smallest symbols are assigned to zero R-LWP, thus the lower line Fig.7.1 indicates the result for clouds without rain. The reverse situation (all LWP is made from LWR) is indicated by the upper line which shows a stronger increase with LWP and a saturation at large LWP values where the atmosphere (sum of gas and liquid constituents) becomes opaque. It is obvious from the different slopes of both extreme cases that a TB measurement can only be converted to a LWP if the mixture of rain and cloud fraction is known. Realistic cloud conditions are represented by a point somewhere between both limiting cases.

### 7.4 Proposed Retrieval Method

Combining the information of TB and PD that refer to a specific combination of cloud LWP (LWC) and rain LWP (LWR) into one diagram (Fig.7.2) shows that the information contained in the two signals is complementary. Fig.7.2 gives the response of all calculated mixtures of LWC and LWR in terms of their radiative response. Isolines of constant LWP are given for three different LWP variables: Dotted red lines indicate calculations with the same LWR but varying LWC, dash-dotted green lines show the results for same LWC, but with varying LWR. The solid blue lines are lines of constant total LWP, which may be formed by any mixture of LWC and LWR.



Pure cloud conditions are indicated by the uppermost horizontal dotted red line (no rain fraction). The increase in cloud liquid water path from 0.0 to 2.5 kg/m<sup>2</sup> leads to an increase in the corresponding TB, but no polarization is produced. Pure rain conditions (in the absence of cloud) produce the lower limit of the PD signal (indicated by the lowest dash-dotted green line). When mixing rain into the cloud, increasing amounts of LWR shift the horizontal line of pure cloud response towards negative PD. However, the lines of constant LWR do not remain

horizontal. This means that a variation of LWC in the presence of considerable LWR (e.g. 0.7 kg/m<sup>2</sup>) not only results in a change of TB, but also affects the PD signal: Increasing amounts of cloud water damp the PD. With further increase of LWR the PD signal ceases to increase in amplitude (beginning saturation due to increasing optical thickness) and then drops back towards zero. It is worth while to note that in the region of initial saturation (beginning of curvature in the dash-dotted green isolines of the LWC) the isolines of LWC and LWR remain roughly orthogonal. This means that LWC and LWR affect the TB/PD response in different ways, which is a prerequisite for a simultaneous retrieval of both properties. If the isolines of both quantities were parallel then a distinction of both quantities would be impossible. This would be the case when assuming spherical particles for all kinds of hydrometeors since spherical rain produces a TB signal with a different sensitivity than cloud drops and only very small positive PD (always below 2 K).

The advantage of the new approach of LWP retrieval by using the PD signal in addition to only the TB signal is obvious when looking at a hypothetical measurement of 110 K brightness temperature and -5 K polarization difference (indicated by the dotted black lines in Fig.7.2). The TB result of 110 K refers to 2.4 kg/m<sup>2</sup> liquid water path when assuming a pure cloud particle size distribution (retrieval (a), uppermost dotted red line) or 0.8 kg/m<sup>2</sup> liquid water path when assuming a composition of pure rain without clouds (retrieval (c), lowest dash dotted green line). These numbers give a good estimate about the uncertainty in LWP retrieval in the presence of raining clouds when only TB measurements are used.

In comparison, when the supplementary PD information is used (measurement (b) in Fig.7.2) the total LWP is reliably estimated to be 1.6 kg/m<sup>2</sup>.

Furthermore, we are now able to separate the LWP between the fraction of cloud water (1.1 kg/m<sup>2</sup>) and the fraction of rain water (0.5 kg/m<sup>2</sup>).

## **7.5 Discussion**

The above results are idealized model calculations that neglect the precise vertical distribution of the hydrometeors and use simplified cloud microphysical assumptions. For example the variability of drop size distribution functions and the effect of the melting layer need to be considered in more detail before a practical retrieval scheme can be based upon such radiative transfer calculations. Variations in water vapour and temperature profile will also affect the numerical results, mainly by an additional shift along the TB axis.

However, the results presented here clearly illustrate the profit of adding the polarization signal that is produced by non-spherical precipitation sized particles to the retrieval process. In addition, multi-frequency observations will help to overcome uncertainties that may arise from unknown drop size distributions. Since modern multi-channel microwave radiometers (solheimetal,1998, Crewell et al, 2000) can determine the temperature (RMS < 2 K) and humidity (RMS < 0.3 g/m<sup>3</sup>) profile in the cloudy (non-raining) troposphere (below 5 km), they will also provide sufficient information about the atmospheric conditions that will improve the retrieval accuracy in case of raining clouds. For this purpose, a final retrieval scheme may also rely on secondary information, such as surface temperature, cloud base height, and humidity profile data from numerical weather prediction models.

For semi-transparent situations (less than 1.5 kg/m<sup>2</sup> LWR at 19 GHz) the vertical distribution of the hydrometeors is of minor importance and will not degrade the general dependence of TB and PD on the different LWP fractions.

Fig.7.3 shows the resulting TB/PD response at 30 GHz (instead of 19 GHz used in Fig.7.2). At higher frequencies the saturation of the PD signal begins at lower rain rates compared to the 19 GHz results. However, the sensitivity of PD to small amounts of LWR is significantly increased. This is partly due to the change in the size parameter (the ratio of particle size to the wavelength under consideration). Another reason is the increased optical thickness due to



the frequency dependence of the refractive index. A lower total optical thickness (e.g. at 10 GHz) decreases the dynamic range of the TB signal, but prevents saturation of the PD and TB signal. Since the accuracy of TB measurements is in the range of 1 K this reduction of the TB signal range is not a severe problem. The insensitivity of 10 GHz observations to smaller drops leads to a total signal that is dominated by the rain generated PD.

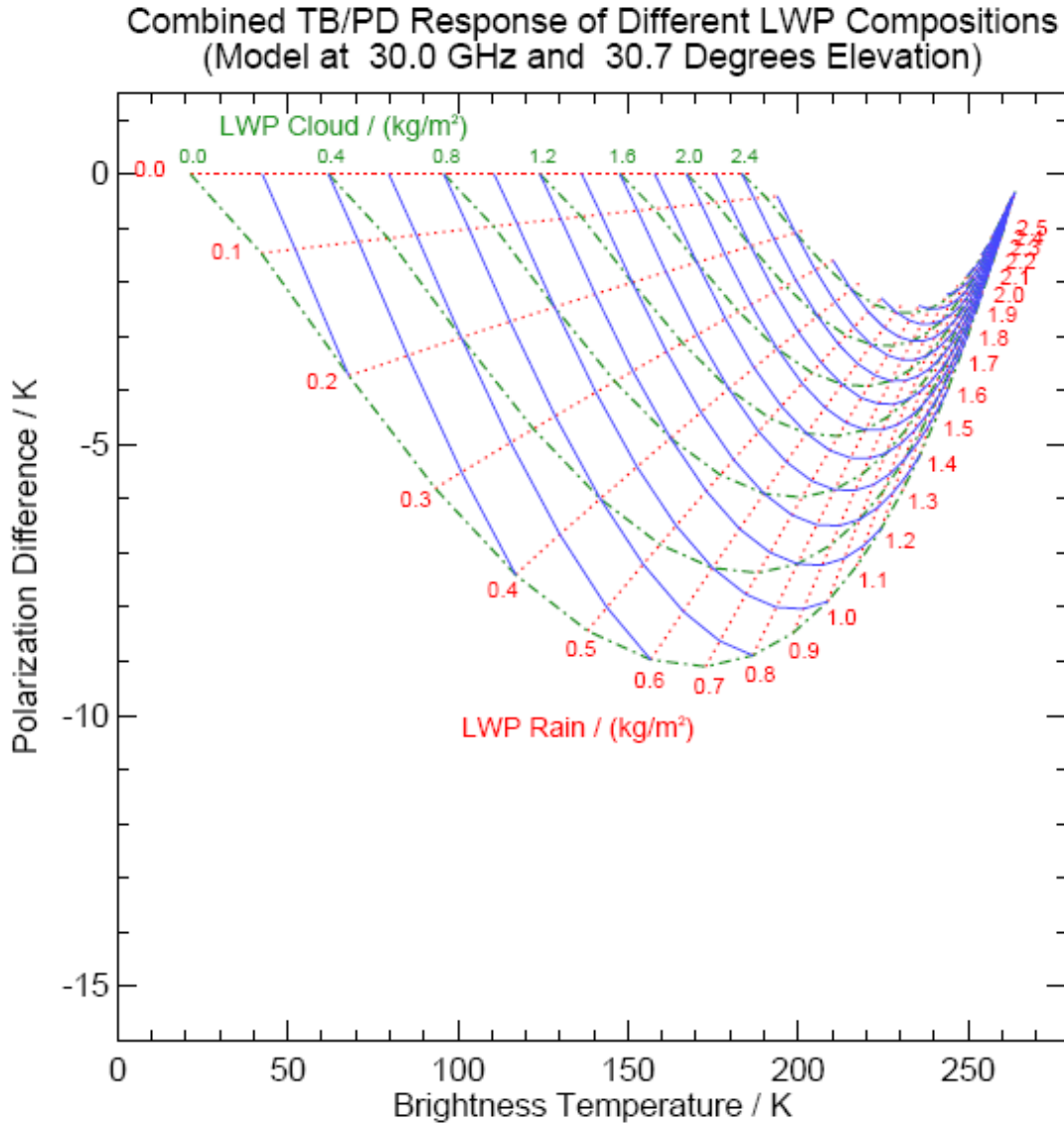


**Fig.7.3**

Similar changes in sensitivity to LWR can also be achieved by variation of the observation angle. Since the total optical thickness increases with increased geometrical path lengths through the atmosphere at lower elevation angles, the saturation of the PD is observed at different LWR fractions. This effect is not the same as a variation in frequency because elevation angle affects the radiation only by changing the optical thickness (due to varied path length). Changes in frequency induce a similar change in optical thickness, but additionally change the ratio of particle size to wavelength and thus lead to different single scattering parameters. Finally, the development of practical retrieval methods also needs to incorporate instrument noise and antenna characteristics, thus leading to instrument specific algorithms.

Current research microwave radiometers have a sufficiently narrow beamwidth (less than 10 degree) to reveal cloud inhomogeneities in process studies (Crewell et al, 2000). With an absolute accuracy of 1 K and a relative calibration of the PD to 0.2 K with clear sky conditions it will be possible to detect the discussed signal.

## **7.6 Conclusions**

The presence of precipitation sized rain drops within clouds inhibits a precise remote sensing of LWP by currently used ground based microwave methods. The brightness temperature is related to LWP, but if the drop size distribution is unknown it is not possible to partition the LWP between cloud droplets and rain drops using such measurements. We have presented a new approach to discriminate between the different contributions to total LWP by exploiting the additional information contained in the negative polarization difference caused by non-spherical rain drops. This signal depends on the drop size and therefore reduces the uncertainty that arises from the unknown partitioning of total LWP between the cloud and rain fractions of the drop size distribution. Future retrieval algorithms that use simultaneous measurements of brightness temperature and polarization difference will allow for a more accurate retrieval of total liquid water path. In addition, we expect that it will be possible to estimate independently the contributions by rain drops and cloud drops to the total LWP.

The uncertainties that may arise from insufficient knowledge of cloud microphysics and vertical distribution of the hydrometeors will be partly mitigated by the additional information that is gained by multi-frequency and making multi-angle measurements.

## **7.7 REFERENCES**

Chuang and Beard, 1990

Chuang, C. and K.-V. Beard, A numerical model for the equilibrium shape of electrified raindrops, *J. Atmos. Sci.*, 47, 1374--1389, 1990.

Crewell et al., 2000

Crewell, S., H.-Czekala, U.-Löhnert, and C.-Simmer, MICCY -- a 22 channel ground-based microwave radiometer for atmospheric research, submitted to *Radio Science*, 2000.

Crewell et al., 2000

Crewell, S., U. Löhnert, A. van Lammeren, and C. Simmer, Cloud remote sensing by combining synergetic sensor information, *Phys. Chem. Earth (B)*, 25, No. 10-12, 1043-1048, 2000.

Czekala et al., 2000

Czekala, H., S. Crewell, A. Hornbostel, A. Schroth, C. Simmer, and A. Thiele, Validation of microwave radiative transfer calculations for non-spherical liquid hydrometeors with ground based measurements, *J. Appl. Meteorol.*, 2000

Czekala and Simmer, 1998

Czekala, H. and C. Simmer, Microwave radiative transfer with non-spherical precipitating hydrometeors, *J. Quant. Spectros. Radiat. Transfer*, 60, 365--374, 1998.

Fox and Illingworth, 1997



Fox, N., and A.J. Illingworth, The potential of space borne cloud radar for the detection of stratocumulus clouds, *J. Appl. Meteorol.*, 36, 676--687, 1997.

Güldner and Spänkuch, 1999

Güldner, J. and D. Spänkuch, Results of year-round remotely sensed integrated water vapour by ground-based microwave radiometry, *J. Appl. Meteorol.*, 38, 981--988, 1999.

Mishchenko, 2000

Mishchenko, M.I., Calculation of the amplitude matrix for a non-spherical particle in a fixed orientation, *Appl. Opt.*, 39, 1026--1031, 2000.

Pruppacher and Pitter, 1971

Pruppacher, H.R. and R.L. Pitter, A semi-empirical determination of the shape of cloud and rain drops, *J. Atmos. Sci.*, 28, 86--94, 1971.

Solheim et al., 1998

Solheim, F., J. Godwin, E.R. Westwater, Y. Han, S. Keihm, K. Marsh, and R.Ware, Radiometric profiling of temperature, water vapor and cloud liquid water using various inversion methods, *Radio Science*, 33, 393--404, 1998.

## 8. Soil Moisture Applications

A polarised radiometer is also very useful for soil moisture and snow measurements. With the vertical polarisation it is straight forward to measure the refractive index of soil samples as shown in the following measurement where a ground scan is performed with a RPG-4CH-DP (18.7 GHz v/h, 36.5 GHz v/h). The elevation angle is scanned between  $-10^\circ$  and  $-80^\circ$ . The result of this scan is shown in Fig 8.1.

As can be seen from the diagram, the Brewster angle for the 18.7 (V) GHz channel is at  $69^\circ$  which corresponds to a refractive index of  $n=2.60$  ( $\tan(69^\circ)$ ). This is consistent with the observation at normal incidence where the reflection coefficient  $R$  is given by  $R=((n-1)/(n+1))^2$  which leads to  $R=0.2$  at 18.7 GHz for normal incidence. With a physical ground temperature  $T_g$  of 273K and a sky temperature of  $T_s=15K$  we get:  $T_b=(1-R)*T_g+R*T_s=220K$  which is really observed. For the 36.5 GHz channel we get:  $n=2.36$  (Brewster angle:  $67^\circ$ ),  $R=0.16$ ,  $T_b=233 K$  which is totally consistent with the observations.

Horizontal and vertical polarizations precisely convert at normal incidence to the same brightness temperature (reflection angle  $0^\circ$  could not be directly measured).

In the horizontal polarization the  $T_b$  is dominated by the reflected sky brightness temperature. The higher the reflection angle, the higher the sky contribution and the lower the total  $T_b$ . But with low elevation angle (El) the sky temperature  $T_s$  becomes larger, roughly the  $T_s$  measured at zenith angle multiplied by the airmass ( $am=1/\sin(El)$ ). At  $10^\circ$  elevation (reflection angle= $80^\circ$ ) the sky temperature is close to 6 times higher compared to the zenith angle  $T_s$ . Therefore the  $T_s$  value at  $80^\circ$  reflection angle is approx. 90 K at 18.7 GHz (cloud free conditions). This is why the  $T_b$ s at high reflection angles tend to increase which is shown in the diagram (sky saturation).

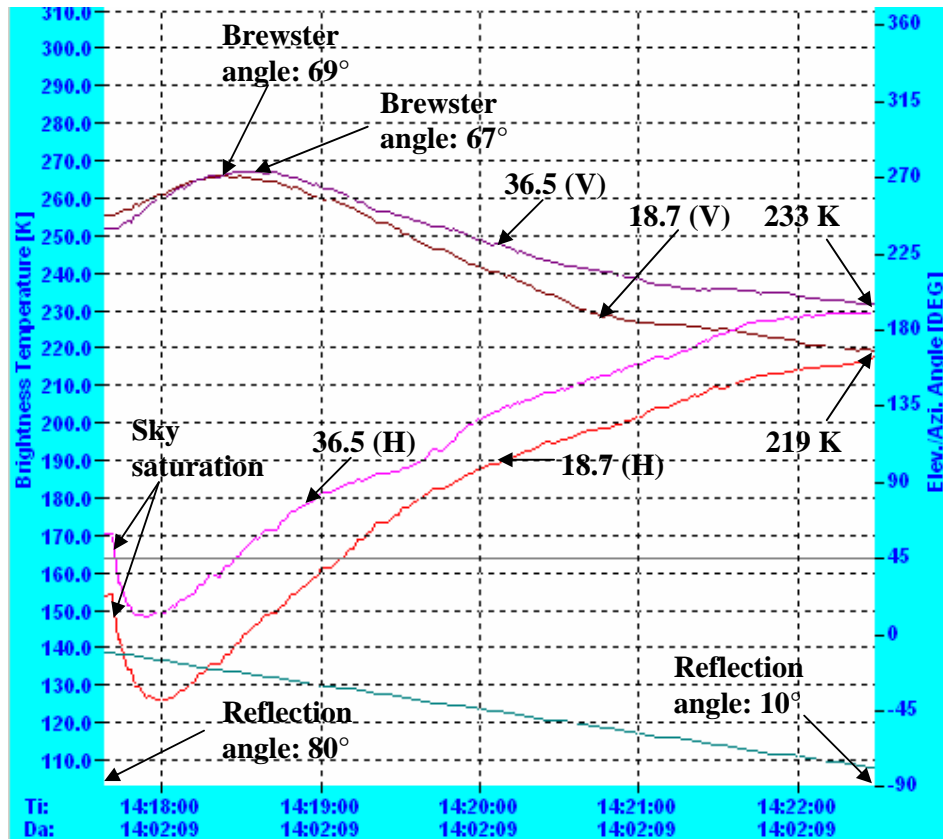


Fig.8.1: Soil measurement scan between  $-10^\circ$  and  $-80^\circ$  elevation.

The refractive index summarizes the soil properties like vegetation content, soil moisture, soil composition, etc. By comparing refractive indices of different frequencies, snow layers can be analyzed. A general rule is that the ground penetration depth increases with decreasing frequency. Therefore a radiometer dedicated for soil moisture measurements should be equipped with 6.925 GHz and 10.7 GHz channels.



**Appendix A (File Formats)**

**A1a: BRT-Files (\*.BRT), Brightness Temperature (Single Channels)**

Variable Name	Type	# Bytes	Description
BRTCode	int	4	BRT-File Code (=837854832)
N	int	4	Number of recorded samples
BRTMin	float	4	Minimum of recorded BRT values
BRTMax	float	4	Maximum of recorded BRT values
T_1	int	4	Time of sample 1 (# of sec. since 1.1.2001)
BRT_1(0)	float	4	Br. Temp. sample 1, frequency 1 [K]
...	...	...	...
BRT_1(7)	float	4	Br. Temp. sample 1, frequency 8 [K]
EL_ANG_1	float	4	Elevation angle of sample 1 (DEG)
AZ_ANG_1	float	4	Azimuth angle of sample 1 (DEG)
...	...	...	...
BRT_N(0)	float	4	Br. Temp. sample N, frequency 1 [K]
...	...	...	...
BRT_N(7)	float	4	Br. Temp. sample N, frequency 8 [K]
EL_ANG_N	float	4	Elevation angle of sample N (DEG)
AZ_ANG_N	float	4	Azimuth angle of sample N (DEG)

**A1b: BRT-Files (\*.BRT), Brightness Temperature (Version 2)**

Variable Name	Type	# Bytes	Description
BRTCode	int	4	BRT-File Code (=837854833)
N	int	4	Number of recorded samples
BRTMin	float	4	Minimum of recorded BRT values
BRTMax	float	4	Maximum of recorded BRT values
Freqs[8]	float	4x8	Field of Frequencies
T_1	int	4	Time of sample 1 (# of sec. since 1.1.2001)
BRT_1(0)	float	4	Br. Temp. sample 1, frequency 1 [K]
...	...	...	...
BRT_1(7)	float	4	Br. Temp. sample 1, frequency 8 [K]
EL_ANG_1	float	4	Elevation angle of sample 1 (DEG)
AZ_ANG_1	float	4	Azimuth angle of sample 1 (DEG)
...	...	...	...
BRT_N(0)	float	4	Br. Temp. sample N, frequency 1 [K]
...	...	...	...
BRT_N(7)	float	4	Br. Temp. sample N, frequency 8 [K]
EL_ANG_N	float	4	Elevation angle of sample N (DEG)
AZ_ANG_N	float	4	Azimuth angle of sample N (DEG)

**A2: HKD-Files (\*.HKD), Housekeeping Data**

Variable Name	Type	# Bytes	Description
HKDCode	int	4	HKD-File Code (=86649438)
N	int	4	Number of recorded samples
T_1	int	4	Time of sample 1 (# of sec. since 1.1.2001)
TEnv_1	float	4	Environmental Temperature [K], sample 1
TRec1_1	float	4	Temperature of Receiver 1 [K], sample 1
TRec2_1	float	4	Temperature of Receiver 2 [K], sample 1
TRec3_1	float	4	Temperature of Receiver 3 [K], sample 1
TRec4_1	float	4	Temperature of Receiver 4 [K], sample 1
StabRec1_1	float	4	Receiver 1 Stability[K], sample 1
StabRec2_1	float	4	Receiver 2 Stability[K], sample 1
StabRec3_1	float	4	Receiver 3 Stability[K], sample 1
StabRec4_1	float	4	Receiver 4 Stability[K], sample 1
Press_1	float	4	Barometric Pressure[mbar], sample 1
RF_1	int	4	Rain Flag, sample 1
Res_1	float	4	Free, for later use, sample 1
...	...	...	...
T_N	int	4	Time of sample N (# of sec. since 1.1.2001)
TEnv_N	float	4	Environmental Temperature [K], sample N
TRec1_N	float	4	Temperature of Receiver 1 [K], sample N
TRec2_N	float	4	Temperature of Receiver 2 [K], sample N
TRec3_N	float	4	Temperature of Receiver 3 [K], sample N
TRec4_N	float	4	Temperature of Receiver 4 [K], sample N
StabRec1_N	float	4	Receiver 1 Stability[K], sample N
StabRec2_N	float	4	Receiver 2 Stability[K], sample N
StabRec3_N	float	4	Receiver 3 Stability[K], sample N
StabRec4_N	float	4	Receiver 4 Stability[K], sample N
Press_N	float	4	Barometric Pressure[mbar], sample N
RF_N	int	4	Rain Flag, sample N
Res_N	float	4	Free, for later use, sample N

**A3: LIW-Files (\*.LIW), Liquid Water Data**

Variable Name	Type	# Bytes	Description
LIWCode	int	4	LIW-File Code (=934501978)
N	int	4	Number of recorded samples
LIWMin	float	4	Minimum of recorded LIW values
LIWMax	float	4	Maximum of recorded LIW values
LIWTimeRef	int	4	Time Reference 0=Local, 1=UTC)
IWRetType	int	4	Retrieval type (0=linear, 1=quadr. regr.)
T_1	int	4	Time of sample 1 (# of sec. since 1.1.2001)
LIW_1(3)	float	3x4	LIW_1(0)=LWP, LIW_1(1)=LWC,



			LIW_1(2)=LWR of sample #1
EL_ANG_1	float	4	Elevation angle of sample 1 (DEG)
AZ_ANG_1	float	4	Azimuth angle of sample 1 (DEG)
...	...	...	...
T_N	int	4	Time of sample N (# of sec. since 1.1.2001)
LIW_N(3)	float	3x4	LIW_N(0)=LWP, LIW_N(1)=LWC, LIW_N(2)=LWR of sample #N
EL_ANG_N	float	4	Elevation angle of sample N (DEG)
AZ_ANG_N	float	4	Azimuth angle of sample N (DEG)

**A4: IWV-Files (\*.IWV), Integrated Water Vapour Data**

Variable Name	Type	# Bytes	Description
IWVCode	int	4	IWV-File Code (=594811068)
N	int	4	Number of recorded samples
IWVMin	float	4	Minimum of recorded IWV values
IWVMax	float	4	Maximum of recorded IWV values
IWVTimeRef	int	4	Time Reference 0=Local, 1=UTC)
IWVRetType	int	4	Retrieval type (0=linear, 1=quadr. regr.)
T_1	int	4	Time of sample 1 (# of sec. since 1.1.2001)
IWV_1	float	4	IWV of sample #1
EL_ANG_1	float	4	Elevation angle of sample 1 (DEG)
AZ_ANG_1	float	4	Azimuth angle of sample 1 (DEG)
...	...	...	...
T_N	int	4	Time of sample N (# of sec. since 1.1.2001)
IWV_N	float	4	IWV of sample #N
EL_ANG_N	float	4	Elevation angle of sample N (DEG)
AZ_ANG_N	float	4	Azimuth angle of sample N (DEG)

**A5: Structure of Calibration Log-File (CAL.LOG)**

Variable Name	Type	# Bytes	Description
STACode	int	4	CAL.LOG -File Code (=657643)
N_Gain	int	4	Number of recorded gain cal. samples
N_Noise	int	4	Number of recorded noise cal. samples
N_SkyTip	int	4	Number of recorded tip curve cal. samples
N_CH_Rec1	int	4	Number of receiver 1 channels
N_CH_Rec2	int	4	Number of receiver 2 channels
Frequ[]	float	4* ChanNo	Frequencies of Rec1 and Rec2
CalType1	int	4	Type of calibration sample 1 (0=gain, 1=noise, 2=tip curve



			results, 3=tip curve with full fit information)
CalTime1	int	4	Time of sample 1 (# of sec. since 1.1.2001)
TipCurveStat1	int	4	Status of tip curve calibration (only if CalType1=2 or 3), 3 = FAILED, 2 = SUCCESS
Gain1[]	float	4* ChanNo	Gains of calibration sample 1
Tsys1[]	float	4* ChanNo	system noise temps of calibration sample 1 (only if CalType1=1 or CalType1=2 or CalType1=3)
LinCorr1[]	float	4* ChanNo	Linear correlations for calibration sample 1 (only if CalType1=2 or 3)
ChiSqr1[]	float	4* ChanNo	Chi square factors for calibration sample 1 (only if CalType1=2 or 3)
NoiseTemp1[]	float	4* ChanNo	Noise source temperatures for calibration sample 1 (only if CalType1=2 or 3)
SkyTipAngAnz1	float	4	Number of sky tip for calibration sample 1 (only if CalType1= 3)
Airmass1[]	float	4* SkyTipAngAnz1	Airmass array (only if CalType1=3)
SkyDipUs1[i][j] i=0, ... , N_CH_Rec1-1 j=0, ... , SkyTipAngAnz1	float	4* N_CH_Rec1* (SkyTipAngAnz1+1)	Sky dip detector voltages (only if CalType1=3). For each frequency the det. Voltage is given at all angles. The last entry is the voltage on the hot target
TauSuccess1[]	int	4* N_CH_Rec1	Flag that indicates if the Tau calculation during the skydip was successful (0=no, 1=yes) (only if CalType1=3)
TauArr1[0][j]	float	4* SkyTipAngAnz1	Tau array for channel 1 (only if CalType1=3 and TauSuccess1[0]=1)
LinFit1A[0]	float	4	Linear Fit parameter A (offset) for channel 1 (only if CalType1=3 and TauSuccess1[0]=1)
LinFit1B[0]	float	4	Linear Fit parameter B (slope) for channel 1 (only if CalType1=3 and TauSuccess1[0]=1)
...	...	...	...
TauArr1[N_CH_Rec1-1][j]	float	4* SkyTipAngAnz1	Tau array for last channel (only if CalType1=3 and TauSuccess1[N_CH_Rec1-1]=1)
LinFit1A[N_CH_Rec1-1]	float	4	Linear Fit parameter A (offset) for channel 1 (only if CalType1=3 and TauSuccess1[N_CH_Rec1-





			1]=1)
LinFit1B[N_CH_Rec1-1]	float	4	Linear Fit parameter B (slope) for last channel (only if CalType1=3 and TauSuccess1[N_CH_Rec1-1]=1)
...	...	...	...
CalTypeN	int	4	Type of calibration sample N (0=gain, 1=noise, 2=tip curve)
CalTimeN	int	4	Time of sample N (# of sec. since 1.1.2001)
TipCurveStatN	int	4	Status of tip curve calibration (only if CalTypeN=2), 3=FAILED, 2=SUCCESS
GainN[]	float	4* ChanNo	Gains of calibration sample 1
TsysN[]	float	4* ChanNo	system noise temps of calibration sample N (only if CalTypeN=1 or CalTypeN=2)
LinCorrN[]	float	4* ChanNo	Linear correlations for calibration sample N (only if CalTypeN=2)
ChiSqrN[]	float	4* ChanNo	Chi square factors for calibration sample N (only if CalTypeN=2)
NoiseTempN[]	float	4* ChanNo	Noise source temperatures for calibration sample N (only if CalTypeN=2)
SkyTipAngAnzN	float	4	Number of sky tip for calibration sample N (only if CalType1=3)
AirmassN[]	float	4* SkyTipAngAnzN	Airmass array (only if CalType1=3)
SkyDipUsN[i][j] i=0, ..., N_CH_Rec1-1 j=0, ..., SkyTipAngAnzN	float	4* N_CH_Rec1* (SkyTipAngAnzN+1)	Sky dip detector voltages (only if CalType1=3). For each frequency the det. Voltage is given at all angles. The last entry is the voltage on the hot target, sample N
TauSuccessN[]	int	4* N_CH_Rec1	Flag that indicates if the Tau calculation during the skydip was successful (0=no, 1=yes) (only if CalType1=3), sample N
TauArrN[0][j]	float	4* SkyTipAngAnzN	Tau array for channel 1 (only if CalType1=3 and TauSuccessN[0]=1)
LinFit1A[0]	float	4	Linear Fit parameter A (offset) for channel 1 (only if CalType1=3 and TauSuccessN[0]=1)
LinFit1B[0]	float	4	Linear Fit parameter B (slope) for channel 1 (only if CalType1=3 and TauSuccessN[0]=1)
...	...	...	...



TauArr1[N_CH_Rec1 - 1][j]	float	4* SkyTipAngAnzN	Tau array for last channel (only if CalType1=3 and TauSuccessN[N_CH_Rec1 -1]=1)
LinFit1A[N_CH_Rec1 -1]	float	4	Linear Fit parameter A (offset) for channel 1 (only if CalType1=3 and TauSuccessN[N_CH_Rec1 -1]=1)
LinFit1B[N_CH_Rec1 - 1]	float	4	Linear Fit parameter B (slope) for last channel (only if CalType1=3 and TauSuccessN[N_CH_Rec1 -1]=1)

with N = N\_Gain + N\_Noise + N\_SkyTip and ChanNo = N\_CH\_Rec1+ N\_CH\_Rec2.

### Appendix B (ASCII File Formats)

Fig.B1 shows an example of an ASCII data file structure (BRT). All ASCII files start with a header giving information about the number of samples in the file, Minimum and Maximum values of the measured quantities for scaling purposes. Comments are preceded by ‘#’.

Each sample line starts with the date and time (Ye = Year, Mo = Month, Da = Day, Ho = Hour, Mi = Minute, Se = Second) this sample was. All data columns are separated by ‘,’ from each other. Each line ends with CR/LF.

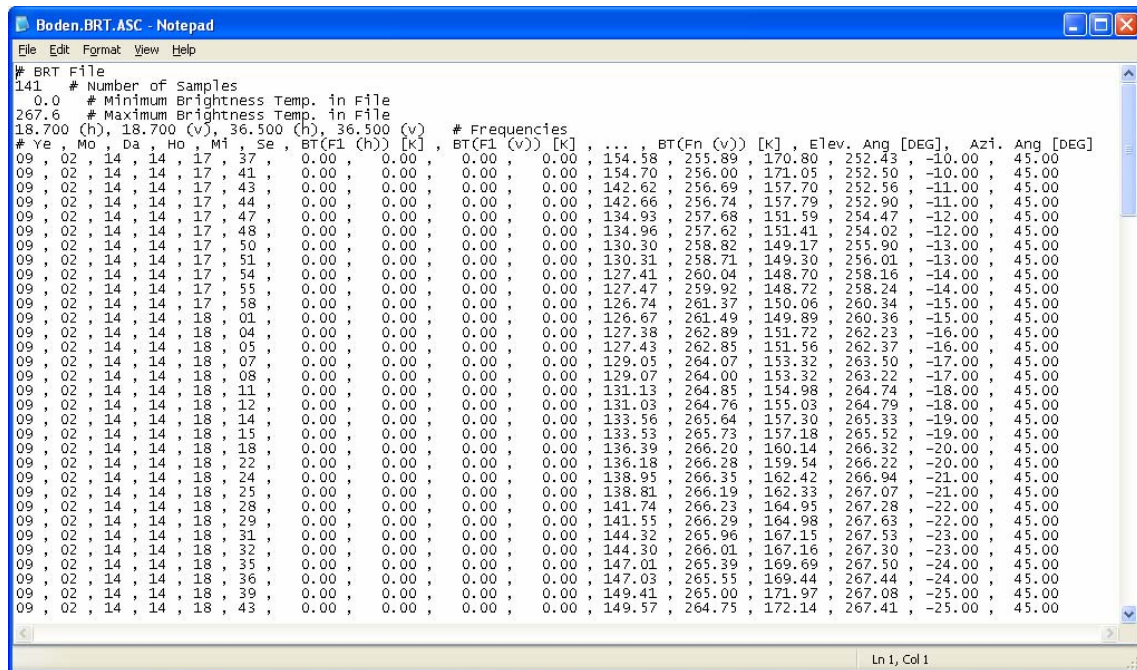


Fig.B1: BRT ASCII data file structure.

Fig.B2 is an example for a housekeeping data file (HKD).



```
09021619.HKD.ASC - Notepad
File Edit Format View Help
# HKD File
2571 # Number of Samples
# Ye, Mo, Da, Ho, Mi, Se, Tenv [K], TR1 [K], TR2 [K], TR3 [K], TR4 [K], SR1 [K], SR2 [K], SR3 [K], SR4 [K], P [mbar], RF,
09, 02, 16, 19, 00, 01, 278.0, 0.0, 0.0, 311.0, 311.0, 0.000, 0.000, 0.008, 0.005, 998.0, 1
09, 02, 16, 19, 00, 02, 278.0, 0.0, 0.0, 310.9, 311.0, 0.000, 0.000, 0.008, 0.005, 998.1, 1
09, 02, 16, 19, 00, 03, 278.0, 0.0, 0.0, 310.9, 311.1, 0.000, 0.000, 0.008, 0.005, 998.1, 1
09, 02, 16, 19, 00, 04, 278.0, 0.0, 0.0, 310.9, 311.1, 0.000, 0.000, 0.009, 0.004, 998.0, 1
09, 02, 16, 19, 00, 05, 278.0, 0.0, 0.0, 310.9, 311.0, 0.000, 0.000, 0.009, 0.004, 998.1, 1
09, 02, 16, 19, 00, 06, 278.0, 0.0, 0.0, 310.9, 311.0, 0.000, 0.000, 0.009, 0.004, 998.0, 1
09, 02, 16, 19, 00, 07, 278.0, 0.0, 0.0, 311.0, 311.0, 0.000, 0.000, 0.009, 0.004, 998.0, 1
09, 02, 16, 19, 00, 09, 278.0, 0.0, 0.0, 311.0, 311.1, 0.000, 0.000, 0.009, 0.003, 998.1, 1
09, 02, 16, 19, 00, 10, 278.0, 0.0, 0.0, 310.9, 311.0, 0.000, 0.000, 0.009, 0.003, 998.1, 1
09, 02, 16, 19, 00, 11, 278.0, 0.0, 0.0, 310.9, 311.1, 0.000, 0.000, 0.009, 0.004, 998.0, 1
09, 02, 16, 19, 00, 15, 278.0, 0.0, 0.0, 311.0, 311.1, 0.000, 0.000, 0.010, 0.004, 998.1, 1
09, 02, 16, 19, 00, 16, 278.0, 0.0, 0.0, 310.9, 311.1, 0.000, 0.000, 0.010, 0.004, 998.1, 1
09, 02, 16, 19, 00, 17, 278.0, 0.0, 0.0, 310.9, 311.1, 0.000, 0.000, 0.010, 0.005, 998.0, 1
09, 02, 16, 19, 00, 18, 278.0, 0.0, 0.0, 311.0, 311.0, 0.000, 0.000, 0.010, 0.005, 998.1, 1
09, 02, 16, 19, 00, 19, 278.0, 0.0, 0.0, 311.0, 311.0, 0.000, 0.000, 0.011, 0.005, 998.0, 1
09, 02, 16, 19, 00, 20, 278.0, 0.0, 0.0, 310.9, 311.0, 0.000, 0.000, 0.011, 0.005, 998.0, 1
09, 02, 16, 19, 00, 21, 278.0, 0.0, 0.0, 310.9, 311.0, 0.000, 0.000, 0.010, 0.005, 998.0, 1
09, 02, 16, 19, 00, 23, 278.0, 0.0, 0.0, 310.9, 311.1, 0.000, 0.000, 0.010, 0.003, 998.1, 1
09, 02, 16, 19, 00, 24, 278.0, 0.0, 0.0, 310.9, 311.1, 0.000, 0.000, 0.010, 0.006, 998.1, 1
09, 02, 16, 19, 00, 25, 277.9, 0.0, 0.0, 311.0, 311.1, 0.000, 0.000, 0.012, 0.007, 998.0, 1
09, 02, 16, 19, 00, 29, 277.9, 0.0, 0.0, 310.9, 311.0, 0.000, 0.000, 0.012, 0.007, 998.0, 1
09, 02, 16, 19, 00, 30, 278.0, 0.0, 0.0, 310.9, 311.0, 0.000, 0.000, 0.012, 0.007, 998.0, 1
09, 02, 16, 19, 00, 31, 277.9, 0.0, 0.0, 311.0, 311.0, 0.000, 0.000, 0.012, 0.007, 998.0, 1
09, 02, 16, 19, 00, 32, 277.9, 0.0, 0.0, 310.9, 311.0, 0.000, 0.000, 0.011, 0.007, 998.0, 1
09, 02, 16, 19, 00, 33, 277.9, 0.0, 0.0, 310.9, 311.0, 0.000, 0.000, 0.011, 0.007, 997.9, 1
09, 02, 16, 19, 00, 34, 277.9, 0.0, 0.0, 311.0, 311.0, 0.000, 0.000, 0.011, 0.007, 998.1, 1
09, 02, 16, 19, 00, 35, 277.9, 0.0, 0.0, 310.9, 311.0, 0.000, 0.000, 0.011, 0.007, 998.0, 1
Ln 1, Col 1
```

Fig.B2: housekeeping ASCII data file structure.

Fig.B3 is an example for a LIW data file (LIW).

```
09021619.LIW.ASC - Notepad
File Edit Format View Help
# LIW File
2571 # Number of Samples
-17.7 # Minimum LWP/LWC/LWR in File
934.3 # Maximum LWP/LWC/LWR in File
0 # Time Reference (1=UTC, 0=Local)
1 # Retrieval Algorithm (0=LR, 1=QR, 2=NN)
# Ye, Mo, Da, Ho, Mi, Se, LWP [g/m^2], LWC [g/m^2], LWR [g/m^2], Elev. Ang [°], Azi. Ang [°]
09, 02, 16, 19, 00, 01, 262.2, 166.2, 96.0, 30.00, 0.00
09, 02, 16, 19, 00, 02, 264.1, 160.3, 103.8, 30.00, 0.00
09, 02, 16, 19, 00, 03, 248.2, 157.2, 91.0, 30.00, 0.00
09, 02, 16, 19, 00, 04, 240.9, 142.5, 98.5, 30.00, 0.00
09, 02, 16, 19, 00, 05, 238.9, 145.1, 93.8, 30.00, 0.00
09, 02, 16, 19, 00, 06, 245.5, 147.9, 97.6, 30.00, 0.00
09, 02, 16, 19, 00, 07, 237.3, 155.0, 82.3, 30.00, 0.00
09, 02, 16, 19, 00, 09, 239.5, 160.3, 79.2, 30.00, 0.00
09, 02, 16, 19, 00, 10, 226.4, 148.1, 78.3, 30.00, 0.00
09, 02, 16, 19, 00, 11, 238.8, 159.4, 79.4, 30.00, 0.00
09, 02, 16, 19, 00, 15, 211.0, 140.5, 70.5, 30.00, 0.00
09, 02, 16, 19, 00, 16, 223.4, 140.0, 83.4, 30.00, 0.00
09, 02, 16, 19, 00, 17, 214.9, 142.5, 72.4, 30.00, 0.00
09, 02, 16, 19, 00, 18, 203.4, 125.5, 77.9, 30.00, 0.00
09, 02, 16, 19, 00, 19, 212.4, 146.7, 65.7, 30.00, 0.00
09, 02, 16, 19, 00, 20, 209.8, 147.2, 62.6, 30.00, 0.00
09, 02, 16, 19, 00, 21, 211.8, 157.5, 54.3, 30.00, 0.00
09, 02, 16, 19, 00, 23, 213.1, 151.7, 61.4, 30.00, 0.00
09, 02, 16, 19, 00, 24, 210.0, 146.5, 63.5, 30.00, 0.00
09, 02, 16, 19, 00, 25, 195.1, 140.6, 54.5, 30.00, 0.00
09, 02, 16, 19, 00, 29, 188.0, 139.8, 48.2, 30.00, 0.00
09, 02, 16, 19, 00, 30, 189.4, 145.3, 44.1, 30.00, 0.00
09, 02, 16, 19, 00, 31, 193.9, 148.6, 45.3, 30.00, 0.00
09, 02, 16, 19, 00, 32, 182.9, 141.8, 41.1, 30.00, 0.00
09, 02, 16, 19, 00, 33, 214.1, 184.2, 29.9, 30.00, 0.00
Ln 1, Col 1
```

Fig.B2: LIW data file structure.

## Appendix C (Measurement Example)

### C1. Zenith Sky Observations

When observing the sky in zenith direction, polarization splitting should be zero, even if clouds are passing the field of view. Falling rain droplets are vertically flattened, but this cannot be seen in zenith direction.

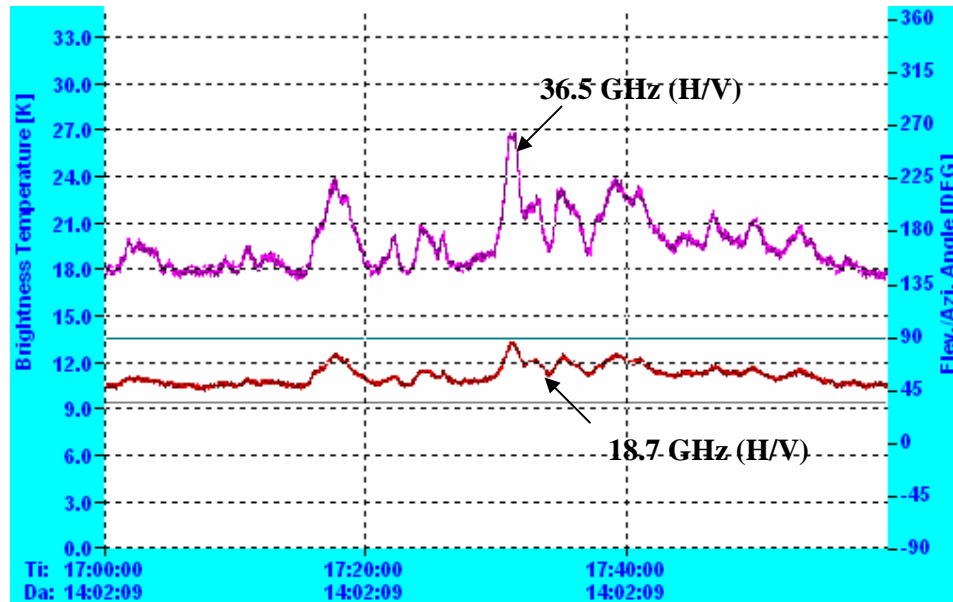


Fig.C.1.1

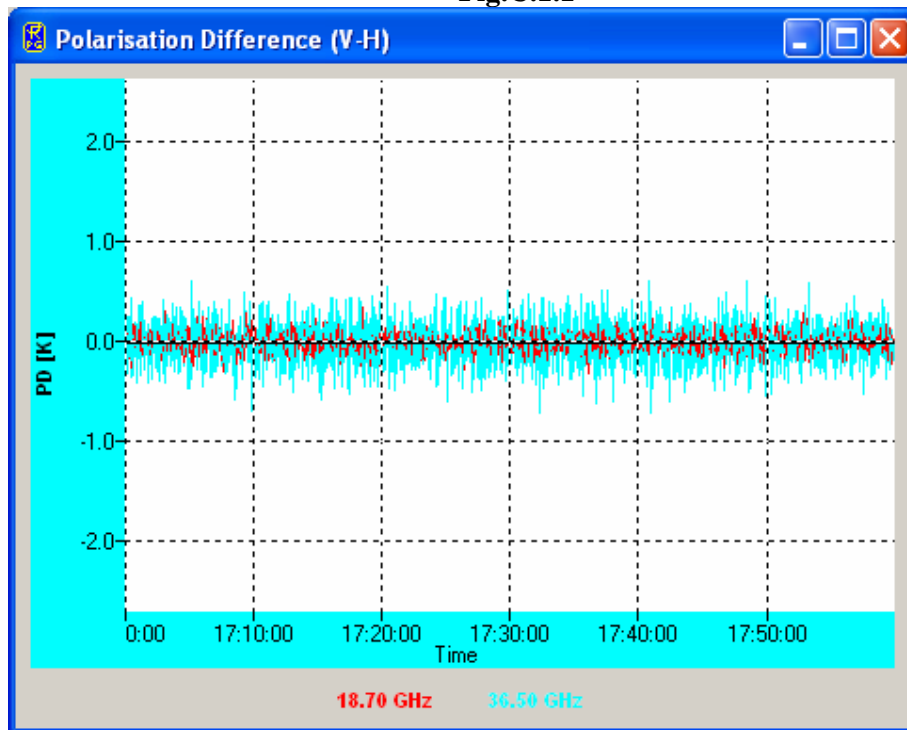
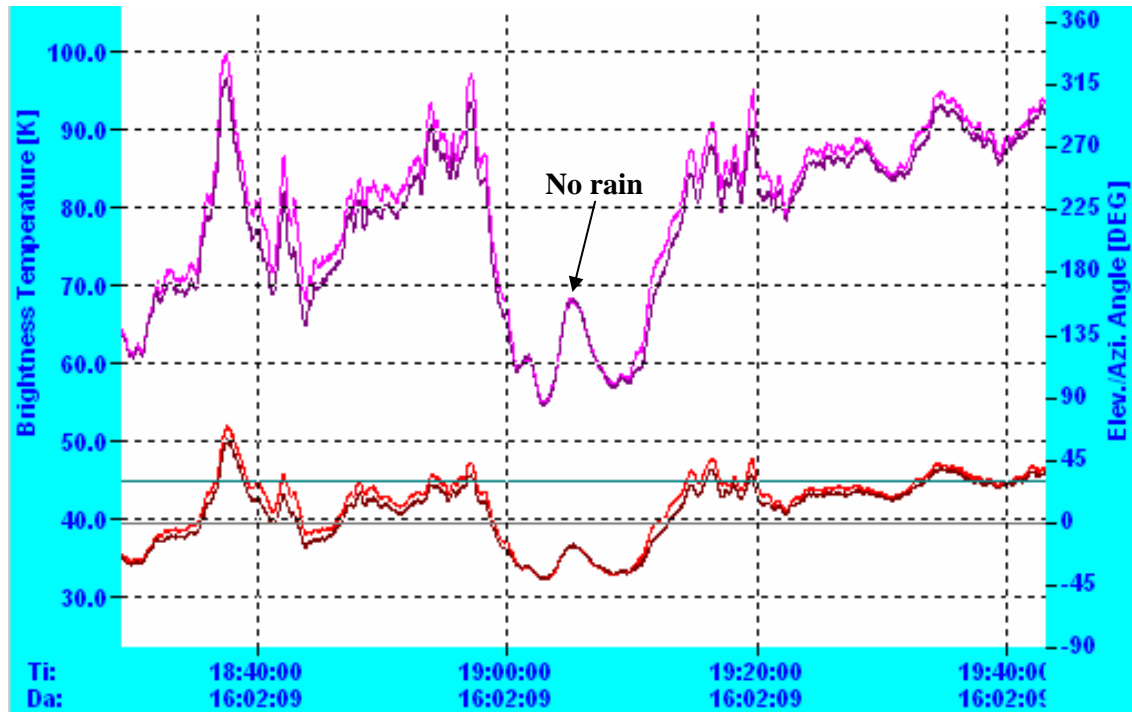


Fig.5.2

Polarisation effects due to falling rain droplets have to be observed under lower elevation angles (e.g. 30°). Therefore, by directing the radiometer to zenith, the polarization difference between V and H should vanish. Fig.C1.1 shows the TBs observed for a cloudy atmosphere and Fig.C1.2 is the polarization difference.

## C2. Observations Under Low Elevation Angles

The following measurements were performed at 30° elevation angle, observing a raining atmosphere (rain rate 5 mm/h). The polarization splitting is very obvious but immediately drops down to zero, when the rain pauses.



As expected, the 36.5 GHz channels respond much more sensitively to the liquid water and the polarization difference is more exaggerated. The 36.5 GHz channels are used for light rain detection while the 18.7 GHz channels cover the strong rain events with rain rates above 20-30 mm/h when the 36.5 GHz channels are starting to saturate.

Fig.C.1 shows the retrieval outputs for the Tb time series above. LWR is the liquid water content of the rain droplets, LWC denotes the cloud liquid and LWP is the total liquid water amount. The three time series are consistent even though the three quantities have been derived by three independent retrieval algorithms, one for each product.

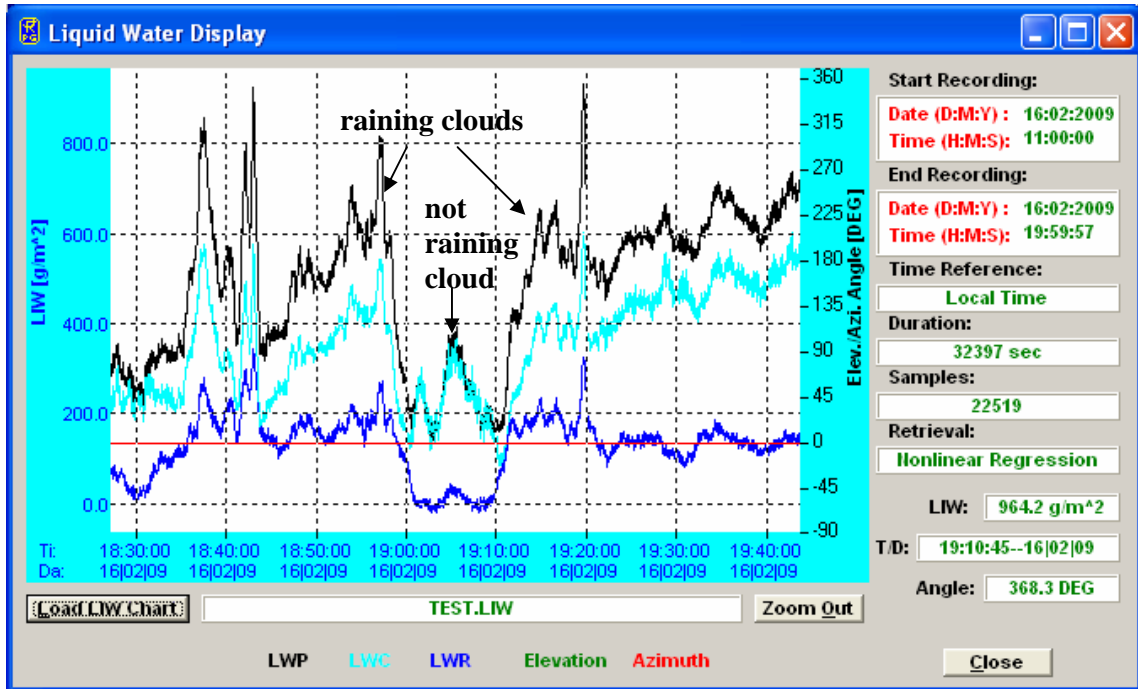
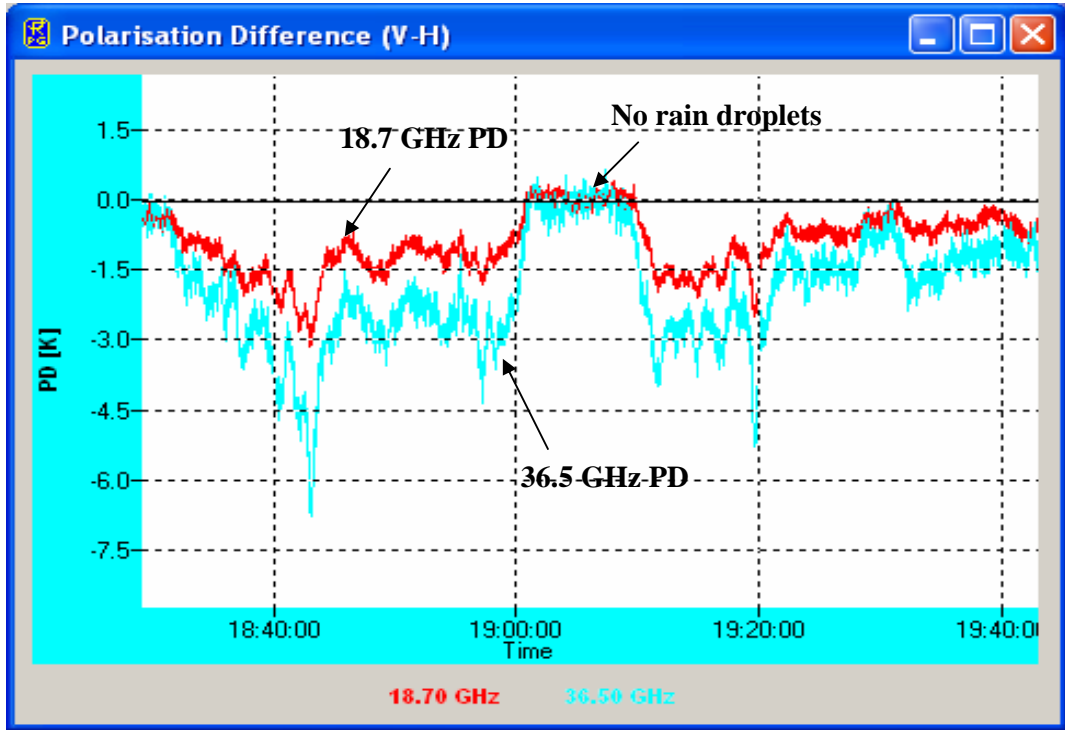


Fig.C.1